

TECHNICAL REPORT STANDARD PAGE

1. Title and Subtitle
Field Implementation of Handheld FTIR Spectrometer for Polymer Content Determination and for Quality Control of RAP Mixtures
2. Author(s)
Nazimuddin Wasiuddin, Rokhsana Hossain, Shams Arafat Lamiya Noor
3. Performing Organization Name and Address
Department of Civil Engineering
Louisiana Tech University, 600 Dan Reneau Dr.
Ruston, LA 71272
4. Sponsoring Agency Name and Address
Louisiana Department of Transportation and Development
P.O. Box 94245
Baton Rouge, LA 70804-9245
5. Report No.
FHWA/LA.17/649
6. Report Date
September 2022
7. Performing Organization Code LTRC
Project Number: 17-1B SIO
Number: DOTLT1000161
8. Type of Report and Period Covered
Research
July 2017- January 2020
9. No. of Pages
147
10. Supplementary Notes
Conducted in Cooperation with the U.S. Department of Transportation, Federal Highway Administration
11. Distribution Statement
Unrestricted. This document is available through the National Technical Information Service, Springfield, VA 21161.
12. Key Words
Quality control; asphalt binder; Styrene-Butadiene-Styrene (SBS); handheld FT-IR spectrometer; reclaimed asphalt pavement (RAP); carbonyl index; sulfoxide index
13. Abstract
Recent development in chemical characterization of asphalt binder with or without modification ascends the scope of using nondestructive techniques to evaluate the characteristics more rapidly in different laboratory and field conditions. Among these techniques, portable Fourier Transform Infrared (FT-IR) Spectroscopy is the most advantageous, considering its applicability and efficacy in terms of quick identification and quantification of chemical components in asphalt binder. In previous studies, application of FT-IR was limited to envisaging the chemical alteration in modified asphalt binder only in laboratory measurement. Therefore, in this study, handheld FT-IR spectrometer was used in the field to predict styrene-butadiene-styrene (SBS) content in modified asphalt binder to identify the type and amount of rejuvenator added in asphalt binder and to determine the reclaimed asphalt pavement (RAP) content in the mix by quantifying the extent of aging of the mix.

For understanding the aging mechanism in unmodified and modified asphalt binder, RTFO (rolling thin film oven), PAV (pressure aging vessel), UV (ultra-violet) chamber, and forced draft oven aging were performed. A dynamic shear rheometer (DSR) test was used to perceive the rheological changes. FT-IR results showed that peak height at 965 cm^{-1} (polybutadiene functional group) did not vary significantly due to SBS polymer structure, cross linking agent, base binder performance grades, and sources used for preparing modified asphalt binder. Based on the results, a universal curve was developed that predicted SBS content (%) in laboratory prepared samples and in field measurement within a percentage error of 0%-5% and 5%, respectively. The universal equation was also used to quantify the SBS content (%) after RTFO and PAV aging.

Carbonyl (I_{CO}) and sulfoxide (I_{SO}) indices were studied to understand the aging behavior of asphalt binder and mixture. Inconsistent increase of sulfoxide index made it unreliable to be considered as a metric for quantification of aging in asphalt binder and mixture. Spectral analysis of unaged binder and RAP can predict the I_{CO} in the fresh mix. The predicted and the measured I_{CO} values were found to be in good agreement in different plant mixes. Based on the study results on 10 plant mixes, the developed procedure can determine the RAP content in the mix within $\pm 5\%$ of the intended RAP content. ATR-FTIRS data collection requires small amount of binder that can be extracted in the field in 15 minutes by the quick extraction method developed in this study. The handheld FT-IRS has the potential to be used as a quality control tool in the field by precisely, accurately, and quickly detecting the SBS content (%) and the percent of aged RAP in the mix.

Project Review Committee

Each research project will have an advisory committee appointed by the LTRC Director. The Project Review Committee is responsible for assisting the LTRC Administrator or Manager in the development of acceptable research problem statements, requests for proposals, review of research proposals, oversight of approved research projects, and implementation of findings.

LTRC appreciates the dedication of the following Project Review Committee Members in guiding this research study to fruition.

LTRC Administrator/Manager

Samuel B. Cooper, III, Ph.D., P.E.
Materials Research Administrator

Members

Samuel Cooper, III
Corey Mayeux
Don Weathers
Phillip Graves
Luanna Cambas
Jason Davis
Brian Owens

Directorate Implementation Sponsor

Christopher P. Knotts, P.E.
DOTD Chief Engineer

Field Implementation of Handheld FTIR Spectrometer for Polymer Content Determination and for Quality Control of RAP Mixtures

By

Nazimuddin Wasiuddin

Roksana Hossain

Shams Arafat

Lamiya Noor

Department of Civil Engineering

Louisiana Tech University

Ruston, LA- 71272

LTRC Project No. 17-1B

SIO No. DOTLT1000161

conducted for

Louisiana Department of Transportation and Development

Louisiana Transportation Research Center

The contents of this report reflect the views of the author/principal investigator who is responsible for the facts and the accuracy of the data presented herein.

The contents do not necessarily reflect the views or policies of the Louisiana Department of Transportation and Development, the Federal Highway Administration or the Louisiana Transportation Research Center. This report does not constitute a standard, specification, or regulation.

September 2022

Abstract

Recent development in chemical characterization of asphalt binder with or without modification ascends the scope of using nondestructive techniques to evaluate the characteristics more rapidly in different laboratory and field conditions. Among these techniques, portable Fourier Transform Infrared (FT-IR) Spectroscopy is the most advantageous, considering its applicability and efficacy in terms of quick identification and quantification of chemical components in asphalt binder. In previous studies, application of FT-IR was limited to envisaging the chemical alteration in modified asphalt binder only in laboratory measurement. Therefore, in this study, handheld FT-IR spectrometer was used in the field to predict styrene-butadiene-styrene (SBS) content in modified asphalt binder to identify the type and amount of rejuvenator added in asphalt binder and to determine the reclaimed asphalt pavement (RAP) content in the mix by quantifying the extent of aging of the mix.

For understanding the aging mechanism in unmodified and modified asphalt binder, RTFO (rolling thin film oven), PAV (pressure aging vessel), UV (ultra-violet) chamber, and forced draft oven aging were performed. A dynamic shear rheometer (DSR) test was used to perceive the rheological changes. FT-IR results showed that peak height at 965 cm^{-1} (polybutadiene functional group) did not vary significantly due to SBS polymer structure, cross linking agent, base binder performance grades, and sources used for preparing modified asphalt binder. Based on the results, a universal curve was developed that predicted SBS content (%) in laboratory prepared samples and in field measurement within a percentage error of 0%-5% and 5%, respectively. The universal equation was also used to quantify the SBS content (%) after RTFO and PAV aging.

Carbonyl (I_{CO}) and sulfoxide (I_{SO}) indices were studied to understand the aging behavior of asphalt binder and mixture. Inconsistent increase of sulfoxide index made it unreliable to be considered as a metric for quantification of aging in asphalt binder and mixture. Spectral analysis of unaged binder and RAP can predict the I_{CO} in the fresh mix. The predicted and the measured I_{CO} values were found to be in good agreement in different plant mixes. Based on the study results on 10 plant mixes, the developed procedure can determine the RAP content in the mix within $\pm 5\%$ of the intended RAP content. ATR-FTIRS data collection requires small amount of binder that can be extracted in the field in 15 minutes by the quick extraction method

developed in this study. The handheld FT-IRS has the potential to be used as a quality control tool in the field by precisely, accurately, and quickly detecting the SBS content (%) and the percent of aged RAP in the mix.

Acknowledgments

The authors would like to thank the following individuals for their invaluable contributions in this study through technical consultations and/or materials.

- Delmar Salomon, Ph.D., Pavement Preservation Systems, LLC
- Sven Eklund, Ph.D., Associate Professor of Chemistry, Thelma Shipp Stewart Endowed Professor, Louisiana Tech University
- Louay Mohammad, Ph.D., P.E. (WY), Fellow-ASCE, Professor of Civil and Environmental Engineering, Holder of the Irma Louise Rush Stewart Distinguished Professorship, Louisiana State University, Louisiana Transportation Research Center
- Ben Holdman, Amethyst Construction, Inc., Ruston
- Sue Davis, Amethyst Construction, Inc., Ruston
- Jonathan Ashley, D & J Construction Company, LLC, West Monroe
- Steven, Diamond B Construction Company, LLC, Monroe
- Johnny Howe, Madden Contracting Company, LLC, Shreveport
- Jay Shane, Benton and Brown, Inc., Bossier City

Implementation Statement

The authors obtained asphalt binders modified with an unknown (one-sided blind study) amount of SBS and determined the percent of SBS. For example, two such binders obtained had 2% SBS (initially unknown to the authors), and in each of the cases, the authors predicted 2.1% SBS, which is highly accurate considering 0.1% variations may occur from other sources of error, such as SBS segregation. An FT-IR test on three samples from any binder in the field will take about 10 minutes, which includes analyses using an excel spreadsheet. Based on this study, the authors recommend that the handheld FT-IR spectrometer is a viable tool for accurate, precise, and quick determination of SBS content in the field and is immediately implementable.

If the liquid binder, RAP, and air-cooled loose mix are given, it is possible to determine the RAP content in the mix within 30 minutes (see the table below). Both the RAP and loose mix need to be extracted in parallel following a quick 15-min extraction procedure developed in this study. Three replicates from each of the three types of binders, virgin binder and two extracted samples, need to be tested. In this way, a total of 9 FT-IR spectra need to be collected using the handheld FT-IR spectrometer. Data will be transferred to the laptop computer for determination of RAP content.

Table 1. Specimen time requirements

Work Step	Required Time					
	5 min	5 min	5 min	5	5 min	5 min
RAP Extraction						
Mix Extraction						
FT-IRS of 3 Replicates (1 Binder)						
FT-IRS of 3 Replicates (1 Extracted RAP)						
FT-IRS of 3 Replicates (1 Extracted HMA w/ RAP)						
Data Transfer and Analysis						

Based on the study results on ten plant mixes, the developed procedure can determine the RAP content in the mix within $\pm 5\%$ of the intended RAP content. The mixes collected from right after the drum (i.e., excluding the short-term aging effect due to hauling time or storage time) were used to determine the accuracy. The authors consider this to be accurate enough because $\pm 5\%$ may come from other potential sources of error, such as inaccurate blending of RAP with virgin aggregates. To this end, the FT-IR spectrometer is

immediately implementable for determining RAP percent in the field precisely, accurately, and quickly.

Table of Contents

Technical Report Standard Page	1
Project Review Committee	3
LTRC Administrator/Manager	3
Members	3
Directorate Implementation Sponsor	3
Field Implementation of Handheld FTIR Spectrometer for Polymer Content	
Determination and for Quality Control of RAP Mixtures	4
Abstract	5
Acknowledgments.....	7
Implementation Statement	8
Table of Contents	10
List of Tables.....	12
List of Figures.....	13
Introduction.....	17
Quantification of SBS Content	17
Degradation of SBS Due to Aging.....	18
Selection of Asphalt Binder Aging Parameter	18
Effect of Laboratory Binder and Mix Aging.....	18
RAP Content Determination	19
Identification and Quantification of Rejuvenators.....	19
Literature Review.....	20
Quantification of SBS Content	20
Degradation of SBS due to Aging.....	21
Selection of Asphalt Binder Aging Parameter	22
Effect of Laboratory Binder and Mix Aging.....	23
RAP Content Determination	25
Identification and Quantification of Rejuvenators.....	25
Objective.....	27
Scope.....	28
Methodology.....	29
Materials and Experimental Plan for Quantification of SBS Content	29
Materials and Experimental Plan for Degradation of SBS Due to Aging.....	40
Materials and Experimental Plan for Selection of Asphalt Binder Aging Parameter	42

Materials and Experimental Plan for Effect of Laboratory Binder and Mix Aging.....	50
Materials and Experimental Plan for RAP Content Determination	53
Materials and Experimental Plan for Identification and Quantification of Rejuvenators	60
Discussion of Results	63
Quantification of SBS Content	63
Degradation of SBS Due to Aging.....	75
Selection of Asphalt Binder Aging Parameter	77
Effect of Laboratory Binder and Mix Aging.....	85
RAP Content Determination	92
Identification and Quantification of Rejuvenators.....	100
Conclusions.....	108
Findings on Quantification of SBS Content	108
Findings on Degradation of SBS Due to Aging.....	109
Findings on Selection of Asphalt Binder Aging Parameter	109
Findings on Effect of Laboratory Binder and Mix Aging.....	109
Findings on RAP Content Determination	110
Findings on Identification and Quantification of Rejuvenator	111
Recommendations.....	112
Acronyms, Abbreviations, and Symbols.....	113
References.....	114
Appendix.....	123
APPENDIX A: Quick Extraction Process in the Field	123
APPENDIX B: Instruction of Operation of Handheld FT-IR.....	127
APPENDIX C: Import Data File from FT-IR to the PC	136
APPENDIX D: FT-IR Spectra Analysis Method.....	139

List of Tables

Table 1. Specimen time requirements	8
Table 2. Previous literatures on SBS quantification in asphalt binder.....	21
Table 3. Functional group in binder susceptible to aging	23
Table 4. Test matrix for developing standard curves for ATR-FTIR	32
Table 5. Polymer content determination by FTIR spectrometer in previous studies.....	34
Table 6. Literature on aging determination of SBS-modified binders by FT-IR	42
Table 7. Experimental variables and their corresponding material properties.....	43
Table 8. Average peak height at different wavenumbers from absorbance spectra of PG 64-22 (NC) binder after different laboratory aging methods.....	48
Table 9. Laboratory aging plan for the study	49
Table 10. Experimental plan for data collection and result analysis.....	51
Table 11. Material properties of bio and aromatic rejuvenators	60
Table 12. Slope, intercept. and correlation among dataset for SBS quantification in 24 cases for absorbance height and area method	65
Table 12. Results from regression analysis between peak height and SBS concentration	72
Table 14. SBS (%) prediction of the laboratory prepared samples	74
Table 15. Field implementation of FT-IR to predict SBS percentage.....	75
Table 16. Reduction in SBS content after RTFO and PAV aging	76
Table 17. Effect of solvent residue in ATR-FTIRS absorbance value	78
Table 18. Details information regarding the plant mix	99
Table 19. Properties of linear regression curves due to bio rejuvenation process at 1744 cm ⁻¹	104
Table 20. Properties of linear regression curves due to bio rejuvenation process at 1162 cm ⁻¹	105

List of Figures

Figure 1. Heating samples in a can in melting pot.....	30
Figure 2. Adding powdered SBS in the liquid asphalt binder.....	30
Figure 3. Mixing in high shear mixture for 2.5 hours.....	31
Figure 4. Sample collection technique for FT-IR spectroscopy.....	33
Figure 5. Placing sample on diamond ATR sensor of FT-IR	33
Figure 6. Effect of SBS addition in different percentages in asphalt binder at wavenumber 965 cm ⁻¹	35
Figure 7. SBS quantification by peak height method	36
Figure 8. SBS quantification by peak area method.....	36
Figure 9. Collecting hot sample from the asphalt tank	37
Figure 10. Storing samples in gallon cans	38
Figure 11. Placing sample on ATR-FTIR sensor by a spatula	38
Figure 12. Ensuring good connection between sensor and sample	39
Figure 13. Collecting FT-IR spectra	39
Figure 14. Repeating same procedure for other samples.....	40
Figure 15. Experimental flow chart	41
Figure 16. Procedure for FT-IR data collection.	41
Figure 17. Dried samples by air blower.....	44
Figure 18. Solution induced with aggregate, binder and DCM solvent.....	44
Figure 19. Filtration technique for HMA mix.....	45
Figure 20. Nicolet IR 100 FT-IR spectrometer	45
Figure 21. Diamond crystal.....	45
Figure 22. Placing sample on crystal	46
Figure 23. Collected spectra for analysis	46
Figure 24. Characteristic functional groups in fingerprint region in unmodified asphalt binder	47
Figure 25. UV aging of PG 64-22 binder	52
Figure 26. Oven aging of PG 64-22 binder.....	52
Figure 27. Sample placed over the FT-IR for data collection.....	53
Figure 28. Detailed experimental plan for the study.....	57

Figure 29. Quick extraction process of asphalt mixture implemented in the field: (a) HMA collection from the truck, (b) pouring loose HMA in the mason jar, (c) use of DCM to extract the binder form mix, (d) the solvent is being filtered, (e) DCM is being evaporated quickly and the asphalt residue is left on the pan, (f) asphalt binder is placed on the FT-IR crystal to collect the spectra.....	58
Figure 30. Change in carbonyl index for various amount of RAP addition. Indices are calculated in six different methods and normalized root mean square error are provided for each method	59
Figure 31. Absorbance height measurement of FT-IR spectra.....	62
Figure 32. Absorbance area measurement of FT-IR spectra.....	62
Figure 33. Slope, intercept, and R ² of the standard curves developed for different scenarios of SBS data collection in FT-IR.....	66
Figure 34. SBS peak height comparison by standard deviation error bars considering different batch mixing in case of preparing SBS-modified binder	67
Figure 35. SBS peak height comparison by standard deviation error bars considering base binder from different sources in cases of preparing SBS-modified binder	67
Figure 36. SBS peak height comparison by standard deviation error bars considering different days' data collection in cases of preparing SBS-modified binder.....	68
Figure 37. SBS peak height comparison by standard deviation error bars considering different PG grade base binder in cases of preparing SBS-modified binder	68
Figure 38. SBS peak height comparison by standard deviation error bars considering effect of SBS polymer structure in cases of preparing SBS-modified binder ...	69
Figure 39. SBS peak height comparison by standard deviation error bars considering effect of cross-linking agents in cases of preparing SBS-modified binder.....	69
Figure 40. Correlation among SBS concentration, peak height at 965 cm ⁻¹ and peak area at 965 cm ⁻¹ with outlier data points	71
Figure 41. Correlation among SBS concentration, peak height at 965 cm ⁻¹ and peak area at 965 cm ⁻¹ without outlier data points	71
Figure 42. SBS content of different types of modified binders after RTFO and PAV aging.....	76
Figure 43. C=O content of different modified binders before and after RTFO and PAV aging.....	77
Figure 44. Comparison of absorbance values for aggregate intrusion at wavenumbers corresponding to oxidative aging.....	78
Figure 45. Absorbance spectra of samples considering aggregate and solvent interruption.....	79
Figure 46. Absorption spectra of extracted binder containing various quantity of fines..	80

Figure 47. Carbonyl (CO) index for PAV aged binder.....	82
Figure 48. Sulfoxide (SO) index for PAV aged binder	82
Figure 49. Sulfoxide index of short-term oven aged mix.	83
Figure 50. Effect of fines on carbonyl and sulfoxide index.....	83
Figure 51. Sulfoxide index for RTFO aged binder	84
Figure 52. Sulfoxide index for short-term oven aged mixture.....	85
Figure 53. Carbonyl index of unaged binder and comparison of those indices to 1-PAV aged binder.....	87
Figure 54. Sulfoxide index of unaged binder and comparison of those indices to 1-PAV aged binder.....	87
Figure 55. Increase in carbonyl index with the duration of different laboratory aging methods: (a) PAV aging, (b) RTFO aging, (c) oven aging at 135°C and (d) oven aging at 85°C.....	88
Figure 56. Sulfoxide index for laboratory aged binder.....	89
Figure 57. I _{CO} peak height index (1695 cm ⁻¹ /1456 cm ⁻¹) for PG 64-22 original and aged binder	90
Figure 58. RTFO and PAV aged (W/O RTFO) PG 64-22 binder at 64°C (a) stiffness (b) phase angle.....	91
Figure 59. Comparison of C=O index of RTFO and PAV aged PG 64-22 binder at similar stiffness	91
Figure 60. Comparison of PAV aged binder and naturally aged RAP: (a) carbonyl index, (b) high temperature grade.....	93
Figure 61. Linear increase in carbonyl index with increase of aged binder	95
Figure 62. Prediction and validation of RAP content in plant produced mix of (a) RAP-8 with 16% design RAP binder, (b) RAP-9 with 15.4% design RAP binder	96
Figure 63. Linear increase in carbonyl index with increase in RAP content in the laboratory mix.....	97
Figure 64. Carbonyl index of short-termed aged mixes in the plant	98
Figure 65. RAP content determined by handheld FT-IRS in the plant	99
Figure 66. Absorbance spectra of aromatic rejuvenator in ATR-FTIR a) spectral region from 650-4000 cm ⁻¹ b) fingerprint spectral region from 650- 1800 cm ⁻¹	101
Figure 67. Absorbance spectra of bio rejuvenator in ATR-FTIR a) spectral region from 650-4000 cm-1 b) fingerprint spectral region from 650- 1800 cm ⁻¹	102
Figure 68. Effect of BR (bio rejuvenator) on unmodified and SBS-modified binder spectra in 650-1800 cm ⁻¹ spectral region.....	103
Figure 69. Effect of AR (aromatic rejuvenator) on unmodified and SBS-modified binder spectra in 650-1800 cm ⁻¹ spectral region.....	103

Figure 70. Effect of BR (bio rejuvenator) on unmodified and SBS-modified binder spectra modified with 20% RAP binder in 650-1800 cm^{-1} spectral region	104
Figure 71. Effect of AR (aromatic rejuvenator) on unmodified and SBS-modified binder spectra modified with 20% RAP binder in 650-1800 cm^{-1} spectral region	105
Figure 72. Linear regression analysis for bio rejuvenated FT-IR spectra at wavenumber 1744 cm^{-1}	106
Figure 73. Linear regression analysis for bio rejuvenated FT-IR spectra at wavenumber 1162 cm^{-1}	107

Introduction

Fourier Transform Infrared Spectroscopy (FT-IRS) has attained its acknowledgement in chemical analysis of asphalt binder considering its simplicity in sampling process and data interpretation proficiency [1]. Recent studies show that FT-IR spectroscopy has been effectively applied in recognizing an array of modifiers used in asphalt binder such as-SBS, polyolefin, crumb rubber, WMA (warm mix asphalt) additives, and polyphosphoric acid (PPA) [2]. Application of FT-IR in quantification of aging in asphalt binder is also well studied. The principle of FT-IR spectroscopy is to detect the molecular structures of a sample based on their vibrational and rotational frequency at a specific wavenumber in the range of 600 cm^{-1} to 4000 cm^{-1} when an infrared beam passes through the sample and is absorbed by it. This absorbance is displayed in the form of an absorbance intensity versus wavenumber. According to Beer's law, this absorbance intensity is proportional to the concentration of the molecule. From this relationship, presence of a functional group in any material can be identified, and the quantity can be determined. So, advantages of the application of FT-IR in asphalt can be taken by quantifying the polymers contents in the binder, and aging of asphalt binder as well as mixes. The whole study can be divided into six subsections for better representation of the findings.

Quantification of SBS Content

SBS is the most frequently used elastomers in the asphalt binder to enhance the life span of the asphalt pavement. Both the physical and rheological properties of the base binder improve by the addition of SBS [3]. In case of SBS-modified asphalt binder, two distinctive functional groups are primarily observed in FT-IR spectrum at wavenumbers 965 cm^{-1} and 700 cm^{-1} which are considered as representative functional groups of polybutadiene and polystyrene compound [4]. It can also be noted that the efficacy of FT-IR spectrometer is not only limited to SBS identification but also visualizing their effect on aged binder due to modification [5], polymer degradation [6-8], the relationship between physical and chemical properties of SBS-modified binder [9-11], and SBS percentage quantification [12]. In this study, a combination of different types of SBS polymers and binder from several sources are tested using FT-IR to investigate if SBS content can accurately be determined.

Degradation of SBS Due to Aging

SBS-modified asphalt binder is used to reduce pavement distress and increase service life. But the main concern of using SBS-modified asphalt binders in pavement construction is the degradation of SBS polymer due to aging [13, 14]. Rheological properties of SBS-modified aged asphalt binder are different that the unaged binder because of the oxidation of base binder and the degradation of SBS polymer. In this study different types of laboratory aging were performed on neat and SBS-modified binders. The laboratory aging methods encompass rolling thin film oven aging (RTFO), pressure aging vessel (PAV), ultraviolet aging (UV) and forced draft oven aging. Degradation of polymer due to aging can be successfully determined by analyzing the FT-IR spectra of unaged and aged SBS-modified binders.

Selection of Asphalt Binder Aging Parameter

Aging reduces the long-term performance of asphalt binder because aging makes the asphalt binder brittle and stiff. Evaluation of asphalt binder and mixture aging can provide an over-all understanding on pavement performance, deterioration, and quality assurance. This study is focused on quantifying the aging of binder and mixes using FT-IR. Key functional groups that are affected by the aging in asphalt binder are carbonyl group (C=O) at wavenumber 1695 cm^{-1} and sulfoxide group (S=O) at wavenumber 1030 cm^{-1} . These two functional groups are used as indicators for quantifying the aging of asphalt. Different indices were developed based on the peak height or area under the spectra at those wavenumbers. In this study, applicability of different indices was investigated, and comparative results were documented for same samples analyzed using different indices. For different types of samples different indices are recommended for data analysis.

Effect of Laboratory Binder and Mix Aging

Aging mechanism can be investigated in the laboratory by various test methods considering their contribution in assessing certain property of the aged binder. Among these tests physical changes in aged binder can be evaluated by penetration, ductility and loss of mass test, and chemical changes can be evaluated by SARA fraction (saturate, aromatic, resin and asphaltene) analysis and FT-IR (Fourier transform Infrared) absorbance or transmittance spectroscopy. In addition, mechanical and rheological

changes can be evaluated by dynamic modulus, resilient modulus, fatigue resistance, rutting potential, cracking susceptibility, viscosity, and complex modulus and phase angles. Since each test has their specific feature to define aging, processing time is also an important factor for accelerating ageing determination in laboratory as well as in the field. Based on this factor, FT-IR spectroscopy requires less time compared to other tests and can also provide reliable results. In this study FT-IR spectrometer has been used as a primary technique to evaluate aging of four different PG grade asphalt binder obtained from four different sources. Both binder aging and mixture aging were conducted to observe their changes under different aging condition. Binders were aged in RTFO and PAV; whereas, mixes were aged in a forced draft oven. Change in carbonyl index for aged binder and mixes were investigated under different aging conditions.

RAP Content Determination

Addition of RAP in asphalt mixture supports the economic and environmental interest, however, quantification of aging state of these RAP aggregates for quality control purpose can help to predict their performance [15]. Incorporation of excess amount of RAP in asphalt mixture has adverse effect on pavement performance. So, continuous quality control during the production phase is crucial. It has been a challenging task to quickly detect the amount of RAP in the hot mix asphalt (HMA) by examining the fresh mix in the plant. As RAP contains highly aged binder, it is possible to detect the presence of RAP by investigating the aging state of the fresh mix. In this study HMA containing RAP from ten different plants were investigated using the FT-IR. The corresponding RAP and the virgin binder were also tested. Based on those spectra, the RAP content in the mix was readily determined in the field using the handheld FT-IR.

Identification and Quantification of Rejuvenators

Application of rejuvenator in aged asphalt binder can improve the binder performance by restoring the ratio of asphaltenes to maltenes. In this study, two types of rejuvenators (bio based, and petroleum based) were used in unmodified, polymer modified, and extracted binder from RAP. Petroleum base rejuvenator is primarily the aromatic oil, and sources of the bio rejuvenator are highly distributed from waste cooking oil to plant derived oils. FT-IR was used as a primary tool to identify the type and amount of rejuvenator added in asphalt binder.

Literature Review

Quantification of SBS Content

Modification of asphalt pavement has become obligatory due to increased heavy loads and high traffic volume. Use of SBS-modified asphalt binder has increased tremendously in the last few decades to enhance that pavement performance. SBS-modified asphalt (SBSMA) binder reduced rutting [16] and increased the fatigue and thermal cracking resistance of the pavement. SBSMA binder showed better performance than the unmodified binder in resisting low temperature cracking [17]. SBS content in asphalt binder has a linear correlation with the physical force parameter [18]. Performance of SBSMA binder depends on the content of SBS, which requires a quantification standard. AASTHO T302-15 proposed a standard test method for polymer content determination of polymer-modified, emulsified asphalt residue and asphalt binder from FT-IR spectroscopy from laboratory prepared samples [12], but its implementation in field samples was not addressed adequately. This standard requires a universal equation for each individual sample for SBS content determination in the field.

The principle of FT-IR spectroscopy involves passing an infrared beam through a material and identifying its molecular structure based on its rotational and vibrational frequency [19]. The chemical bonds in a material absorb the infrared beam in a specific wavenumber and display as an absorbance spectrum in FT-IR spectroscopy. In most of the cases, the FT-IR spectrometer reported a spectrum in 400 cm^{-1} - 4000 cm^{-1} region where 600 cm^{-1} - 1500 cm^{-1} is known as fingerprint region due to the presence of complex functional group which differs from sample to sample [20]. After analyzing this absorbance spectrum, chemical functional groups of a material can be identified and quantified. The handheld FT-IR spectrometer is considered more feasible for implementation in the field for its quick identification and quantification of chemical compound [21].

Table 2 lists a magnitude of research related to FT-IR spectroscopy that has been done in the past. Hu et al. [22] considered all the variabilities in SBS mixing with asphalt binder; however, SBS percentage quantification and field implementation of FT-IR spectrometer in predicting SBS percentage in unknown samples were not performed. In summary, these studies only consider laboratory samples; therefore, application of such results to represent

field condition is not viable since SBS concentration is highly susceptible to storage and handling temperature during construction [23].

Table 2. Previous literatures on SBS quantification in asphalt binder

References	FT-IR sensors	No. of Base binders	No. of Base binder sources	Types of SBS	Use of cross-linking agents	% of SBS	Quantify SBS in field
Hu et al. [22]	ATR-FTIR	3	3	4	yes	3,3.5,4, 4.5,5 100%	No
Wang et al. [24]	ATR-FTIR	2	1	-	no	PG76-22, 85% PG76-22, 70% PG76-22, and 0% PG76-22	No
Wang et al. [25]	ATR-FTIR	1	1	1	no	3.5, 4.0, 4.5 and 5	No
Ye et al. [26]	-	1	1	2	no	2,3,3.5,4, 4.5, and 5	No
Lu et al. [27]	ATR-FTIR	1	1	-	no	0,1,3,5,7,9, and 10	No
Masson et al. [28]	Transmission	2	1	3	no	3,6, and 10	No

Degradation of SBS due to Aging

The performance of SBS was better when it was coated with asphalt binder. Degradation of SBS in the air was more than in the asphalt binder. Due to the aging of SBS-modified asphalt binder, low temperature cracking resistance decreased [29]. Again, the rheological properties of the aged SBSMA showed better performance than the original aged base binder [30]. From the FT-IR spectrum, C=O, C=C, C-H, and S=O bonds are observed at 1700 cm^{-1} , 1600 cm^{-1} , 1460 cm^{-1} , and 1030 cm^{-1} wavenumbers respectively [31]. C=C content in butadiene of SBS copolymer in SBS-modified asphalt binder decreased after RTFO, PAV, and UV aging. As a result, butadiene content reduced after these three types of aging of SBS-modified asphalt binder [5, 31, 32].

Selection of Asphalt Binder Aging Parameter

Atmospheric oxidation of asphalt binder during different stages of the pavement life cycle leads to deterioration of pavement, which is known as oxidative aging. It occurs at a high temperature when asphalt binder meets atmospheric oxygen. At temperature greater than 150°C, the chemical composition of asphalt is altered even when the oxygen is not present [33]. Generally, asphalt binder contains hydrocarbon compounds of different weight which forms a complex colloidal mixture and any changes in this mixture due to volatilization and oxidation causes aging [34]. Oxidation amount of asphalt binder can be associated with changing in six functional groups: carboxylic acids, aldehydes, amides, anhydrides, esters, and ketones [35].

In addition to carbonyl group, sulfoxides, which form at a high temperature, are also responsible for oxidative aging and form at a rapid rate compared to carbonyl group [34]. Previous studies show that FTIR spectroscopy is one of the most effective tools for monitoring the chemical composition of aged asphalt binder, identifying the oxidation product, evaluating carbonyl and sulfoxides compounds, producing aliphaticity, aromaticity and long chain indices, and analyzing the nature of modified asphalt binder and the effect of modifiers [33].

In FTIR spectroscopy, absorbance values indicate the aging extent of different functional groups. Previous literatures on FTIRS used various techniques such as peak to peak ratio, valley to valley integration which is known as area ratio method, and normalizing band area by dividing each band area by the sum to find compound indices. For peak to peak ratio, absorbance at 1700 cm^{-1} and 2920 cm^{-1} were considered to evaluate oxidation signal. On the other hand, aromaticity, carbonyl, sulfoxide, and hydroxyl band areas were used to determine the indices responsible for aging [36]. In most of the studies, the wavenumber, which was not susceptible to aging, was 2920 cm^{-1} (C-H stretching) whereas the wavenumbers 1700 cm^{-1} (C=O), 1030 cm^{-1} (S=O), 1210- 1320 cm^{-1} (C-O), and 2500-3330 cm^{-1} (O-H) were noted responsible for aging. Table 3 shows the functional groups which were susceptible to aging in previous literatures.

In previous studies, three different FTIRS methods: T-FTIRS (transmittance), ATR-FTIRS (Attenuated Total Reflectance) and DR-FTIRS (Diffuse Reflectance) were used by different researchers to evaluate aging characteristics in asphalt binder. Studies by ATR-FTIRS showed that laboratory-aged, polymer-modified binders did not exhibit significant oxidation rates compared to neat asphalt binder, and polymer degradation was also not significant when concentration was less than 3.5 wt. %. [37]. T- FTIRS was also

used to analyze Polymer Modified Nano Clay (PMN), Nonmodified Nano Clay (NMN) and Nano Silica (NS) modified asphalt binders at laboratory aging which concluded that nanomaterial exhibited anti-aging effect on asphalt binder [35]. In summary, many researchers used T-FTIRS and ATR-FTIRS to evaluate laboratory aging and effect of polymers. In one study, DR- FTIRS and ATR- FTIRS were used to analyze the blending characteristics of RAP with neat binder for samples collected from lab mix, plant mix, and pavement surfaces considering only carbonyl oxidation and its increase corresponding to RAP percentage [38]. However, the previous studies did not consider the effect of extraction solvent, remaining aggregate intrusion effect, and sulfur oxidation due to RAP aggregate.

Table 3. Functional group in binder susceptible to aging

Literatures on functional group	Functional groups and corresponding wave numbers (cm ⁻¹) susceptible to aging			
	C=O	C-O	O-H	S=O
Yut et al. 2011 [37]	1700		3400-3100	1030
Dehdezi et al. 2014 [39]	1702	1695	1670-1820	1108
Bower et al. 2014 [40]	1695		1210-1320	
Marsac et al. 2014 [34]	1635-1800			1030
Sun et al. 2014 [41]	1654			1024
Yao et al. 2015 [35]	1670-1820	1210-1320	2500-3300	
Salomon et al. 2016 [38]	1700			
Nivitha et al. 2016 [33]	1678-1725			1010-1043

Effect of Laboratory Binder and Mix Aging

Aging degraded the chemical, physical, and rheological performance of neat asphalt binder [16]. Aging is not only a physical phenomenon of stiffening the asphalt binder, but also chemical and rheological changes that occur during this process. It is crucial to understand the aging mechanism to improve the service life of asphalt pavement. Several researchers [42-44] studied the aging behavior and tried to find the relationship between chemical and rheological properties of aged asphalt binder. The oxidation process reduces the fatigue life of asphalt pavement as well as initiates embrittlement and subsequent cracking [45].

Aging mechanism can be investigated in the laboratory by various test methods considering their contribution in assessing certain properties of the aged binder. Among these tests physical changes in aged binder can be evaluated by penetration, ductility, and loss of mass tests, and chemical changes can be evaluated by SARA fraction (saturate, aromatic, resin, and asphaltene) analysis and FT-IR absorbance or transmittance spectroscopy. In addition, mechanical and rheological changes can be evaluated by dynamic modulus, resilient modulus, fatigue resistance, rutting potential, cracking susceptibility, viscosity, complex modulus, and phase angles [46, 31].

Since each test has their specific feature to define aging, processing time is also an important factor for accelerated aging determination in the laboratory as well as in the field. Based on this factor, FT-IR spectroscopy requires less time compared to other tests and can also provide reliable results. Besides, a portable FT-IRS has the potential to examine the aging state of the binder or mix in the field. FT-IRS can detect the carbonyl and sulfoxide content in asphalt binder. Previous studies with FT-IR spectrometer in aging determination showed that C=O (carbonyl) compound in asphalt binder increased with the increase in temperature and aging duration. It signifies the oxidation chemistry of asphalt binder [47, 48].

Different analysis methods for quantifying C=O and S=O aging indices were performed by several researchers [49, 50]. Jing et al. also showed the effect of temperature, pressure and aging duration on C=O and S=O indices of FT-IR spectra and their correlation with rheological properties [51]. Hofko et al. conducted an extensive study on FT-IR to visualize its capability in different analysis methods for quantifying C=O and S=O aging indices and recommended the importance of analysis method selection for FT-IR measurement [52]. Previous study conducted by the authors concluded that only carbonyl index can effectively identify the aging level of the asphalt mix. A universal model was developed by Liu et al. to predict the carbonyl content after long-term aging behavior [42]. Overlapped absorbance spectra of sulfoxide (from aged binder) and silicon oxide (from aggregate) makes it indecisive to use the sulfoxide index as an aging indicator for the asphalt mix [53]. In addition, S=O oxidation was observed in early stage of aging and the increasing pattern in oxidation was inadequate in later stages.

Oxidation reaction occurring in service life is significantly higher compared to RTFO (rolling thin film oven) and PAV (pressure aging vessel) aging of asphalt binder in respect with C=O oxidation [54]. The aging rate in PAV for different duration is also higher compared to field aging due to escalated exposure temperature. It was also found that high PG (performance grade) binder aged slower in field aging. Inter-laboratory studies suggested that C=O aging index in unaged and RTFO aged binders are significantly different compared to PAV aged binder [52]. Liang et al. showed that C=O absorbance area in FT-IR spectra had a linear relationship with aging duration at PAV condition [18].

RAP Content Determination

From the previous studies, it was evident that FT-IR spectrometer has a potential to quantify aging in terms of C=O and S=O oxidation measurement. However, in most of the studies, the FT-IR spectrometer has been used as a supporting tool to show the chemical changes due to oxidation. In addition, the effect of binder performance grade (PG) and binder sources in the chemical oxidation process was not addressed significantly. In one study, Diffuse Reflectance (DR) FT-IRS and ATR FT-IRS were used to analyze the blending characteristics of RAP with neat binder for samples collected from lab mix, plant mix, and pavement surfaces considering only carbonyl oxidation and its increase corresponding to RAP percentage [38]. However, chemical changes during the oxidation process in asphalt mixture and the oxidation stage of the RAP aggregate were not addressed properly in previous studies.

Identification and Quantification of Rejuvenators

In previous studies, FT-IR has been used as supporting technique with other chemical and rheological tests to evaluate the rejuvenation mechanism in asphalt binder. Researchers have shown that aging mechanism in asphalt binder was reversed by soybean oil due to the changes in carbonyl (C=O) and sulfoxide (S=O) functional groups in FT-IR spectra during the rejuvenation process [55]. In addition, 10% bio rejuvenator can restore the aging mechanism of PAV aged binder [56]. Studies also showed that 5% bio-based rejuvenators (seed oil, cashew nutshell oil, and tall oil) can exhibit aging restoration mechanism by unstiffened the RAP binder. It was concluded that bio rejuvenator added a functional group form ester at wavenumber 1750 cm^{-1} and increased C=O functional group in FT-IR spectra [57]. Bio rejuvenator obtained from sawdust can be used at a 15% dosage for the rejuvenation of lower graded PAV aged binder. Besides, it was also concluded that S=O and C=C indices reflected the rejuvenation process more precisely than C=O index which was increased due to the C=O groups incorporated from the bio rejuvenator [58].

Previous studies also presented the rejuvenation mechanism in unmodified and SBS-modified asphalt binder and concluded that the rejuvenation process was unable to restore SBS crosslinking structures. It showed that physical properties of rejuvenated SBS-modified asphalt binder were more stable than the rejuvenated unmodified asphalt [59]. Recent studies also recommended the necessity of characterizing rejuvenated binder

based on their chemical properties to understand the interaction between asphalt binder and rejuvenator, [16] as well as addressing the recent challenges on implementation of the rejuvenating agent in field application and to understand the chemical characterization of rejuvenating agents and their interaction on polymer modified binders [15].

Objective

The main objectives of this study were:

- To develop a universal curve that can be used to successfully predict SBS content (%) in a modified asphalt binder in the field.
- To implement the handheld FT-IR spectrometer in the field as a tool for quality control of plant mix containing RAP.

To achieve this goal, the following specific objectives were accomplished:

- Investigated the effects of different base binders (source and grade), different SBS polymer types, and crosslinking agent on FT-IR spectra.
- Evaluated the degradation of SBS in SBS-modified asphalt binder because of different types of laboratory aging (RTFO, PAV, UV, and forced draft oven).
- Selected a suitable index derived from FT-IR spectral analysis that can quantify both the binder and mix aging.
- Understood and quantified the laboratory aging of the binder and mix using ATR FT-IR.
- Determined the RAP content in the hot mix asphalt at the plant by a handheld FT-IR using a quick extraction method developed in the study.
- Quantified the amount of rejuvenator present in asphalt binder by analyzing absorbance spectra.

Scope

PG 52-34, PG 58-28, and PG 64-22 binders were collected from LA, MS, TX, and NC. Polymer modified binders PG 64-28, PG 70-22, PG 70-28, and PG 76-22 were collected from LA, MS, TX, AR, and NV. Both asphalt binders and mixture were used to achieve the goals of this study. The FT-IR spectrometer was used for the data collection of different type of original binders, modified (with polymer, rejuvenator and RAP) binders, and aged binders. Aging of binders was performed by RTFO, PAV, UV, and forced draft oven. The DSR test was performed to perceive the rheological properties. DCM solvent was used to extract the binder from the mixture and RAP. Two different plants were visited to implement the SBS content determination technique. RAP and mixture were collected from 10 different sources and five plants were visited twice to implement the RAP content determination technique.

Methodology

Materials and Experimental Plan for Quantification of SBS Content

Materials

PG52-34, PG58-28, and PG64-22 were used as base binders. PG64-22 was obtained from two different sources- one from Louisiana and the other from North Carolina. For preparation of polymer modified binder, two types of SBS polymer structure—triblock and diblock—were considered. For triblock SBS copolymers, both linear and radial molecular configurations were examined [60]. As a result, a total of three types of SBS copolymers named as linear, radial, and diblock were used to prepare polymer modified asphalt binder. The Styrene-Butadiene weight ratio (%) in these copolymers were 31/69, 31/69, and 33/67 respectively. The percentage of diblock contents in these copolymers were 16%, 16%, and 78%. All these copolymers were provided in powder form from the manufacturers. A reagent grade 100 mesh particle size sulfur was used as a crosslinking agent for avoiding phase separation of SBS-modified asphalt binder [61].

Preparation of SBS-modified Binders in Laboratory

SBS-modified asphalt binders were prepared in the laboratory using a high shear mixer. SBS copolymer was added to the asphalt binder based on the total weight of the binder. 1%, 2%, 3%, and 4% SBS copolymer were added to the base binders as follows:

- At first, 600 gm of asphalt binder was placed in the melting pot as shown in Figure 1. The setting temperature of the melting pot was 170°C. When the binder achieved its workability, SBS copolymer was added to the asphalt binder as shown in Figure 2.
- The setting temperature and rotation for the high shear mixer were maintained at 170°C and 5000 rpm, respectively. The mixing procedure continued for 30 minutes at 5000 rpm and then for another 2 minutes at 8000 rpm. The high shear mixer which was used in this study is shown in Figure 3.
- The increment in temperature of the melting pot was monitored by adjusting the speed of the high shear mixer so that it could not cross the temperature of 185°C.
- After repeating this process for 2.5 hours, data for SBS-modified samples were collected.

- On the other hand, the mixing process for preparing SBS-modified binder with cross-linking agent consisted of mixing the asphalt binder with SBS for 1.5 hours at 170°C and 5000 rpm in high shear mixer followed by adding 0.5% sulfur and mixing for another one hour.
- After 2.5 hours of total mixing, data for SBS-modified samples with the cross-linking agent were collected.

Figure 1. Heating samples in a can in melting pot



Figure 2. Adding powdered SBS in the liquid asphalt binder



In this process, a total of 36 mixes were prepared for different percentages of SBS-modified binder. For repeatable data collection in different days, remixing was conducted in a high shear mixer at 170°C for 30 minutes at 5000 rpm. At 15-minute intervals, speed was increased to 8000 rpm and mixing was continued for 2 minutes. After that, speed was reduced to 5000 to complete the 30-minute cycle of remixing. Table 4 shows the sample preparation matrix which is used in this study. In Table 4, “Batch” indicates the SBS-modified samples which were prepared in the same procedure for the second time. “Days” indicates the repeatability in data collection for different days from the same batch. In each case, except case 2, a total of 50 samples were collected.

Figure 3. Mixing in high shear mixture for 2.5 hours



Table 4. Test matrix for developing standard curves for ATR-FTIR

Binder	Type of polymer	%SBS	Batch	Day	Sample tested in ATR-FTIR	Standard curve ID
PG52-34	Radial	0%,1%, 2%, 3%, 4%	1	1	50	Case1
				2	25	Case2
				3	50	Case3
PG58-28	Radial	0%, 1%, 2%, 3%, 4%	1	1	50	Case4
				2	50	Case5
				3	50	Case6
				4	50	Case7
			2	1	50	Case8
				2	50	Case9
				3	50	Case10
PG64-22 (Source A)	Radial	0%, 1%, 2%, 3%, 4%	1	1	50	Case11
				2	50	Case12
				3	50	Case13
			2	1	50	Case14
				2	50	Case15
				3	50	Case16
PG64-22 (Source B)	Radial	0%, 1%, 2%, 3%, 4%	1	1	50	Case17
				2	50	Case18
	Linear	0%,1%, 2%, 3%, 4%	1	1	50	Case19
				2	50	Case20
	Diblock	0%, 1%, 2%, 3%, 4%	1	1	50	Case21
				2	50	Case22
Radial+ 0.5% Sulfur	0%, 1%, 2%, 3%, 4%	1	1	50	Case23	
			2	50	Case24	

FT-IR Spectroscopy

A 4300 handheld FT-IR spectrometer was used to obtain spectra considering its flexibility, robustness, carrying capability for field data collection, and easy sampling procedure. The diamond ATR sensor was considered since collected spectra remained unaffected by the sample amount placed on the sensor [12]. Again, it has corrosion and scratching resistivity which makes it suitable for field measurement. Each sample was placed on the sensor area by a spatula. The connection between the sample and the sensor of the instrument was ensured. Each spectrum collected by the FT-IR spectrometer was

converted to the absorbance spectrum by the default Microlab PC software provided with the instrument. A total of 24 scans for each sample was conducted in $650\text{-}4000\text{ cm}^{-1}$ region and reported in the form of 4cm^{-1} resolution. Before each scan, background spectra were collected to check if the sensor was properly clean. Figure 4 shows the sample collection technique and Figure 5 shows the instrumentation with a 4300 handheld FT-IR spectrometer [62].

Figure 4. Sample collection technique for FT-IR spectroscopy



Figure 5. Placing sample on diamond ATR sensor of FT-IR



Data Analysis

Table 5 represents some of the previous studies that used FT-IR spectroscopy. Spectroscopy data obtained from the FT-IR spectrometer were analyzed both qualitatively and quantitatively.

Table 5. Polymer content determination by FTIR spectrometer in previous studies

FT-IRS Method	Index Used	Comment
AASHTO T302 [12]	FTIR-T: Ratio of peak value of absorbance at 965 cm ⁻¹ and at 1375 cm ⁻¹ is used FTIR-ATR: Peak area at 965 cm ⁻¹ : to quantify the presence of polymer. No normalization is required	FT-IRS results are plotted against polymer content this curve is calibration curve. It will be used further to find unknown polymer content from FTIR spectrum
Yut et al. [37]	FTIR-ATR: Normalized band area was used to find the Polybutadiene index and Polystyrene index	SBS and SB Latex was mixed in variable proportion into the base binder and change in different indices was observed
Nivitha et al. [33]	FTIR-T: Normalized band was used to calculate PS, PB and N-H indices	Modifiers (PS, PB and Crumb rubber) were mixed in the laboratory
Diefenderfer et al. [63]	Used the peak ratio of at 965 and 1375 cm ⁻¹ to detect the SBS or specifically SB polymer content.	Constructed a calibration curve with peak ratio vs different polymer content: useful for quick determination of polymer in field
Fernandez et al. [46]	Peak at 815, 960 and 700 cm ⁻¹ : to identify Natural rubber, SB and PB. Absorption band of C-H (2960-2820): to normalize	Amount of styrene and butadiene were determined from a calibration curve
Ghebremeskel et al. [64]	Peak ratio 1602/1639 was used to quantify SBR and ratio of 2237/1639 was used to quantify NBR in SBR/NBR blend	When these two peak ratios are plotted against the %SBR the with R ² 0.99
Curtis et al., [65]	Quantified SBR latexes, ethylene vinyl acetate (EVA) and SBS polymers	Calibration curves with R ² 0.92 to 0.99
Nasrazadani et al. [66]	FTIR-T, AASHTO T302 was followed FTIR-ATR, AASHTO T302 was followed	Calibration curve with R ² 0.9949 Calibration curve with R ² 0.99

- For qualitative analysis, SBS-modified spectrum was superimposed on the unmodified spectrum, and characteristic functional group due to modification was identified.
- After that, regression analysis was performed to visualize the relationship between the absorbance intensity of the added functional group and the concentration of the modifier. According to Beer's law, the absorbance intensity

in terms of peak height or peak area is directly proportional to the concentration [20].

- In this study, absorbance intensity of the characteristic functional group was quantified by both height and area method to find the appropriate method which would provide repeatable measurements. These two methods were selected considering their ability to eliminate noise and baseline shift effects [67].
- The height of the functional group was determined by drawing a baseline considering the two lowest points on either side of the characteristic functional group as shown in Figure 6. After that, the mid-point of the baseline and top point of the peak was added to determine the peak height as shown in Figure 7.
- On the other hand, the absorbance area was calculated by the trapezoidal rule method as shown in Figure 8. The baseline was drawn following a similar process as the peak height method.

Figure 6. Effect of SBS addition in different percentages in asphalt binder at wavenumber 965 cm⁻¹

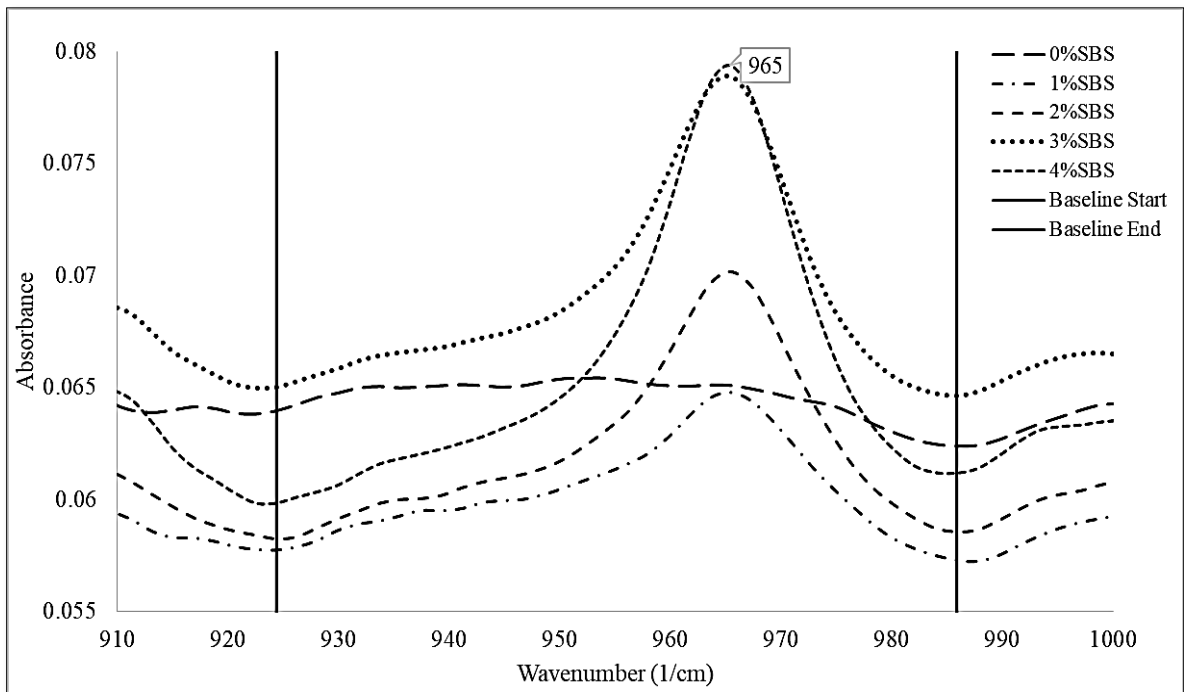


Figure 7. SBS quantification by peak height method

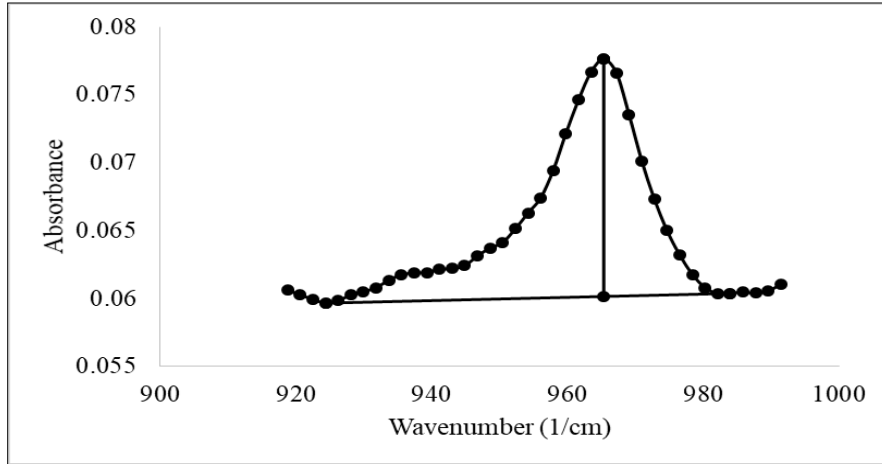
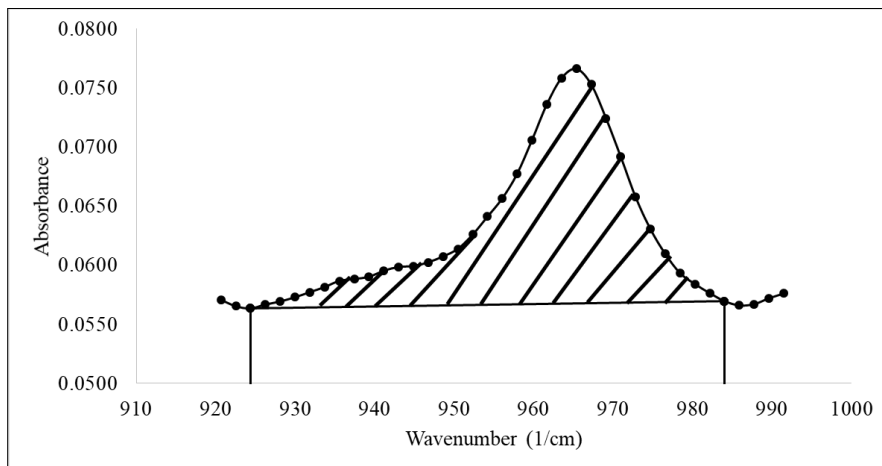


Figure 8. SBS quantification by peak area method



- After drawing the baseline, the area under the baseline was subtracted from the total area under the peak which provided the desired area for developing a universal curve.
- After that, peak height values and slope of the universal curves were analyzed in terms of standard deviation (SD) and coefficient of variation (CV) to visualize the effect of polymer structure, presence of cross-linking agents, and binder performance grade (PG).
- Finally, preferred analysis method for SBS quantification was selected based on the correlation values among SBS concentration, peak height at 965 cm⁻¹, and peak area at 965cm⁻¹. After selecting the best method based on its correlation,

regression analysis was performed to obtain the regression model for predicting SBS percentage in the asphalt binder with unknown amount of SBS in it.

- Subsequent cross-validation was also conducted to validate the model performance in terms of R^2 , RMSE (root mean square error), and MAE (mean absolute error).
- All statistical analysis was performed in RStudio programming language.

Field Demonstration

Six different field measurements were conducted to quantify the SBS percentage in modified asphalt binder.

- At first, asphalt binder was collected in 1-gallon cans from the designated tank of the asphalt plant as shown in Figure 9 and 10.
- After that, using a spatula, asphalt binder was placed on the FT-IR sensor as shown in Figure 11 and 12. The FT-IR spectrum were collected by Microlab mobile software.
- In this process, 10 samples were collected for each field observation as shown in Figure 13 and 14.
- After collecting each sample, the sensor was cleaned using cleaning solvent.
- The total process for sample collection and data processing in each field demonstration required 15 minutes.

Figure 9. Collecting hot sample from the asphalt tank



Figure 10. Storing samples in gallon cans



Figure 11. Placing sample on ATR-FTIR sensor by a spatula



Figure 12. Ensuring good connection between sensor and sample



Figure 13. Collecting FT-IR spectra



Figure 14. Repeating same procedure for other samples



Materials and Experimental Plan for Degradation of SBS Due to Aging

Materials

Four SBS-modified asphalt binders, namely PG 64-28, PG 70-22, and PG 76-22, were collected from Nevada (NV) and Mississippi (MS). Those binders were RTFO and PAV aged according to AASHTO T240 and AASHTO R28 respectively. Figure 15 represents the experimental flowchart of this study.

FT-IR Data Collection

In this study, a 4300 handheld FT-IR spectrometer with a diamond ATR (Attenuated total reflectance) sensor was used to obtain the spectrum. This type of ATR FT-IR spectrometer was considered because the collected spectrum remained unaffected by the amount of sample placed over the crystal. For the FT-IR data collection, at first, polymer modified binders were heated at 170°C to melt adequately for data collection. The FT-IR spectrometer was connected with the laptop and Microlab PC software was opened. After starting the software, cleaning of crystal and background checking were done. When it was shown that “ensure contact with the sample,” then a small amount of the binder was taken at the tip of the spatula and kept over the crystal of the FT-IR spectrometer. After

that absorbance was collected by the FT-IR spectrometer from 4000 cm^{-1} to 650 cm^{-1} wavenumber region and a resolution of 4 cm^{-1} . A total of 10 spectra were collected for each of the binders. Figure 16 represents the data collection method for FT-IR spectroscopy.

Figure 15. Experimental flow chart

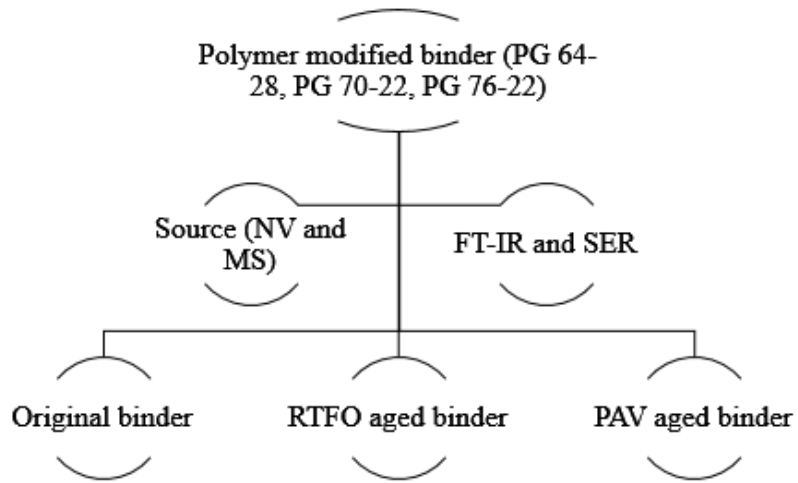
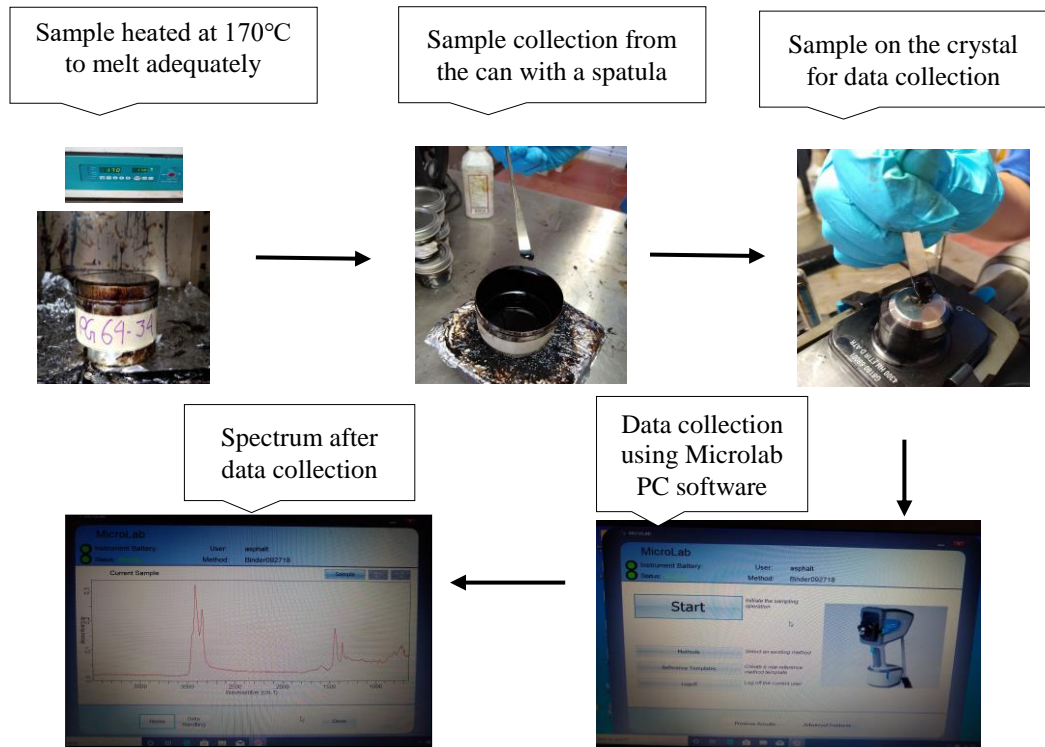


Figure 16. Procedure for FT-IR data collection



FT-IR Data Analysis

Table 6 represents the FT-IR spectra analysis by different authors for understanding the aging of SBS-modified asphalt binder before and after RTFO, PAV, and UV aging. In this study, equation (3) was followed which was proposed by Hossain et al. (2020) to determine the SBS content (%) before and after RTFO and PAV aging. For the calculation of the carbonyl index and sulfoxide index, equation (1) and (2) was followed.

Table 6. Literature on aging determination of SBS-modified binders by FT-IR

Author, year	FT-IR data analysis for aging	
	Wavenumber	Index
Wu et al., [32]	1700 cm ⁻¹ , 1030 cm ⁻¹ , and 968 cm ⁻¹	Carbonyl, butadiene, and sulfoxide.
Xue et al., [68]	1700 cm ⁻¹ and 1031cm ⁻¹	Carbonyl and sulfoxide.
Zhang et al., [14]	1603 cm ⁻¹ , 1458 cm ⁻¹ , 1375 cm ⁻¹ , 1030 cm ⁻¹ , and 966cm ⁻¹	Carbonyl, butadiene, and sulfoxide.
Singh and Kumar, [5]	1700 cm ⁻¹ , 1600 cm ⁻¹ , 1460 cm ⁻¹ , 1370 cm ⁻¹ , 1240 cm ⁻¹ , 1030 cm ⁻¹ , and 968 cm ⁻¹	Aromaticity, Aliphatic, Carbonyl, sulfoxide, trans-butadiene, and trans-acetate.
Zhao et al., [29]	1700cm ⁻¹ , 1030 cm ⁻¹ , and 966 cm ⁻¹	Carbonyl, butadiene, and sulfoxide

$$I_{C=O} = \frac{\text{Peak height at } 1695\text{cm}^{-1}}{\text{Peak height at } 2920\text{cm}^{-1}} \dots\dots\dots(1)$$

$$I_{S=O} = \frac{\text{Peak height at } 1031\text{cm}^{-1}}{\text{Peak height at } 1456\text{cm}^{-1}} \dots\dots\dots(2)$$

Materials and Experimental Plan for Selection of Asphalt Binder Aging Parameter

Effects of Extraction Solvent and Fine Particles

Experimental Variables. Laboratory aging was evaluated in ATR-FTIRS after analyzing various experimental variables, including effect of residual solvent and aggregate intrusion. At first, absorbance spectra of virgin binder samples were collected in the laboratory. After that, a series of laboratory tests were undertaken to evaluate the experimental variables. Table 7 presents the materials and description of samples evaluated in the laboratory.

Development of Simple Binder Extraction Procedure. As mentioned earlier, the effect of different amount of residual extraction solvent, residual aggregate fines and amount was investigated which aided to develop a simple field procedure for sample preparation in ATR-FTIRS. The developed sample preparation procedure allowed obtaining spectra for analyzing without taking consideration of solvent amount and aggregate size. This made the procedure quicker and simpler to be performed in the field for RAP aging analyses.

Table 7. Experimental variables and their corresponding material properties

Experimental Variables	Base Binder PG grade	Materials
Solvent		a. DCM b. N-Propyl Bromide (ASTM 5404-03)
Aggregate size	PG64-22	a. #200 passing b. #200 retain c. #100 retain d. HMA (passing #100)

Development of Sample Preparation Procedure and Collection of Spectra in ATR-FTIRS. For this study, samples were prepared in two stages. At the first stage, solvent induced samples were considered to evaluate the effect of residual solvent in the binder. In this case, DCM was used as a solvent considering its evaporating power and less reactivity [69]. Five samples were prepared with 4% unaged binder and 96% of DCM solvent according to their weight. After a complete dissolution of binder to solvent, immediate spectra were collected by placing 2-3 drops of solution on ATR-FTIRS. For assessing the residual influence, samples were dried at varying time periods using an electric hand dryer (air blower) as shown in Figure 17. After the evaporation of the solvent (27%- 95%) from samples, the effect of residual solvent in spectra was observed.

Figure 17. Dried samples by air blower



In the second stage, aggregate intrusion and size were considered to establish whether the aggregate initiated any effect in absorbance spectra or not. At first, three types of aggregate fines (#200 passing, #200, and #100) were used in this experiment to prepare samples with equal amount of binder for making a homogenous mix. 87%-90% DCM solvent added later to establish a sample like field extraction as shown in Figure 18. The binder, aggregate, and solvent ratio was 1:1:23 in five samples. Spectra were collected in the similar process mentioned above for both immediate samples and samples dried up to 80% of their initial weight. Secondly, an HMA (4.6% binder) sample was prepared in the laboratory and binder was extracted by DCM solvent. The obtained solution was filtered with #100 nylon mesh filter as shown in Figure 19 and spectra were collected in the similar process mentioned above. For the mentioned stages stated above, infrared spectra were collected using a Nicolet IR 100 FTIR spectrometer with a diamond ATR crystal as shown in Figure 20 and 21.

Figure 18. Solution induced with aggregate, binder and DCM solvent



Figure 19. Filtration technique for HMA mix



Figure 20. Nicolet IR 100 FT-IR spectrometer



Figure 21. Diamond crystal

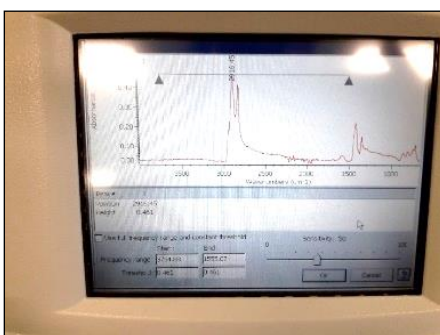


Samples were placed directly on the diamond crystal as shown in Figure 22. Using default software settings (wavenumber range of 4000 to 650 cm^{-1} and resolution of 4 cm^{-1}), 24 scans for each sample were averaged and the resultant spectrum was collected as shown in Figure 23.

Figure 22. Placing sample on crystal



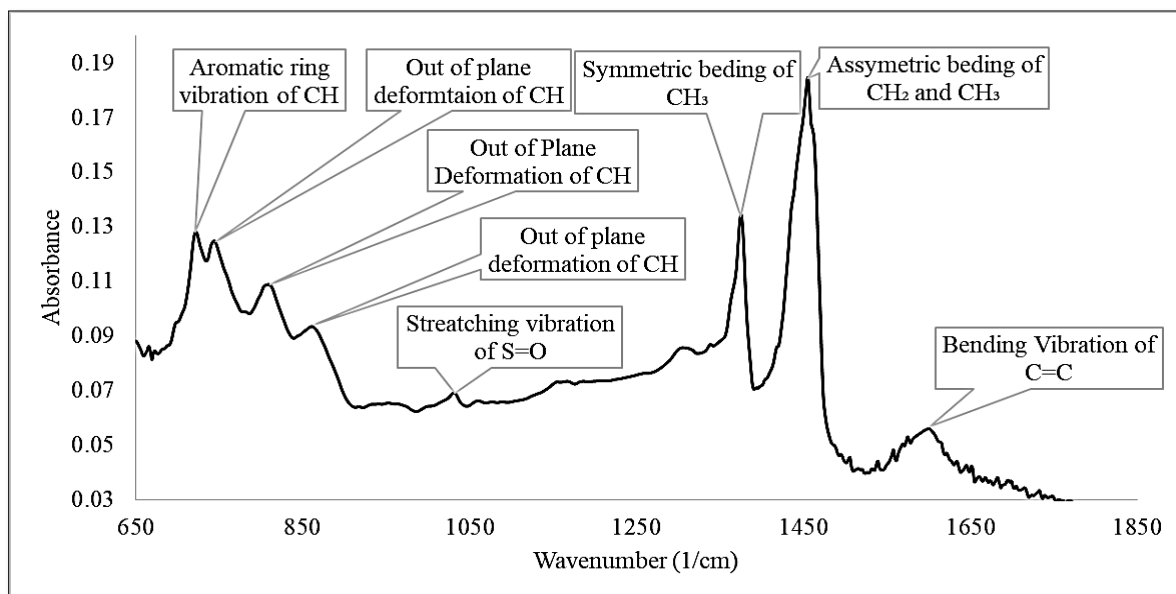
Figure 23. Collected spectra for analysis



Method for Data Analysis: Selection of Appropriate Peak

Qualitative Analysis. In this study, FT-IR spectral interpretation was conducted by both qualitatively and quantitatively. For qualitative analysis, spectra were analyzed in the fingerprint region (650 cm^{-1} - 1800 cm^{-1}) to identify the presence of new functional group added to the asphalt binder and extracted mix due to different aging conditions. In addition, difference between spectra of neat binder and extracted binder from mix was also observed. From qualitative analysis, principal functional groups susceptible to aging were identified. After this identification, quantitative analysis was performed to measure the degree of aging. In this study, peak height ratio was used for quantitative measurement of aging. This measurement was obtained by dividing the peak height of aging susceptible functional group to the height of functional group which is unsusceptible to aging [70]. The height was measured by drawing a baseline considering two lowest points (can be named as valley) on each side of the peak and then added the middle point of the baseline to the top point of the peak.

Figure 24. Characteristic functional groups in fingerprint region in unmodified asphalt binder



From qualitative analysis it was observed that key functional groups in unaged asphalt binder are- asymmetric stretching vibration of CH₂ at 2920 cm⁻¹; symmetric stretching vibration of CH₂ at 2851 cm⁻¹; stretching vibration of C=C at 1600 cm⁻¹; asymmetric bending vibration of CH₂ and CH₃ at 1455 cm⁻¹; symmetric bending vibration of CH₃ at 1375 cm⁻¹; stretching vibration of S=O at 1030 cm⁻¹; out-of-plane deformation of CH at 870 cm⁻¹, 817 cm⁻¹, and 745 cm⁻¹; and aromatic ring vibration of CH at 721 cm⁻¹ as shown in Figure 24. After aging it was observed that absorbance of C=O functional group at 1695 cm⁻¹ became intense in asphalt binder as well as in asphalt mixture. In addition, increase in peak intensity of S=O functional group at 1030 cm⁻¹ was also observed in aged binder and mix samples.

Quantitative Analysis. After qualitative analysis, quantitative analysis was performed by measuring the peak heights of C=O and S=O functional group at 1695 cm⁻¹ and 1030 cm⁻¹ and divided them with the height of asymmetric stretching vibration of CH₂ at 2920 cm⁻¹ which was considered unsusceptible to aging. This quantification process for C=O and S=O functional groups were symbolized as carbonyl index (I_{CO}) and sulfoxide index (I_{SO}). For measuring peak height, baseline was drawn by connecting the valleys on both sides of the peak. It was observed that the location of the valleys remained unchanged irrespective to the binder type or intensity of aging. Baseline for C=O functional group vibration of CH₂ and CH₃ groups extended from the wavenumber 1684 to 1718 cm⁻¹ and

1394 to 1487 cm^{-1} , respectively. For S=O and asymmetric stretching vibration of CH_2 , the limits of the base lines were 978 cm^{-1} to 1080 cm^{-1} and 2753 to 2995 cm^{-1} , respectively.

Peak Height Ratio Process. Table 8 contains the values as well as the coefficient of variation (CV) of peak height at six different wavenumbers (cm^{-1}). This table is produced using PG64-22 (NC) binder of different aging levels using all four aging methods. Except at wavenumber 1695 cm^{-1} , peak height remains unaffected by aging conditions as expected. Similar type of table can be prepared for other binders too. The CV% provides the measure of repeatability of the data collection procedure. Each data point in the table is the average of 10 individual spectra collected from at least three different locations of the specimen container.

Table 8. Average peak height at different wavenumbers from absorbance spectra of PG 64-22 (NC) binder after different laboratory aging methods

Aged Samples	1375		1455		1600		1695		2851		2920	
	Avg.	CV%										
Unaged-Binder	0.057	1	0.125	1	0.016	8	0.005	12	0.207	2	0.288	2
2hr-RTFO	0.056	1	0.125	1	0.017	3	0.006	10	0.208	2	0.289	2
16hr-RTFO	0.054	2	0.123	2	0.019	3	0.010	8	0.203	2	0.282	2
1-PAV	0.055	2	0.125	1	0.017	3	0.008	7	0.205	1	0.286	1
4-PAV	0.053	4	0.120	4	0.018	6	0.010	9	0.198	5	0.272	5
Unaged-Mix	0.057	2	0.126	1	0.017	4	0.005	7	0.210	2	0.293	1
2hr-at 135C	0.057	1	0.126	1	0.016	2	0.005	11	0.207	1	0.289	1
24hr-at 135C	0.056	1	0.125	1	0.017	2	0.008	7	0.205	1	0.285	1
1day-at 85C	0.057	0	0.126	0	0.017	2	0.006	8	0.209	0	0.291	0
5day-at 85C	0.055	1	0.124	1	0.019	3	0.011	6	0.205	1	0.284	1

Effect of Sulfoxide Index

Materials. In this study, eight unmodified/neat binders of four different performance grades and from four different sources were used to investigate if the aging indices are dependent of binder grades or sources. The binders are named by the grade followed by the location where it came from. The names of the binder are provided in the Table 7. Hot mix asphalt was produced in the lab using ½ inch NMS aggregate following the SUPERPAVE aggregate gradation requirement. The design asphalt content was found to be 4.6%.

Experimental Plan. ATR-FTIR spectra of binder and extracted mix were recorded in the laboratory. Different binders were subjected to standard and extended RTFO aging and PAV aging and afterward the absorbance spectra were collected for analysis. Similar spectra were obtained for laboratory aged mix also. Table 9 describes the different types of aging methods applied for binder and mix aging in this study.

Table 9. Laboratory aging plan for the study

Materials	Aging Method	Duration (hours)	Binder Types
Binder	Unaged		Additional: PG58-28(LA), PG64-22(LA), PG67-22(MS) PG52-34(LA), PG58-28 (TX), PG64-22(MS, NC), PG67-22(TX)
	RTFO	1,2,4,8,6,24	
	PAV	20,40,60,80	
Mix	Unaged		PG52-34 (LA), PG58-28 (TX) PG64-22 (NC)
	STOA	2,4,12,24	
	LTOA	24, 72, 120	

Laboratory Aging of Binder and Mixture. Binders were aged using RTFO and PAV whereas, the mixture was aged in forced draft oven. RTFO aging was performed at 163°C and PAV aging was performed at 100°C under 2.1 MPa pressure. Duration for RTFO and PAV aging are provided in the Table 1. Loose mixes were subjected to short-term oven aging (STOA) as well as long-term oven aging (LTOA). Temperature for STOA and LTOA were selected as 135°C and 85°C respectively and duration of mixture aging is given in Table 1. Binder from mixture was extracted using dichloromethane (DCM). For the extraction process 100 grams of loose mix and 100 milliliters of DCM was required for each mix sample. Whole extraction process can be performed in the lab or field within 15 minutes by one person having minimal laboratory support.

Method of FT-IR Data Analysis. Agilent 4300 handheld FT-IR was used for the spectroscopy. A single reflection diamond ATR (Attenuated Total Reflectance) sample interface was used for data collection. Each spectrum was collected in the spectral region of 600 cm⁻¹ to 4000 cm⁻¹ at 4 cm⁻¹ resolution by the default Microlab Mobile software equipped with the instrument and reported as an average of 24 spectra.

Quantitative analysis was performed by measuring the peak heights of C=O and S=O functional group at 1695 cm⁻¹ and 1030 cm⁻¹ respectively. The corresponding peak height

was then divided by the height of asymmetric stretching vibration of CH₂ at 2920 cm⁻¹ which was considered unsusceptible to aging [71]. This quantification process for C=O and S=O functional groups were symbolized as carbonyl index (I_{CO}) and sulfoxide index (I_{SO}). For measuring peak height, baseline was drawn by connecting the valleys on both sides of the peak. It was observed that the location of the valleys remained unchanged irrespective of the binder type or intensity of aging. Baseline for C=O functional group was extended from the wavenumber 1684 to 1718 cm⁻¹. For S=O and asymmetric stretching vibration of CH₂, the limits of the base lines were 978 to 1080 cm⁻¹ and 2753 to 2995 cm⁻¹ respectively.

Materials and Experimental Plan for Effect of Laboratory Binder and Mix Aging

Materials

To understand the aging mechanism at equal stiffness of asphalt binder after RTFO, PAV, UV, and oven aging, a neat unmodified PG 64-22 asphalt binder was selected to conduct the RTFO, PAV, UV, and forced draft oven aging. Eight neat/unmodified binders of different performance grade obtained from various sources were used to visualize if their aging indices are different or not in unaged condition. These binders are- PG52-34 (LA), PG58-28 (MS, TX), PG64-22 (LA, MS, and NC), and PG67-22 (MS and TX). Hot mix asphalt having ½ inch nominal maximum size of granite aggregate with 4.6% asphalt content was used to investigate the mix aging.

Experimental Plan

Different degrees of RTFO and PAV aging was performed to simulate the extreme aging of asphalt binder at similar stiffness. RTFO aging was performed by following the AASHTO T240 standard. PAV aging was performed by following the AASHTO R28 standard except performing RTFO aging before placing the binder in the PAV chamber. Table 10 represents the experimental plan for the data collection and result analysis.

ATR-FTIR spectra of binder and extracted mix were recorded in the laboratory and in the plant/field. Different binders were subjected to standard and extended RTFO aging and PAV aging and absorbance spectra were collected for analysis. Similar spectra were obtained for laboratory aged mix also.

Laboratory Aging of Binder and Mixture

Laboratory aging of binder was conducted by using two accelerated aging methods: RTFO (AASHTO T240) and PAV (AASHTO R28). For RTFO aging procedure, samples were kept at 163°C for 1 hour to 24 hours and sample were collected at different interval. For PAV aging procedure, unaged binder samples were kept at 100 °C under 2.1 MPa pressure for 20, 40, 60, and 80 hours which is referred as 1-PAV, 2-PAV, 3-PAV, and 4-PAV respectively in further discussion in this paper.

Loose mix was aged in forced draft oven in the lab at two different temperatures. According to NCAT recommendation, one aging temperature was selected as 135°C which is also recommended by AASHTO R30 for short-term aging [72]. Mix was aged up to 24 hours at 135°C and samples were collected after 2, 4, 12, and 24 hours. Another set of mix was aged at 85°C up to five days and samples were collected after 1, 3, and 5 days. Oven aged mix was then extracted using the quick extraction method developed in this study and the binder residue was used for data collection in FT-IR.

Table 10. Experimental plan for data collection and result analysis

Binder Type	Binder Condition	Aging Duration	Test	
PG64-22 (original unmodified binder)	Original		DSR (Rheology test) and RT- IRS (Chemical test)	
	RTFO Aging	1RTFO		1h 25 min
		2RTFO		2h 50 min
		3RTFO		4h 15 min
		4RTFO		5h 40 min
		6RTFO		8h 30 min
		PAV Aging (W/O RTFO)		1PAV
		2PAV		40hr
		3PAV		60hr
	UV aging (W/O RTFO)	24hr, 36hr, 48hr and 60hr		
	Forced draft oven aging (W/O RTFO)	24hr, 36hr, 48hr and 60hr		

UV and Oven Aging Simulation Test in Laboratory

2g of binder was taken in a small can and mixed with dichloromethane (DCM) to make the binder enough liquid to spread on a 14.1 cm circular PAV plate uniformly. The UV

chamber reached at a constant temperature of 70°C after about 45 minutes. The PAV plate with asphalt binder and DCM solvent was kept under the hood for drying. The dried PAV plate was placed inside the UV chamber when the UV chamber had reached at 70°C as shown in Figure 25. Similarly, dried PAV plate was placed inside the forced draft oven at 70°C as shown in Figure 26. The thickness of the asphalt binder film was calculated to be 32 μ , and intensity of the UV aging chamber was 100mW/m².

Figure 25. UV aging of PG 64-22 binder



Figure 26. Oven aging of PG 64-22 binder



Figure 27. Sample placed over the FT-IR for data collection



FT-IR Data Collection and Analysis

No separate sample preparation method was required to collect the FT-IR spectrum. Sample was directly placed with a spatula over the FT-IR crystal as shown in Figure 27. For data collection, unmodified binders were heated at 163°C. A total of 10 spectra were collected for each of the binders. Data analysis for unmodified binders were performed as the process mentioned in the section “Aging Parameter Selection.”

Materials and Experimental Plan for RAP Content Determination

Materials

RAP from 10 different sources were collected from RAP piles in mixing plants and from milling sites to characterize the RAP content. Age of those RAP varies from roughly 3 to 20 years. Plant visits were made to two different places in Louisiana to collect data with a vision to implement the quality control procedure using the handheld FT-IR spectrometer. All those plants were producing hot mix asphalt containing 15% RAP using a PG 67-22 binder. DCM procured from Sigma-Aldrich was used to perform the quick extraction procedure in the field to collect binder residue from RAP as well as from the fresh mix.

To determine the RAP content, ten different types of asphalt mix were collected from five plants in northern Louisiana, USA. Three to five samples for each mix were collected at certain time interval and a total of 10 different mixes were collected. The liquid binder was collected from the binder tank and RAP was collected from the RAP pile for each of the ten mixes.

Experimental Plan

RAP from ten different sources were analyzed to investigate the extent of aging. Finally, FT-IR spectra were collected in the plant during the production phase. Unaged binder from tank, RAP from the pile before mixing and fresh mix were collected to record the spectra to predict the RAP present in the mix as a measure of quality control. Besides the FT-IR testing plan, DSR tests were also performed on unaged and PAV aged PG58-28 (TX), PG64-22 (NC), and PG67-22 (TX) binders to determine the stiffness/ high temperature grade. RAP from five different sources were extracted and recovered to find the high temperature grade which was then compared with PAV aged binder. Figure 28 is the ATR FT-IR spectra collection plan for the study.

The ATR-FTIRS was performed on the unaged binder, binder residue obtained from the RAP and mix samples FT-IR spectra were recorded in the plants in Northern LA, USA. Binder residues were prepared by quick extraction process and the FT-IR spectra were recorded. A total of 10 mixes were used for this study and three to five samples for each mix were tested. The result provided here is the average of ten spectra for each sample.

Binder Aging

Laboratory aging of binder was conducted by using two accelerated aging methods: RTFO (AASHTO T240) and PAV (AASHTO R28). For RTFO aging procedure, samples were kept at 163°C for 1 hour to 24 hours and sample were collected at different interval. For PAV aging procedure, unaged binder samples were kept at 100 °C under 2.1 MPa pressure for 20, 40, 60 and 80 hours which is referred as 1-PAV, 2-PAV, 3-PAV, and 4-PAV respectively.

Mix Aging

Loose mix was aged in forced draft oven in the lab at two different temperatures. According to NCAT recommendation, one aging temperature was selected as 135°C which is also recommended by AASHTO R30 for short-term aging [73]. Mix was aged up to 24 hours at 135°C and samples were collected after 2, 4, 12, and 24 hours. Another set of mix was aged at 85°C up to five days and samples were collected after 1, 3, and 5 days. Oven aged mix was then extracted using the quick extraction method developed in this study and the binder residue was used for data collection in FT-IR.

Dynamic Shear Rheometer (DSR) Test on Extracted Binder

PAV aged and extracted binders from RAP were tested in DSR following the AASHTO T315 to determine the complex modulus. Binder from RAP was extracted and recovered following the ASTM D2172 and ASTM D5404 respectively. Ensolvex (nPB) was used as the extraction solvent in this part of the study. DSR tests were performed using 25 mm parallel plate geometry at 10 rad/sec angular frequency and 12% strain rate. Those parameters were selected because the target of the test was to determine the temperature at which the $G^*/\sin\delta$ value equals 1.0 kPa. Each sample was tested at least at three different temperatures at a 6°C temperature interval. The test temperature was chosen in such a way that the temperature corresponding to $G^*/\sin\delta$ value of 1.00 kPa could be determined directly from the plot.

Quick Extraction Process of Asphalt Mixture in the Field

A quick extraction method is developed in this study which can be implemented in the field in less than 15 minutes with minimal supplies and effort. A hot asphalt mix sample was collected and was allowed to cool (Figure 29a). Approximately 100 grams of loose asphalt mix was taken in a 16-oz mason jar (Figure 29b). Then around 100 milliliter of DCM was poured into the jar (Figure 29c). Proper care should be taken to make sure that the mix is air cooled so that the DCM does not get evaporated as soon as it comes in contact with the mix. The jar was then shaken moderately and left for 5 minutes with closed lid. The solvent with dissolved asphalt was then filtered through an 80-micron nylon mesh filter and the liquid was collected in a metal pan with large surface area (Figure 29d).

In this case a standard PAV pan with 5-inch diameter was used. It is not necessary to drain the whole liquid as very small amount of binder residue is required for FT-IR analysis. The pan with few millimeters depth of liquid was left in an open place for 10 minutes while all the DCM evaporated (Figure 29e). The binder residue was then collected using a metal spatula and placed on the FT-IR crystal for spectra collection (Figure 29f). Figure 29 shows the step by step procedure that was followed in the field for quick extraction of plant mix. RAP was also extracted by following the same procedure.

Different Calculation Method of Carbonyl Index

Different amount of RAP was added in the laboratory and carbonyl index was calculated in six different methods. Carbonyl index can be calculated considering the peak height or area under the curve at wavenumber 1696 cm^{-1} . The change in the carbonyl index with the change of added RAP is shown in Figure 30. It is expected that the index will vary linearly with the addition of RAP. Carbonyl Index corresponding to 0% and 100% RAP are connected by a straight line. The indices at intermediate RAP content are shown in the figure. Considering the straight line as predicted index, root mean square error is calculated using the equation:

$$RMSE = \sqrt{\frac{\sum[(Predicted - Measured)^2]}{\text{Number of data points}}}$$

The RMSE is then normalized by dividing it by the carbonyl index of the mix with zero percent RAP. This normalized RMSE is presented as percent in each figure. From the Figure 30(f) it can be observed that normalized RMSE for the area ratio at 1696 cm^{-1} to 1456 cm^{-1} yields the lowest error. Although the area ratio at 1696 cm^{-1} to 1601 cm^{-1} also yields the same value, this ratio is not considered for further calculation as the previous one predicts more closely at lower RAP content. For quantification of RAP content in the mix, the area ratio at 1696 cm^{-1} to 1456 cm^{-1} is considered in the later sections.

Figure 28. Detailed experimental plan for the study

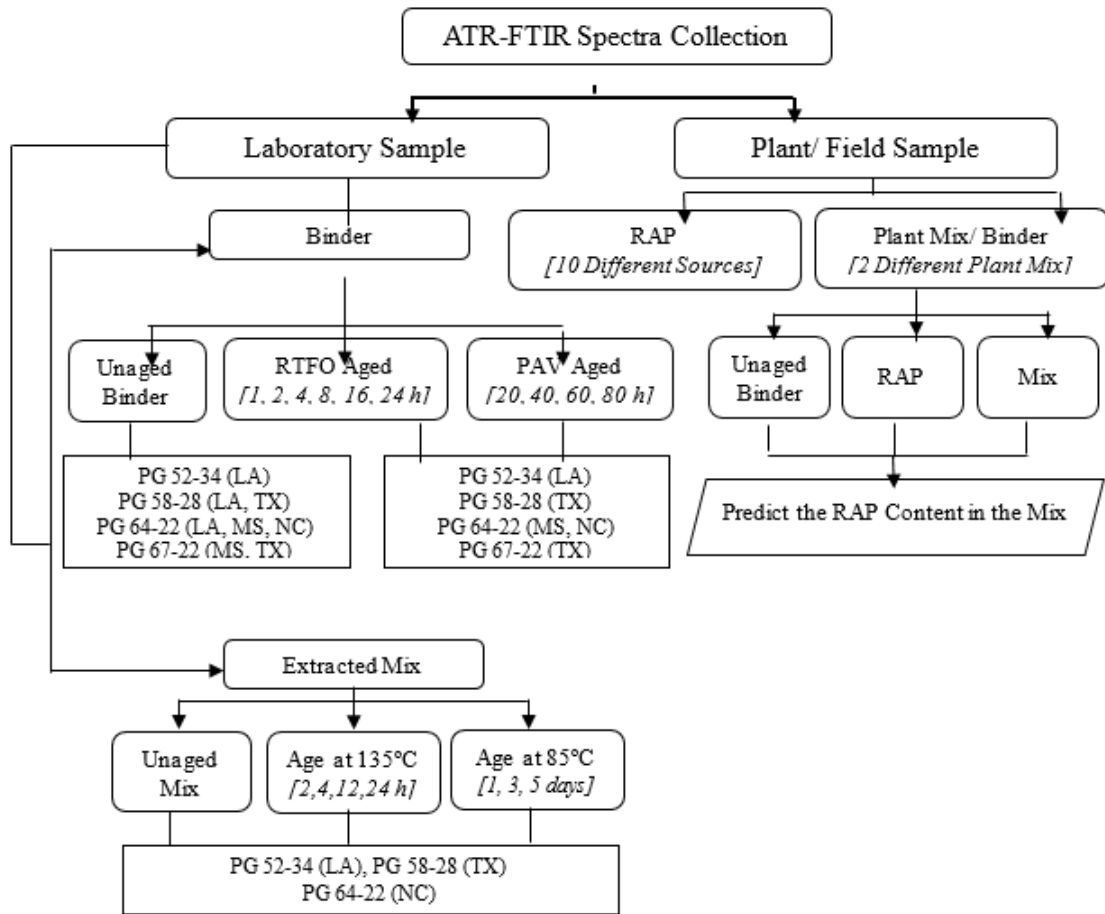


Figure 29. Quick extraction process of asphalt mixture implemented in the field: (a) HMA collection from the truck, (b) pouring loose HMA in the mason jar, (c) use of DCM to extract the binder from mix, (d) the solvent is being filtered, (e) DCM is being evaporated quickly and the asphalt residue is left on the pan, (f) asphalt binder is placed on the FT-IR crystal to collect the spectra

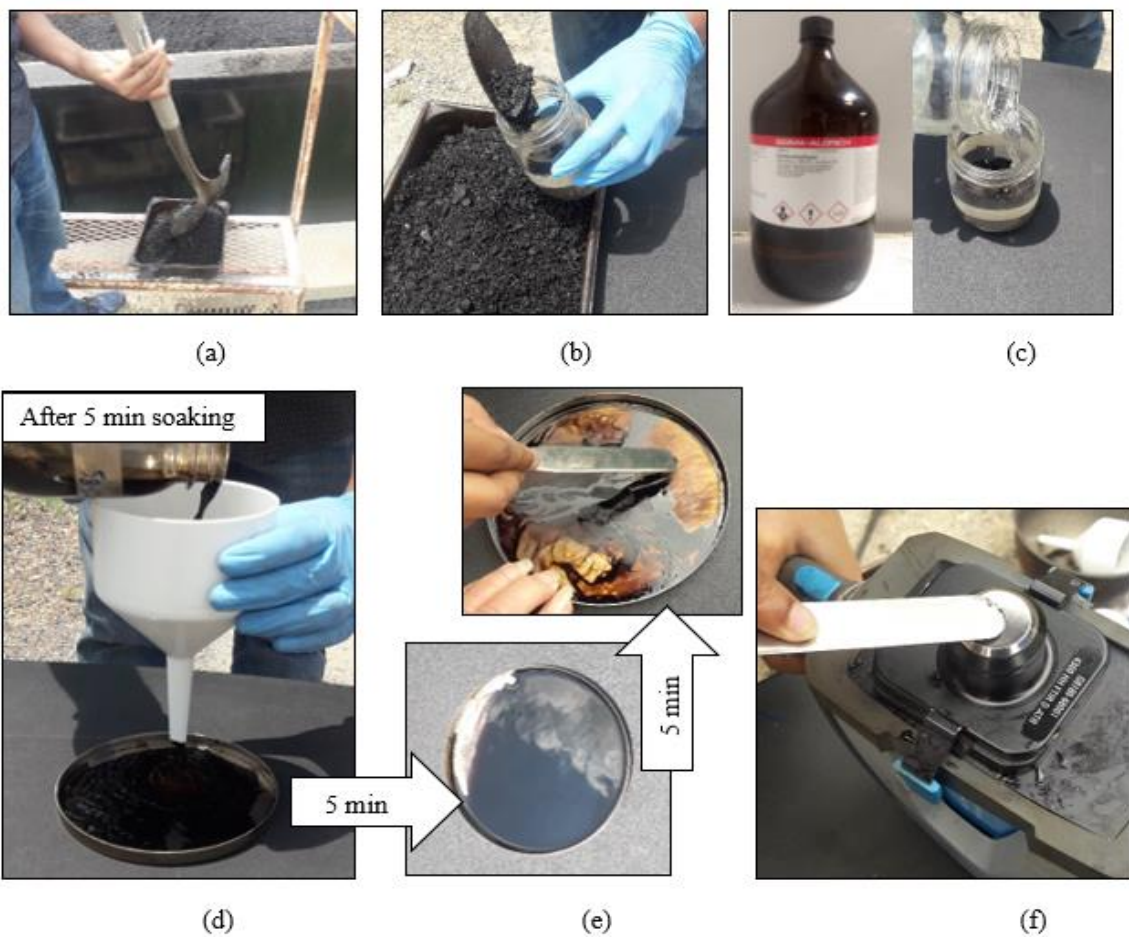
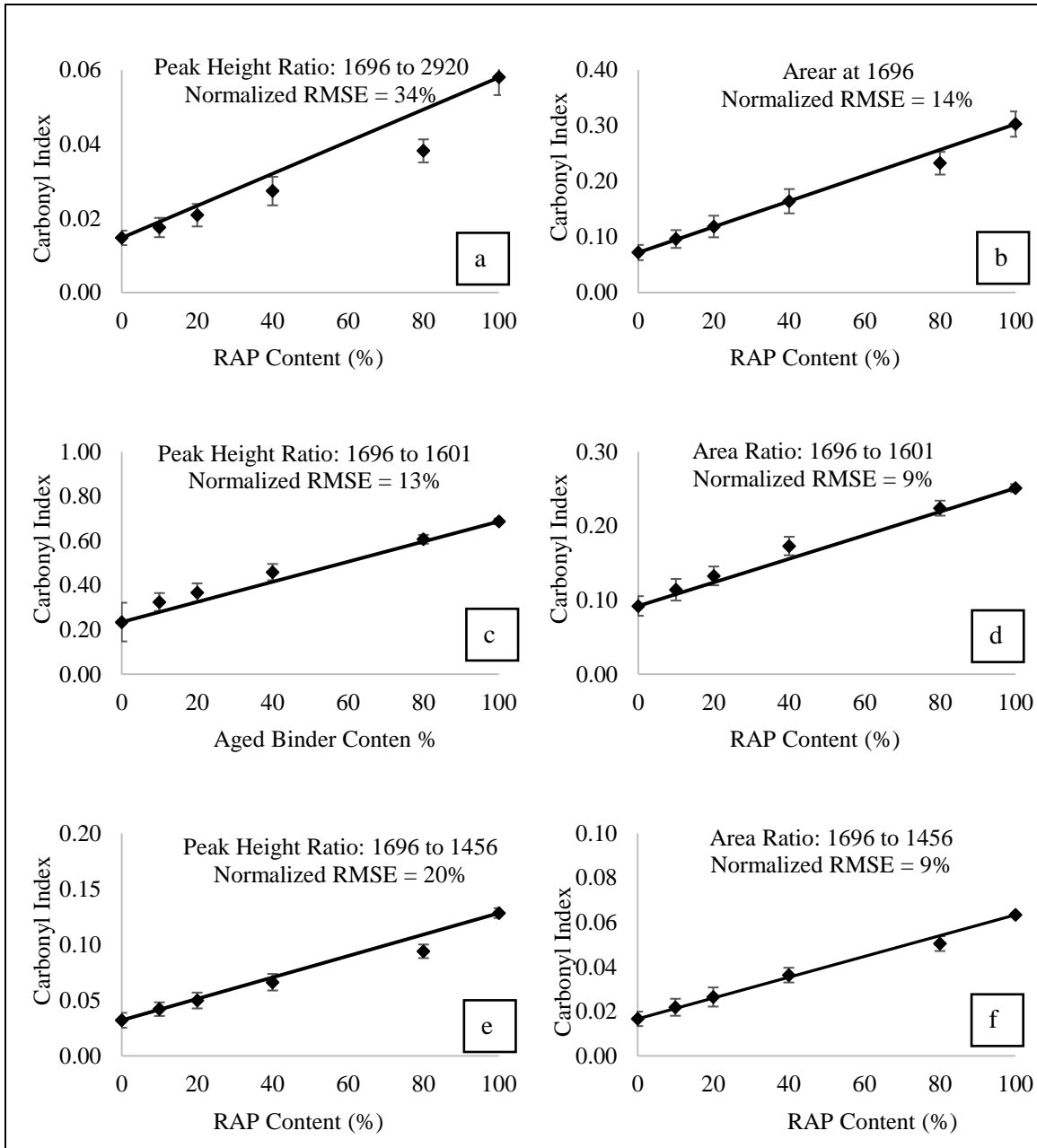


Figure 30. Change in carbonyl index for various amount of RAP addition. Indices are calculated in six different methods and normalized root mean square error are provided for each method



Materials and Experimental Plan for Identification and Quantification of Rejuvenators

Materials

PG58-28 binder was used as a base binder. Commercially available plant-based rejuvenator was used as a bio rejuvenator, whereas petroleum extracted residual oil was used as an aromatic rejuvenator. Properties of the rejuvenators used in this study are listed in Table 11. SBS polymer was used for the modification of the base binder in which styrene-butadiene ratio was 31/69. The polymer structure was radial and was provided in powder form from the manufacturer. RAP aggregate was collected from the construction plant stockpile. After collection, proper sieving was conducted to find the nominal size of RAP aggregate to carry out the extraction of RAP binder.

Table 11. Material properties of bio and aromatic rejuvenators

Property	Bio-Rejuvenator	Aromatic Rejuvenator
Appearance, 77 °F (25 °C)	Dark-Colored Liquid	Dark-Colored Liquid
Odor	Mild Hydrocarbon	Slight
Density, 77 °F (25 °C)	7.6 lb/gal	8.0 lb/gal
Viscosity	100 cP; 77 °F (25 °C)	4.29 cm ² /s; 140°F (60°C) [ASTM D445]

Preparation of the RAP Binder

RAP binder was extracted and collected using standard test method for quantitative extraction of bitumen from bituminous paving mixtures (ASTM D2172-05) and standard practice for recovery of asphalt from solution using the rotary evaporator (ASTM D5404-03). Nominal maximum size of the RAP aggregate was ½ inch and 1500gm RAP aggregated was used for obtaining extracted RAP binder.

Preparation of the Rejuvenated Asphalt Binder

Both bio and aromatic rejuvenator was added with the base binder, polymer modified binder, base binder with 20% RAP binder, and polymer modified binder with 20% RAP binder. In these four cases, the dosage of the bio rejuvenator was kept at 5% and 15%, whereas aromatic rejuvenator was maintained at 15% and 35%. Rejuvenated asphalt binder with polymer and RAP binder was prepared as follows:

- At first, 50 gm of base binder was poured in an 8 oz. tin can and heated on hotplate at 100°C for 15 minutes.
- When it became soft, rejuvenator was added to the base binder according to its weight.
- Preparation of polymer modified rejuvenated asphalt followed the same procedure as adopted for base binder.
- For preparing RAP binder induced rejuvenated samples, 10 gm of RAP binder was added to 40 gm of base binder. After that, rejuvenator was added in the same way as before.

Analysis Methods

Both qualitative and quantitative analysis were performed to visualize the effect of rejuvenator modification.

- For qualitative analysis, rejuvenator modified spectra was compared with the standard spectra without rejuvenator modification to identify the presence of unknown substance due to modification. This unknown substance was categorized as characteristic functional group of the sample.
- After that, a linear relationship was established based on the absorbance intensity and concentration of the rejuvenator. The absorbance intensity was analyzed by three methods: absorbance value, and absorbance height, and absorbance area.
- For absorbance value, a universal curve was produced with the absorbance value at the characteristic wavenumber without any pretreatment of the spectra. It is considered as the simplest method to visualize the linear relationship but highly affected by the shift of the baseline [2].
- After that, absorbance height and absorbance area of the characteristic band were calculated. In both cases, a baseline was drawn considering two lowest bands on both side of the definite absorbance band.
- For absorbance height determination, the top point and middle point of the baseline was added, and peak height was calculated (Figure 31). Absorbance area was calculated using trapezoidal rule. Region of the definite absorbance band was considered as a function of trapezoid and the total area under the band was calculated from the x-axis.
- After that, area under the baseline was calculated and subtracted from the whole area which gave the interested area under the absorbance band (Figure 32).

Figure 31. Absorbance height measurement of FT-IR spectra

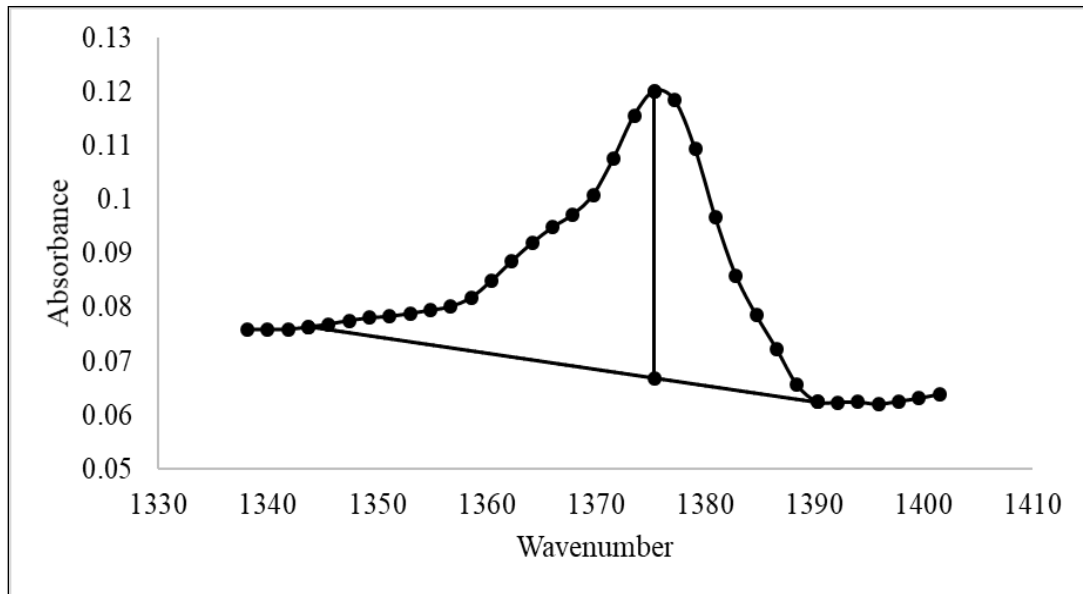
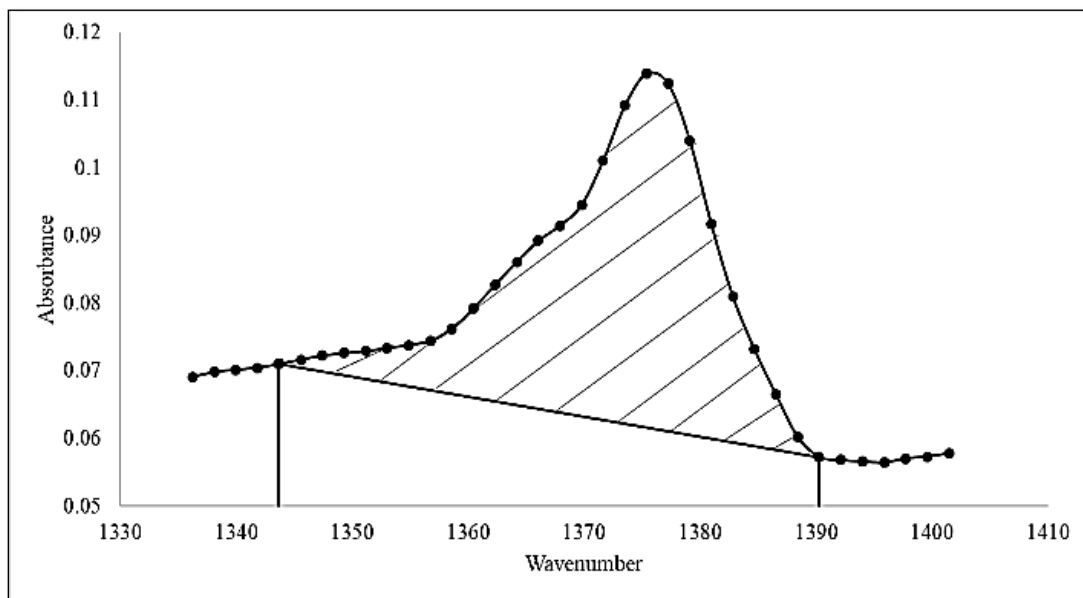


Figure 32. Absorbance area measurement of FT-IR spectra



Discussion of Results

Quantification of SBS Content

Qualitative Analysis

Effect of SBS modification in asphalt binder was analyzed qualitatively at first by studying FT-IR spectra of unmodified and modified asphalt binders respectively. This analysis was done by overlapping both spectra and categorizing inclusion of any unknown functional group in the fingerprint region of $650\text{-}1800\text{ cm}^{-1}$. Figure 22 shows the characteristic functional groups present in the fingerprint region of an unmodified asphalt binder. These functional groups were persistent in all the unmodified base binders used in this study. From this, it can be inferred that functional groups in FT-IR spectra of all unmodified base binders remained identical even though their performance grade (PG) were different.

However, when base binders were modified by SBS copolymers, two additional functional groups were added (a) out-of-plane (wagging) vibrations of the CH groups at 965 cm^{-1} which was accountable for polybutadiene block, and (b) out-of-plane bending of the CH groups in the aromatic ring at 699 cm^{-1} for polystyrene block [74]. No additional functional groups were added due to the difference in SBS polymer structure and presence of sulfur as a cross-linking agent. Besides, peak positions and peak shapes of these functional groups were also unaffected by these changes in material. In this study, only polybutadiene functional group was considered for developing the first order linear curves from laboratory prepared samples and quantifying SBS percentage in the field samples, since polybutadiene functional group was more correlated with SBS content compared to polystyrene functional group [12, 75]. Figure 6 showed the increasing pattern in absorbance intensity of the FT-IR spectra at wavenumber 965 cm^{-1} due to the addition of different percentage of SBS in asphalt binder.

Quantitative Analysis for Linear Regression

In this study, a total of 48 calibration curves were developed in view of two analysis methods- peak height and peak area considering all contributing factors such as difference in SBS polymer structure, presence of sulfur as cross-linking agent, base

binder performance grades, base binder sources, different batch mixing and different days' data collection from same batch mixed samples.

For the peak height method, height of the polybutadiene block was measured from the baseline drawn in the range of 984 cm^{-1} to 924 cm^{-1} . This baseline range was kept constant in measuring absorbance area also. Figure 6 shows the baseline selection and position of the polybutadiene functional group in the specified wavenumber region. It was also noticeable that intensity of the polybutadiene functional group increased with respect to SBS percentages. Using these two analysis methods, absorbance heights and areas of the polybutadiene copolymer at wavenumber 965 cm^{-1} for different percentage of SBS (0%, 1%, 2%, 3%, and 4%) was measured and for each case subsequent standard curve was developed. Table 12 showed the slope, intercept and R^2 for the standard curves for each case. Figure 33 shows the standard curves with slope, intercept, and R^2 value.

However, for unmodified samples (0% SBS), negligible peak height and area was encountered due to the scattering effect of the IR beam and no pretreatment of the raw spectra were conducted [76]. Preprocessing techniques were not applied since the proposed method was intended to apply for in-situ data measurement. In both analysis methods, average R^2 was 0.97 for all different 24 cases which indicated that the correlation between variables (peak height or peak area vs. concentration) are highly linear.

Results also showed that coefficient of variation (CV) among the slopes were 12% in absorbance height method and 11% in absorbance area methods. It indicated that the standard deviation among the slopes in both analysis methods were 12% and 11% of the average slope values, supporting the fact that slopes in both analysis methods did not vary significantly due to binder performance grades, base binder sources, SBS polymer structure, different days' data collection, different batch mixing in the sample procedure, and presence of crosslinking agents (0.5% Sulfur). In addition, standard deviation error bars were also produced for both analysis methods to find if there is any significant difference among individual dataset. Figures 34, 35, 36, 37, 38, and 39 show the standard deviation error bars in calibration curves as well as individual values for peak height measurement. The standard deviation error bars indicated that height of the polybutadiene copolymer was unaffected by the conditions stated above.

Table 12. Slope, intercept, and correlation among dataset for SBS quantification in 24 cases for absorbance height and area method

Groups	Absorbance Height			Absorbance Area		
	Slope	Intercept	R ²	Slope	Intercept	R ²
Case1	0.0041	-0.0032	0.99	0.0659	-0.0123	0.99
Case2	0.0034	-0.0014	0.97	0.0504	0.026	0.96
Case3	0.0042	-0.0023	0.99	0.0663	0.004	0.99
Case4	0.0031	0.0002	0.95	0.0494	0.0575	0.97
Case5	0.0035	-0.0005	0.97	0.0561	0.0445	0.97
Case6	0.0052	-0.0035	0.96	0.0796	0.0055	0.96
Case7	0.004	-0.0011	0.98	0.0643	0.0388	0.96
Case8	0.003	-0.0004	0.94	0.0521	0.0358	0.95
Case9	0.0043	-0.0023	0.96	0.0702	0.0041	0.96
Case10	0.0038	-0.0016	0.97	0.0562	0.0457	0.96
Case11	0.0036	-0.0007	0.96	0.0579	0.042	0.97
Case12	0.0038	-0.0017	0.94	0.061	0.0254	0.95
Case13	0.0036	-0.002	0.94	0.059	0.0197	0.95
Case14	0.0034	-0.0007	0.98	0.0557	0.0312	0.98
Case15	0.0034	0.0001	0.95	0.0551	0.0473	0.94
Case16	0.0038	-0.0013	0.99	0.0603	0.0291	0.99
Case17	0.0035	-0.0009	0.97	0.0581	0.0336	0.98
Case18	0.0037	-0.0013	0.99	0.0579	0.0389	0.99
Case19	0.0038	-0.001	0.99	0.0613	0.0358	0.99
Case20	0.0035	-0.0003	0.98	0.0547	0.0554	0.98
Case21	0.004	-0.0012	0.99	0.0609	0.0411	0.98
Case22	0.0042	-0.0016	1.00	0.0647	0.0369	1.00
Case23	0.0037	-0.0009	0.98	0.058	0.0409	0.98
Case24	0.0042	-0.0023	0.97	0.0661	0.0169	0.97
CV (%)	12	-	-	11	-	-

Since quantitative measurement of polybutadiene height and area were not affected by the mentioned factors and were only governed by the SBS concentration, correlation (Corr.) among these three variables were determined. Figure 39 shows the correlation among these three variables considering all 1175 data points obtained from 24 cases for peak height and peak area measurements individually. From Figure 39, it can be observed that peak height data points showed slightly greater correlation (0.929) with SBS concentration compared to peak area measurements (0.922). It was also observed that 2% and 4% SBS data points contained some outlier values in both analysis methods.

Figure 33. Slope, intercept, and R^2 of the standard curves developed for different scenarios of SBS data collection in FT-IR

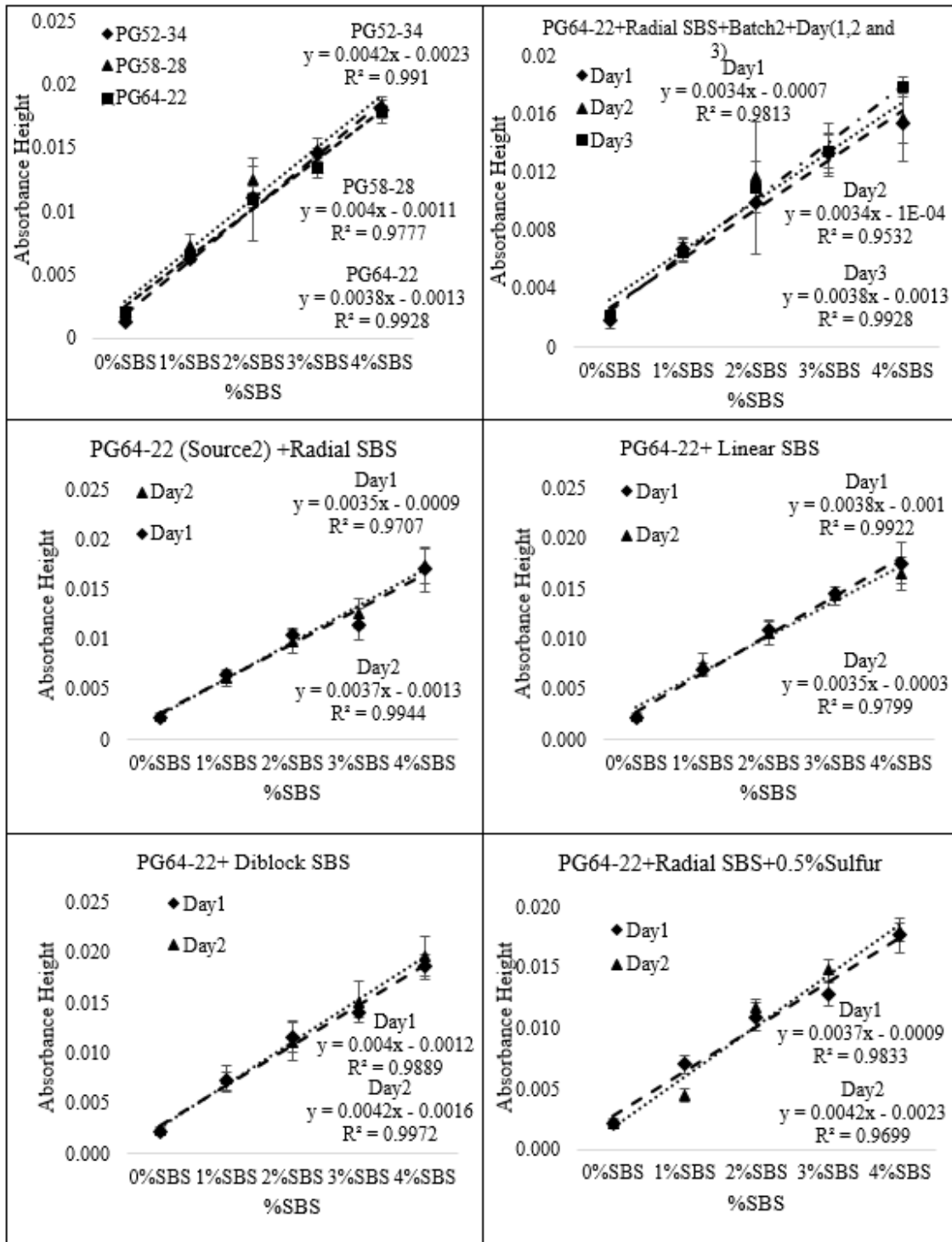


Figure 34. SBS peak height comparison by standard deviation error bars considering different batch mixing in case of preparing SBS-modified binder

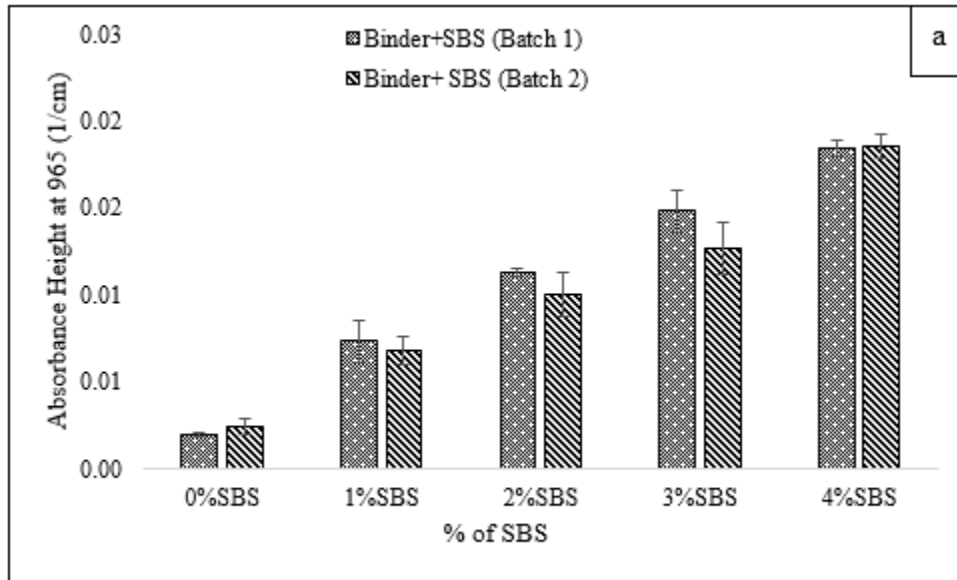


Figure 35. SBS peak height comparison by standard deviation error bars considering base binder from different sources in cases of preparing SBS-modified binder

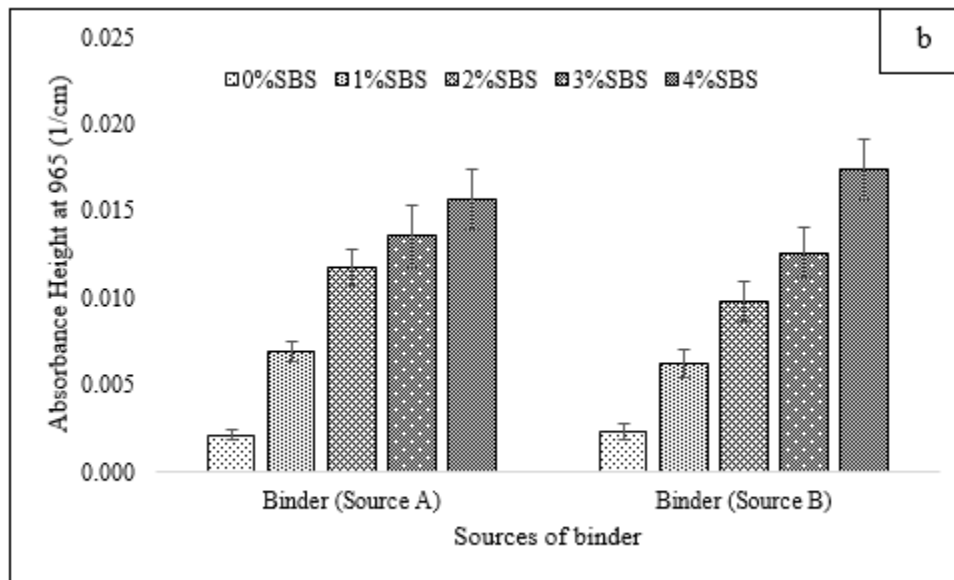


Figure 36. SBS peak height comparison by standard deviation error bars considering different days' data collection in cases of preparing SBS-modified binder

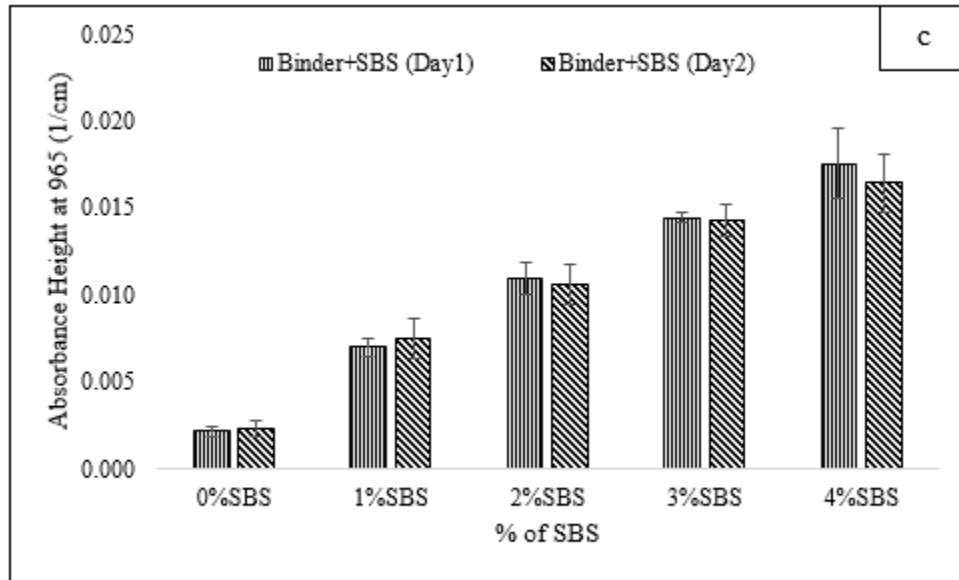


Figure 37. SBS peak height comparison by standard deviation error bars considering different PG grade base binder in cases of preparing SBS-modified binder

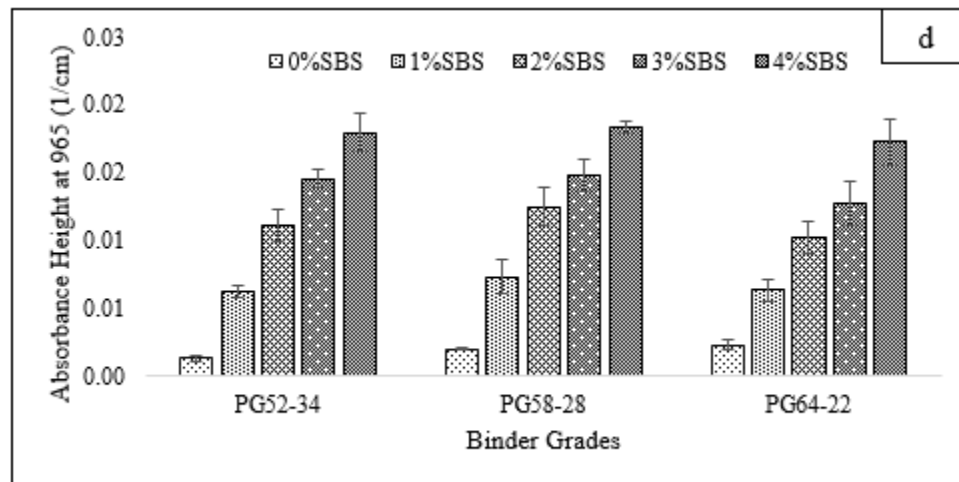


Figure 38. SBS peak height comparison by standard deviation error bars considering effect of SBS polymer structure in cases of preparing SBS-modified binder

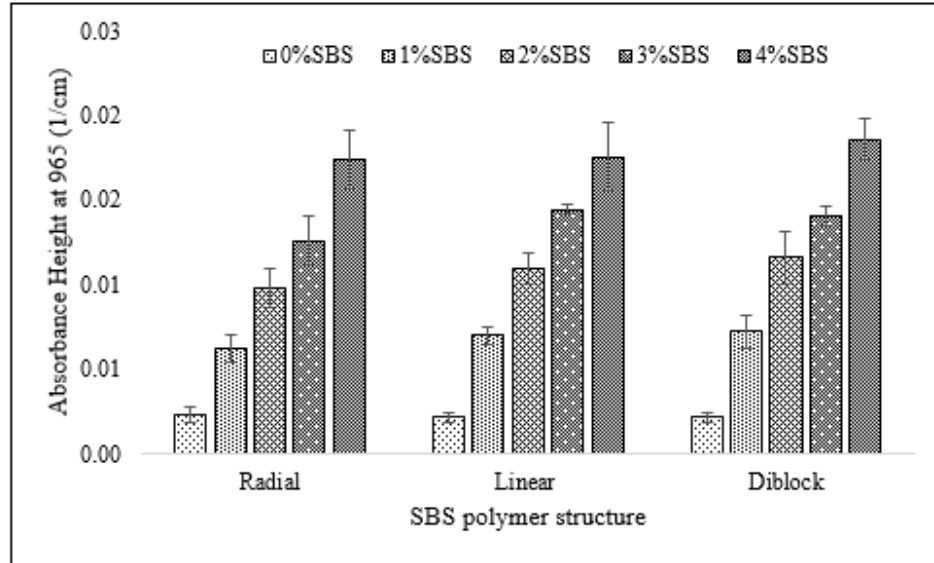
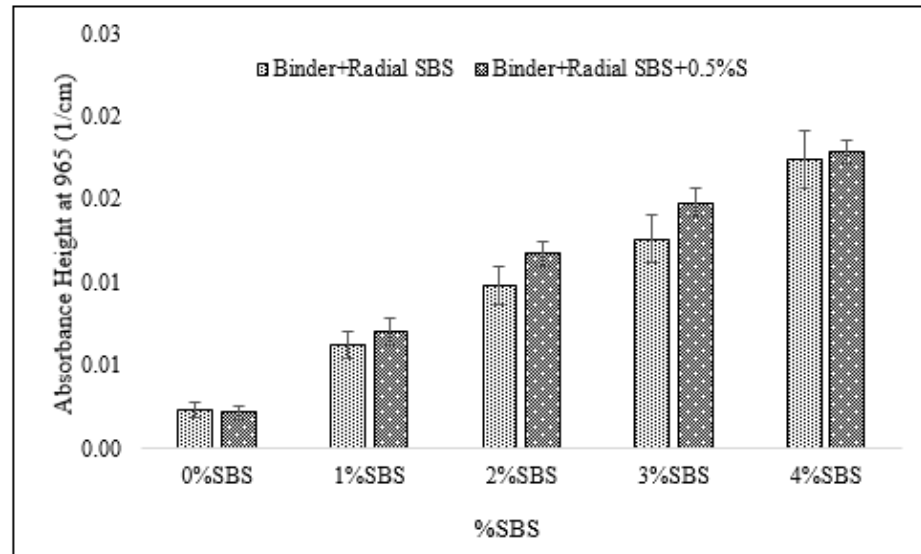


Figure 39. SBS peak height comparison by standard deviation error bars considering effect of cross-linking agents in cases of preparing SBS-modified binder



To remove the outliers, Cook's distance [75] algorithm was applied. In this study, influential points which negatively affected the regression model [77, 78] were selected when the Cook's distance of an observed value was greater than four times of the average Cook's distance. Among 1175 data points, 39 data points were identified as influential

points for the regression model. After deleting these points, the regression model was built again, and their correlation was observed. It was found that, correlation among variables increased significantly which is illustrated in Figure 40 and 41. For peak height data points correlation increased to 0.967, where for peak area measurement correlation was 0.953. Since the correlation between peak height and SBS concentration was higher compared to peak area measurement, final linear regression model was developed based on these two variables. Table 12 showed the parameters of the regression model considering with and without outlier condition. The regression equation found in both cases stated below-

$$\text{With outlier: Peak height at } 965 \text{ cm}^{-1} = 0.003814 * \text{SBS concentration} + 0.002419 \quad (3)$$

$$\text{Without outlier: Peak height at } 965 \text{ cm}^{-1} = 0.003809 * \text{SBS concentration} + 0.002413 \quad (4)$$

From equation (3) and (4), it can be observed that the co-efficient of the regression equations did not change significantly after removing the outlier data points although the correlation between the variables was improved. Comparing other parameters obtained from the developed regression models, it can be observed that standard error (St. Error) which represents the precision of the coefficients reduced significantly after removing the outlier. In addition, t-value increased when the outlier data points were deleted directing to the improvement of the regression model. Pr ($>|t|$) was the same in both cases, lower than 2×10^{-16} , which indicated that the estimations of the coefficients were significant. After that, accuracy of both models was compared based on RSE (residual standard error), multiple R^2 , adjusted R^2 , and F-statistics.

Here, RSE value reduced from 0.0021 to 0.0014 which indicated that regression model developed without outlier was more fitted and provided less prediction error compared to the model developed with outlier data points. Both multiple R^2 and adjusted R^2 increased to 0.93 from 0.86, directing to the fact that regression model developed without outlier can explain more variation in the outcome. In addition, a higher F-statistic and a lower p-value (<0.05) was also observed in the regression model developed without outliers. The developed model is a highly significant prediction model and the prediction from this model will not be interpreted as a coincidental event. Here, 0.05 represented the significance level for 95% confidence interval.

Figure 40. Correlation among SBS concentration, peak height at 965 cm⁻¹ and peak area at 965 cm⁻¹ with outlier data points

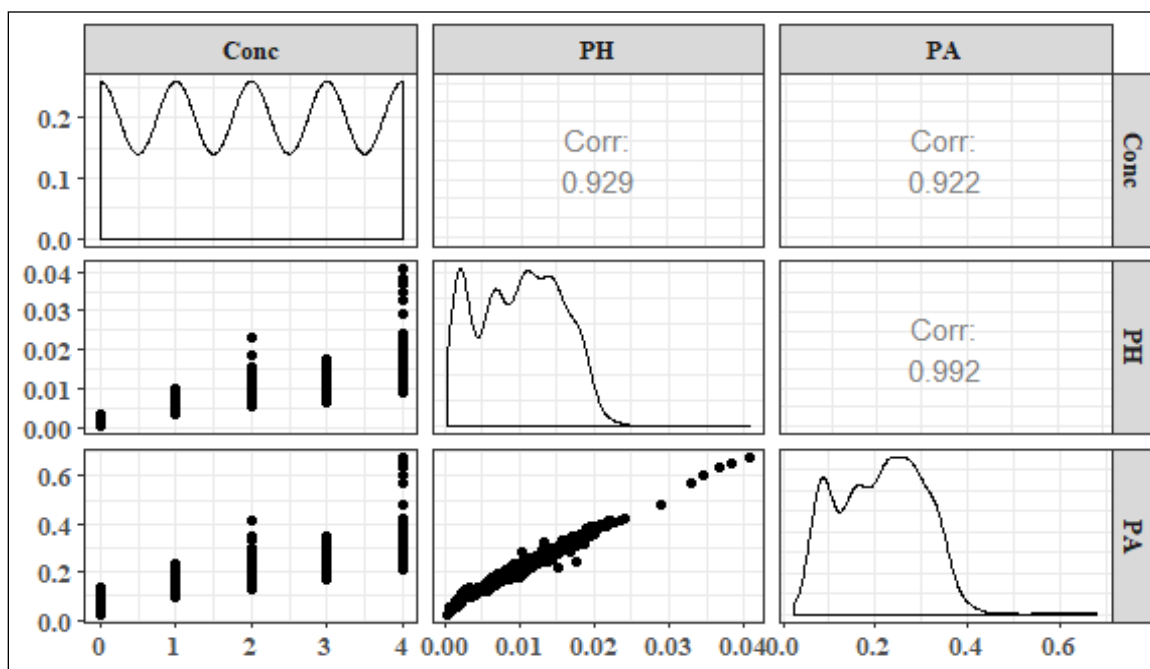


Figure 41. Correlation among SBS concentration, peak height at 965 cm⁻¹ and peak area at 965 cm⁻¹ without outlier data points

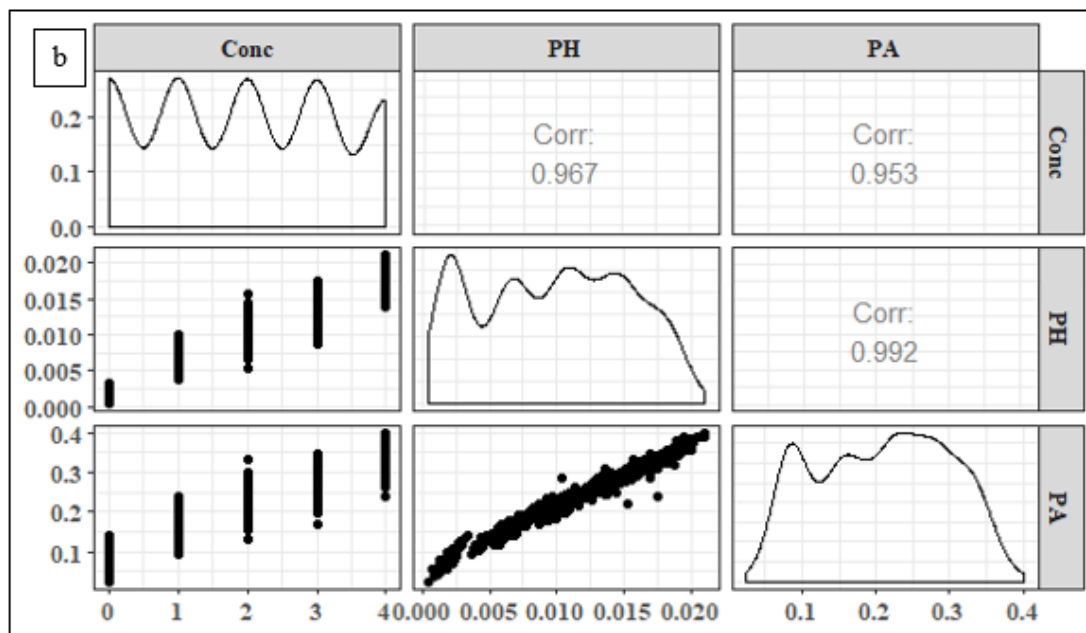


Table 13. Results from regression analysis between peak height and SBS concentration

Parameters of regression model	With outlier		Without outlier	
	Intercept	Concentration	Intercept	Concentration
Coefficients	0.002419	0.003814	0.002413	0.003809
St. error	1.084×10^{-4}	4.427×10^{-5}	7.13×10^{-5}	2.99×10^{-5}
t- value	22.30	86.16	33.84	127.51
Pr (> t)	$<2 \times 10^{-16}$	$<2 \times 10^{-16}$	$<2 \times 10^{-16}$	$<2 \times 10^{-16}$
RSE		0.002146		0.001403
Multiple R ²		0.8636		0.9348
Adjusted R ²		0.8634		0.9347
F-statistics		7424		1.63×10^4
P-value		$<2.2 \times 10^{-16}$		$<2.2 \times 10^{-16}$

Cross-Validation of the Predictive Model

The performance of the regression model developed without outlier data points in the previous section was evaluated by cross-validation approaches [76]. The basic principal of cross-validation is to divide the dataset into two subsets named as training set and testing set, where the data points for training set were used to build the model and testing set was used to validate the model in terms of prediction error. In this study, two cross-validation methods were applied to assess the performance of the prediction model –(a) data splitting approach, and (b) repeated K-fold cross validation.

In the data splitting approach, 80% of the dataset was used as a training set to build the model and 20% of the data points were used as a testing set to validate the model. After that, the prediction error was measured in terms of RMSE (root mean squared error) and MAE (mean absolute error). Results showed that, R² from data splitting cross-validation approach was 0.94, RMSE= 0.0014, and MAE= 0.0009. It indicated that the observed values and predicted values were highly correlated. RMSE represented the average prediction error between the observed value and the predicted value where MAE represented mean absolute difference of the observed and predicted value. Both RMSE and MAE were found significantly lower indicating the validation of the model. Although the data splitting approach is the simplest form of all the validation approaches, it unfolded some bias regarding how observed values are distributed between training set and testing set.

To support the result from this validation approach, further analysis was conducted using repeated K-fold cross validation. K-fold cross validation evaluated the model

performance by arbitrarily distributing the datasets into K-subsets (K= 5 or 10). One subset was reserved as testing set and the others were reserved as training set. Using these two sets, the model was evaluated and the prediction error was recorded. This whole process was repeated for K-subsets and their average prediction error was recorded. When the K-fold cross-validation approach was repeated multiple times, it was known as repeated K-fold cross validation. In this study 10- fold cross validation was conducted with 3 repetitions. After performing this, the R^2 was 0.94, RMSE was 0.0014 and MAE was 0.0010. From the cross-validation approaches, it was concluded that the predictive model developed from linear regression analysis was significant to predict SBS percentages in laboratory as well as in the field with least prediction error.

SBS Prediction in Laboratory Samples

Using the standard equation (4) developed in the preceding section, five laboratory measurements were carried out to predict the percentage of SBS in modified asphalt by two different operators who were not informed about the actual percentage of SBS. Table 14 showed the prediction result of the samples prepared in the laboratory. Among these five samples, sample #1 and #2 were used in developing the regression model, where the remaining ones were not used in the regression analysis. The measurements were carried out by two different operators to ensure the repeatability and reproducibility of predicting SBS percentage. Here, predicted SBS percentages were reported to the nearest 0.1%. In addition, SD (standard deviation), CV (co-efficient of variation), and 95% CI (confidence interval) were calculated.

Results exhibited that, developed regression model predicted SBS concentration for five laboratory prepared samples with ± 0.14 , ± 0.08 , ± 0.22 , ± 0.06 , and ± 0.21 concentration (%) accuracy at 95% confidence interval. The differences between observed and predicted values in all five measurements were found in the range of 0%-5%, which indicated the high accuracy of the model in predicting SBS concentration (%).

SBS Prediction in the Field Samples

For field implementation, SBS concentration (%) prediction study was carried out in six different field sites and their subsequent SBS concentration (%) was predicted using equation (4). In each case, a total of 10 samples were collected, and maximum allowable CV was 12% to avoid the variation in measurement caused by nonhomogeneous polymer phase distribution in asphalt binder [36]. Table 15 shows the results obtained from field

observations. For field demo 1 and 2, binder performance grade was PG76-22 and PG70-22 respectively. Their predicted SBS percentages were reported as 1.1%-1.2% and 1.6%-1.9%. Since the actual percentage of SBS was unknown in these two cases due to supplier trade guideline, a range for predicted SBS percentage was reported.

On the other hand, for field demo 3 and 4, the manufacturer specified the SBS percentage range. Results showed that, predicted SBS percentage falls within the specified range mentioned by the manufacturer. For field demo 5, predicted SBS percentage was 1.9% where actual SBS percentage was 2%. The percentage error in prediction was 5% with respect to actual value. Again, for field demo 6, SBS percentage was predicted 2.1% with 5% error with respect to actual value. For field demo 7 and 8, supplier specified that both the samples have SBS content (%) more than 3%. The predicted SBS content (%) from the universal equation was more than 3% in both the cases. All predicted results of the field measurements were reported to the nearest 0.1%. The confidence interval of all measurements did not vary that much, which indicated the prediction accuracy of the measurement.

Table 14. SBS (%) prediction of the laboratory prepared samples

Sample ID	1	2	3	4	5
Sample used in regression analysis	Yes	Yes	No	No	No
Operator	A	B	A	A	B
Avg. height	0.018	0.014	0.017	0.017	0.015
Predicted SBS (%)	4.2	3.0	3.9	4.0	3.4
SD	0.197	0.115	0.301	0.077	0.295
CV	4.745	3.856	7.814	1.940	8.802
CI	0.141	0.082	0.215	0.055	0.211
95%CI Upper	4.3	3.1	4.1	4.0	3.6
95%CI Lower	4.0	2.9	3.6	3.9	3.1
Actual SBS (%)	4	3	4	4	3.5
% error $\left \frac{\text{Actual} - \text{Predicted}}{\text{Actual}} \right * 100$	5	0	2.5	0	2.9

Table 15. Field implementation of FT-IR to predict SBS percentage

Field demo	Avg. height from FT-IR	Predicted SBS (%)	SD	CV	CI	95%CI Upper	95%CI Lower	Actual SBS (%)
1	0.007	1.1	0.1	5.1	0.042	1.2	1.1	unknown
2	0.009	1.8	0.2	11.2	0.142	1.9	1.6	unknown
3	0.011	2.2	0.2	9.0	0.140	2.3	2.0	1%-3%
4	0.010	2.1	0.1	7.1	0.107	2.2	2.0	1.5%-3%
5	0.010	1.9	0.2	10.5	0.140	2.0	1.7	2%
6	0.011	2.1	0.1	2.8	0.042	2.2	2.1	2%
7	0.018	4.2	0.03	1.37	0.02	4.2	4.2	> 3%
8	0.015	3.2	0.15	9.95	0.13	3.2	3.2	> 3%

Degradation of SBS Due to Aging

Prediction of SBS Content (%) Before and After Aging.

Figure 42 represents the SBS content of different types of modified binders before and after RTFO and PAV aging. All the four binders showed a reduction in SBS content (%) after RTFO aging and further reduction after PAV aging. The SBS content (%) in Figure 42 was determined by using equation 4. The use of equation 4 also showed the exact same result as equation 4. Table 16 represents the percentage reduction in SBS content (%) after RTFO and PAV aging. It was found that 7.5 to 14.5% SBS content (%) was reduced after RTFO aging. After PAV aging, 16-30% SBS content (%) was reduced in all the four modified binders. For predicting the SBS content (%), SD, CV, and 95% confidence interval (CI) were calculated. It was observed that the developed regression model predicted SBS concentration in the binders before and after aging varying with ± 0.02 to ± 0.22 concentration (%) accuracy at 95% CI. From the above result, it can be concluded that SBS polymer degraded after RTFO and PAV aging.

C=O in SBS-Modified Binders After Aging

Figure 43 represents the C=O content of different types of SBSMA binders from different sources before and after RTFO and PAV aging. It was clearly observed from the figure that I_{CO} index increased after RTFO and PAV aging in all the four modified binders. In the case of RTFO aging, I_{CO} index was increased by 40%, 6%, 10%, and 65% for NV PG 64-28, MS PG 70-22, and NV PG 76-22 binder respectively (compared to original

binder). After PAV aging, I_{co} index was increased by 97%, 20%, 20% and 93% of the original binder for NV PG 64-28, MS PG 70-22 and NV PG 76-22 binder respectively.

Figure 42. SBS content of different types of modified binders after RTFO and PAV aging

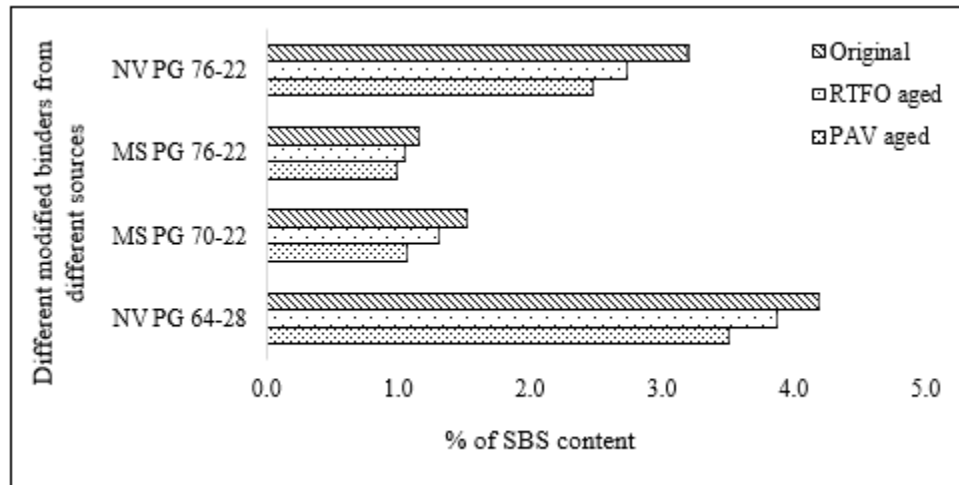
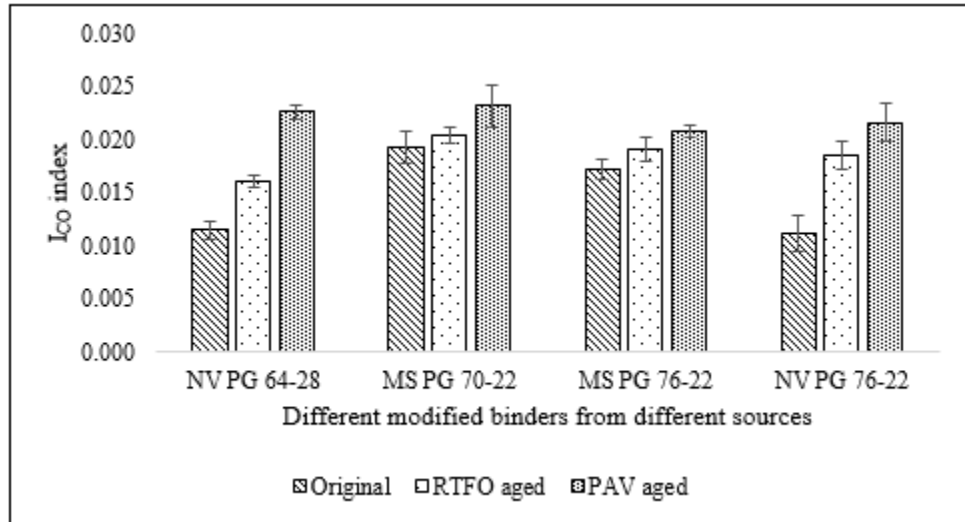


Table 16. Reduction in SBS content after RTFO and PAV aging

Binder	Source	Binder condition	SBS content (%)	% reduction after aging	SD	CV	CI	95% upper CI	95% lower CI
PG 64-28	NV	Original	4.2		0.0003	1.37	0.02	4.2	4.2
		RTFO aged	3.9	7.46	0.0008	4.48	0.06	3.9	3.9
		PAV aged	3.5	16.06	0.0005	3.15	0.04	3.5	3.5
PG 70-22	MS	Original	1.5		0.000	5.99	0.04	1.5	1.5
		RTFO aged	1.3	13.19	0.000	4.32	0.02	1.3	1.3
		PAV aged	1.1	29.91	0.000	6.35	0.03	1.1	1.1
PG 76-22	MS	Original	1.2		0.0003	3.83	0.02	1.2	1.2
		RTFO aged	1.1	8.88	0.0003	5.36	0.03	1.1	1.0
		PAV aged	1.0	14.59	0.0004	7.26	0.04	1.0	1.0
PG 76-22	NV	Original	3.2		0.0015	9.95	0.13	3.2	3.2
		RTFO aged	2.7	14.46	0.0009	7.01	0.11	2.7	2.7
		PAV aged	2.5	22.33	0.0007	6.26	0.09	2.5	2.5

Figure 43. C=O content of different modified binders before and after RTFO and PAV aging



Selection of Asphalt Binder Aging Parameter

Effect of Solvent Amount Residue

The effect of residual DCM was observed significantly in the absorbance value of samples which were dried up to 0%-76% of their initial weight. Initial weight of the samples was 4g, where the binder was 4% and the solvent was 96%. The absorbance values at the wavenumbers 1700 cm^{-1} , 1030 cm^{-1} , and 2920 cm^{-1} were analyzed since these were considered as the fingerprints for aging in the binder. It was found that solvent residue did not display any effect after maximum (95 %) evaporation of the solvent. Table 17 shows the effect of solvent residue in the ATR absorbance value at wavenumber 1700 cm^{-1} . Similar patterns were observed in the absorbance values of wavenumbers 2920 cm^{-1} and 1030 cm^{-1} .

Effect of Aggregate Size

In this study, fine aggregates equal to the binder amount did not exhibit any significant difference in the absorbance values at 1700 cm^{-1} , 2920 cm^{-1} , and 1030 cm^{-1} after drying the samples up to 85%-90% (Figure 44). The only deviations in absorbance spectra were observed in the region of 1150 cm^{-1} to 650 cm^{-1} (Figure 45) which indicated that aggregate intrusion affected the absorbance value at 1030 cm^{-1} , but statistically (5% level of significance), the deviation is not significant. Additionally, aggregate size did not

display any significant deviation at the wavenumbers 1700 cm^{-1} and 2920 cm^{-1} , but in wavenumber 1030 cm^{-1} , #200 passing aggregate caused a 0.1 unit deviation compared to unaged binder absorbance value.

Table 17. Effect of solvent residue in ATR-FTIRS absorbance value

Wavenumber (1/cm)	Samples (DCM Solvent + Binder)	Mean Abs. value	Standard Deviation	CI (95%)	Mean Abs. value of neat binder	Statistical Significance
1700	no dry (immediate collection)	0.01707	0.002644	0.006567	0.02890	Significantly different from binder absorbance value
	27% Dry	0.0170	0.001722	0.004277		
	55 % Dry	0.01463	0.004085	0.010146		
	76 % Dry	0.01804	0.001717	0.004264		
	95 % Dry	0.02924	0.003874	0.009624		No significant difference

Figure 44. Comparison of absorbance values for aggregate intrusion at wavenumbers corresponding to oxidative aging

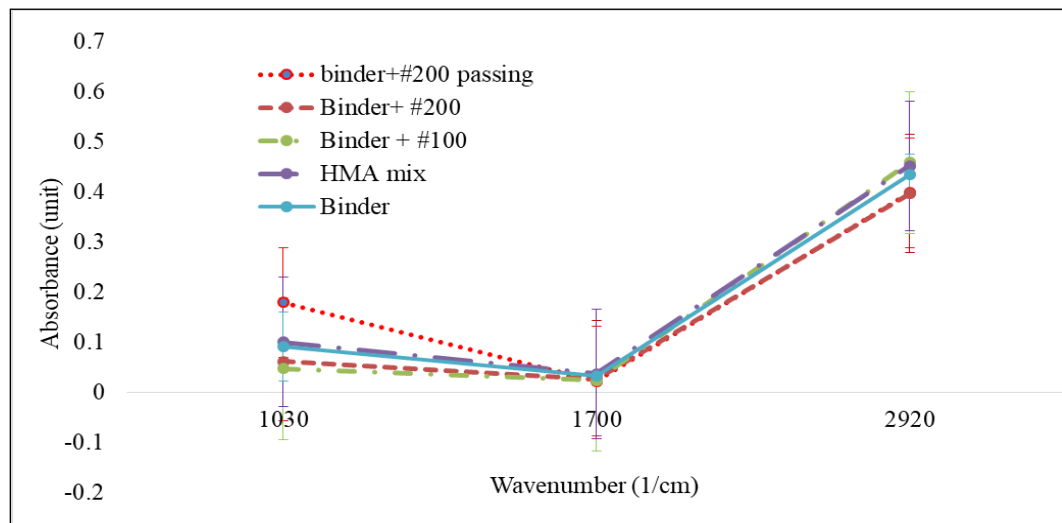
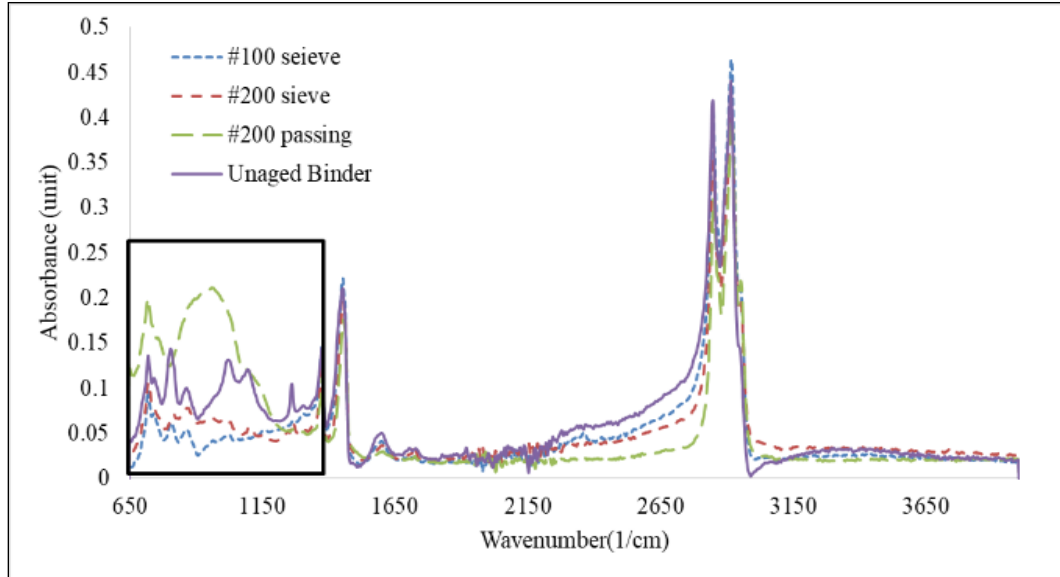


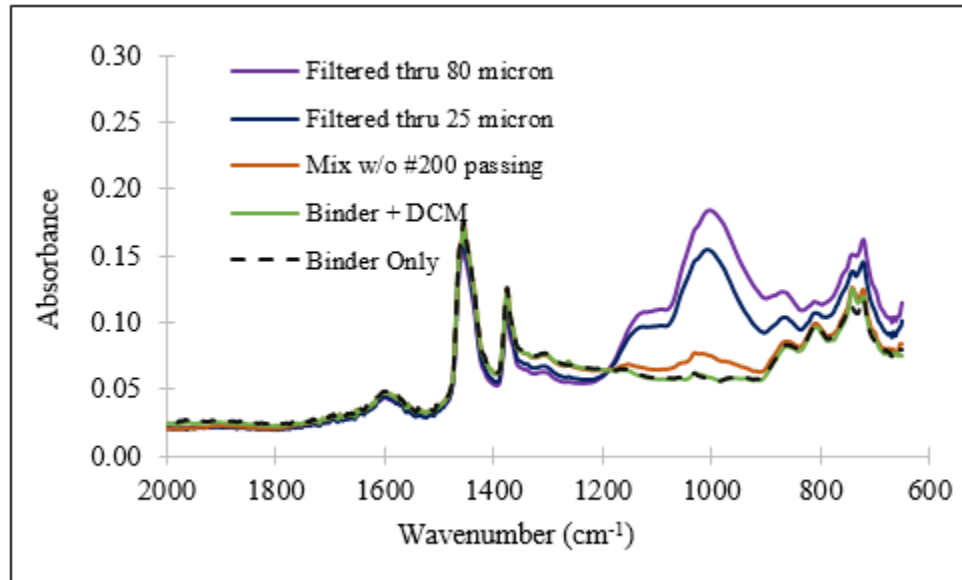
Figure 45. Absorbance spectra of samples considering aggregate and solvent interruption



Effect of Quick Extraction Process on Carbonyl and Sulfoxide Indices

A quick extraction process was developed in this study which can be performed in 15 minutes and can produce enough extracted binder for recording FT-IR spectra. For this quick extraction process, dichloromethane (DCM) was used as a solvent to dissolve the binder from the mix. Rationale behind choosing the solvent was that, it has distinct peaks at wavenumber 746 and 1265 cm^{-1} which do not overlap or interfere with the peak at 1695 cm^{-1} corresponding to carbonyl in aged asphalt binder. Of course, rate of evaporation was much faster, which was an added advantage to perform the extraction in the field. Influence of quick extraction process on binder FT-IR spectra was explained with the aid of Figure 46. Spectra of the neat and residue of dissolved PG 58-28 binder overlap on each other indicating the complete evaporation of the DCM from the binder. So, presence of DCM in the binder residue should not be a concern.

Figure 46. Absorption spectra of extracted binder containing various quantity of fines



Two different extractions were performed where afterward the extraction processes the solution was filtered through 80-micron and 25-micron nylon filter separately. Spectra of the residue show that there exist significantly large peaks with different absorption value at wavenumber 1030 cm^{-1} . In either aged or unaged asphalt binder, sulfoxide shows a peak at 1030 cm^{-1} , but for similar extent of aging the peak height is supposed to be equal. There is a probability that fine particles which could pass through the filter added some silica in the residue. Silicon oxide shows a peak at wavenumber 1000 cm^{-1} . Because of the interference of the molecular vibration at this region a peak with wide area is observed. Residue filtered through 25-micron filter shows smaller peak as it contains less fines. But the filtration process requires much longer time and still cannot remove all the fines. To eliminate the effect of fines in the residue a mix was prepared with aggregate larger than #200 particles and extracted through 25-micron filter. Still some fines are present as observed in the Figure 16. For this reason, aging of extracted binder cannot be quantified by sulfoxide index. There is no interference at wavenumber 1695 cm^{-1} corresponding to carbonyl either because of the solvent of the fines. So, the extraction method can successfully quantify the aging of mix using the carbonyl index.

The effectiveness of the quick extraction method can be supported by providing the carbonyl index of unaged binder and extracted binder from unaged mix. Theoretically both should have the similar indices. Average I_{CO} for unaged and extracted binder were found to be 0.0146 and 0.0140 respectively which differs by only 4.1%.

Inconsistent Increase in Sulfoxide Index with Duration of Aging

Concentration of both carbonyl and sulfoxide increased due to aging. Increase in carbonyl index for different hours of PAV aged binder are shown in the box plot (Figure 47 and 48). Box plot corresponding to unaged and aged binder contain I_{CO} for eight and five different binders respectively. A gradual increase in I_{CO} for PAV aged binder is noticeable from Figure 47. A similar pattern is observed in RTFO aged binder too, which is not shown here. In case of sulfoxide index, the increasing trend ceases after a certain level of aging and then starts decreasing as observed from Figure 48. Extended duration of accelerated aging may cause some sulfoxide to decompose to sulfones and lower the I_{SO} . For this reason, a known value of I_{SO} cannot be directly correlated to the extent of aging of a binder. With the increase in aging duration, unlike carbonyl index, the variability of sulfoxide index value due to different binder grade increases. As the increasing trend of sulfoxide index is not consistent and varies a lot because of the binder grade, this index might not be suitable for quantifying aging of unknown binder.

Unusually High Sulfoxide Index of Unaged Mixture

In this study, I_{SO} of short-term and long-term aged mixture was determined using ATR-FTIR. It was observed that I_{SO} of unaged mix was much higher than the unaged binder (Figure 49) and this value varies considerably from mix to mix. Moreover, no noticeable trend is observed in the STOA mixture. Similar observation was made in the LTOA mixture too. It can be noted that a small amount of binder was extracted in the field to determine the I_{SO} of the mix. There might be a chance that the I_{SO} is influenced by the mixing process.

Five different extractions were performed using the same binder and the I_{SO} was calculated. It is observed from Figure 48 that the solvent does not have any effect on the I_{SO} as both the neat binder and binder residue from the solvent have the similar sulfoxide index. There exists a large increase in I_{SO} when binder is extracted from the mixture. Usually the dissolved binder from the mixture is filtered through an 80-micron nylon filter. If it was filtered using a 25-micron filter the I_{SO} decreases.

Figure 47. Carbonyl (CO) index for PAV aged binder

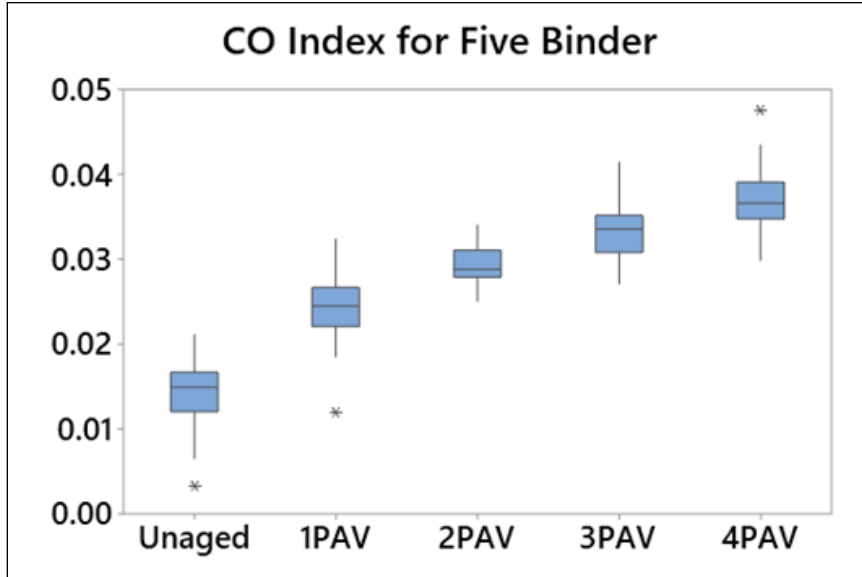
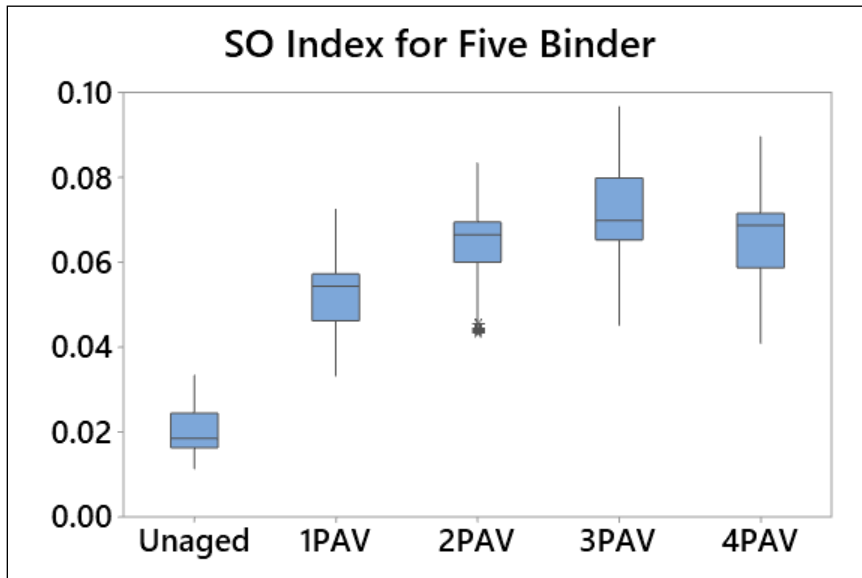


Figure 48. Sulfoxide (SO) index for PAV aged binder



Binder extracted from mix made without #200 and fine particles reduces the I_{SO} significantly. Still it was much higher than that of the unaged binder. Some fine particles present in the mix can be present in the extracted binder which influences the I_{SO} . Interference of the molecular vibration of silicon oxide (at wavenumber 1000 cm^{-1}) from the fines and sulfoxide (at wavenumber 1030 cm^{-1}) creates higher peak value in the spectra and consequently results to higher sulfoxide index. Determination of carbonyl

index is not influenced by the fines present in the mixture (Figure 50). That is why, sulfoxide index cannot be considered as a reliable metric to quantify the aging of the mixture.

Figure 49. Sulfoxide index of short-term oven aged mix.

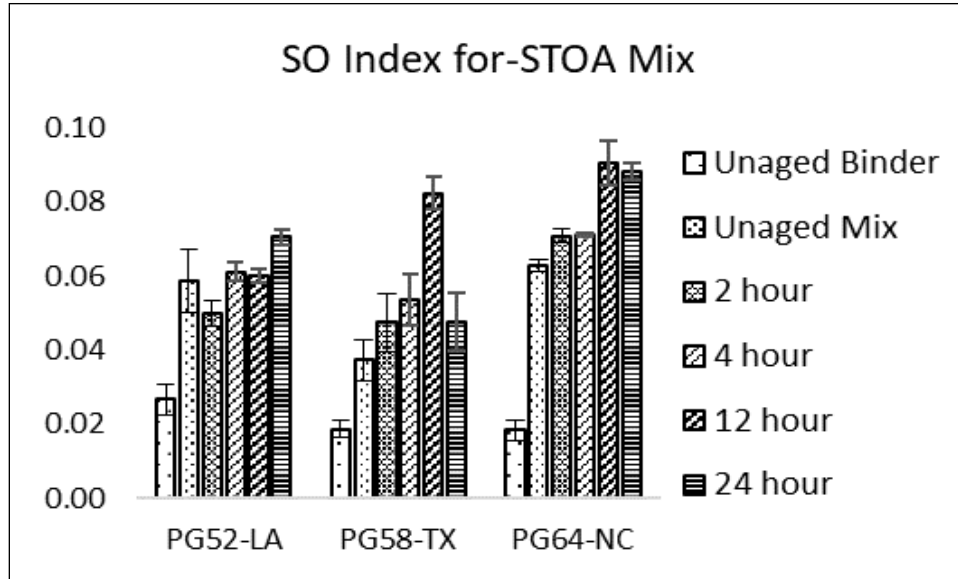
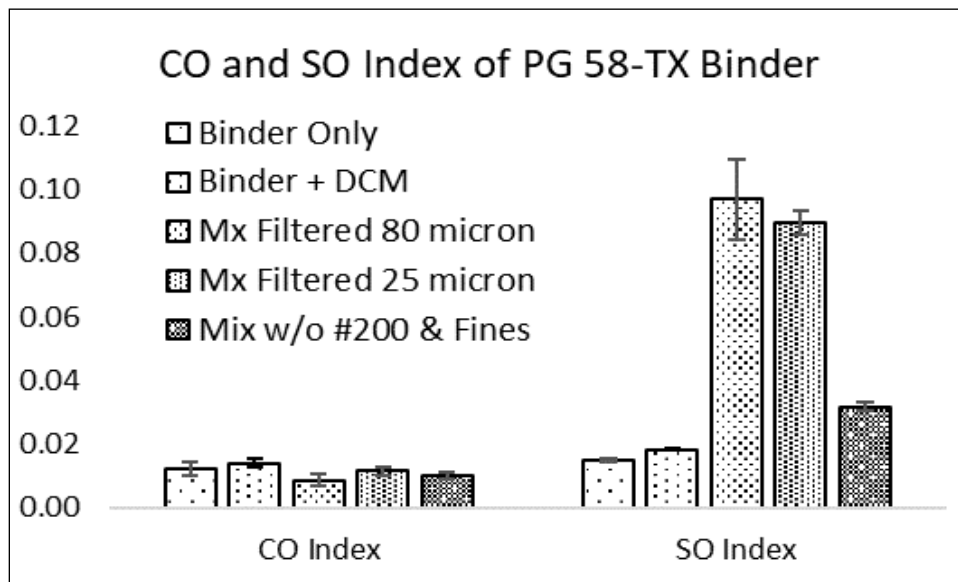


Figure 50. Effect of fines on carbonyl and sulfoxide index.



Different Behavior in RTFO and PAV Aging

Sulfoxide index for the PAV and RTFO aged of five binders are provided in Figure 51 and 52. It is observed that ISO for PAV aged binders are much higher than the RTFO aged binder. Even sulfoxide index of 1-PAV aged binder is much higher than the 24-hour of RTFO aged binder. Another study performed by the authors verified that, 8-hour of RTFO aging created an equivalent effect to 1-PAV aging in terms of carbonyl index. But similar types of relationships cannot be established for I_{SO} index. Moreover, I_{SO} depends on the aging method. Aging at higher pressure and longer duration (in PAV) creates more sulfoxide than aging at a higher temperature (in RTFO). Since the concentration of sulfoxide is dependent on the aging process, this index may be unreliable to quantify aging of a mixture in the field or aging of RAP.

Figure 51. Sulfoxide index for RTFO aged binder

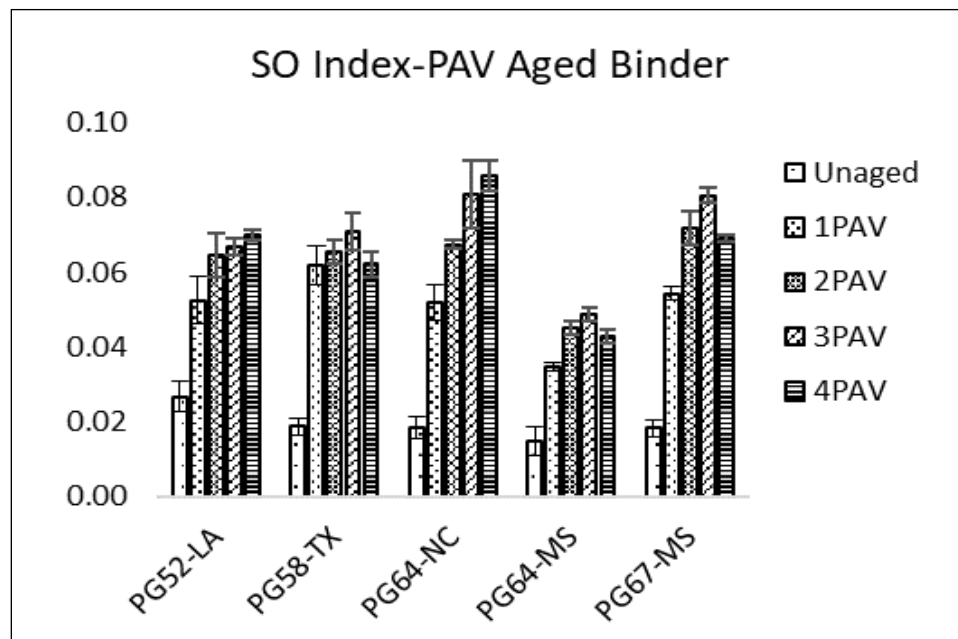
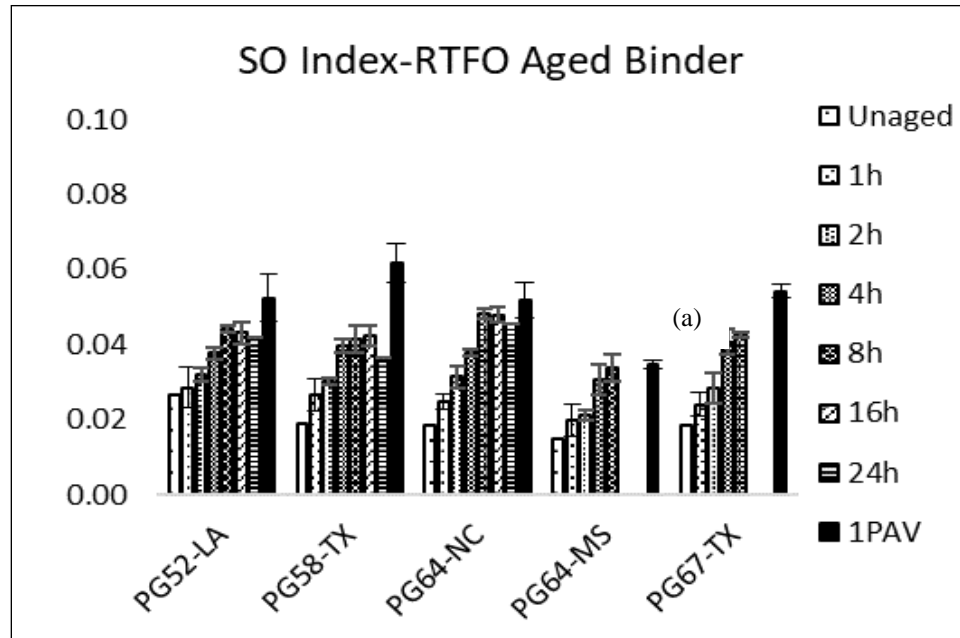


Figure 52. Sulfoxide index for short-term oven aged mixture



Effect of Laboratory Binder and Mix Aging

Aging Indices of Unaged Binders

Two types of aging index parameters were considered to quantify the laboratory aging of both the binder and the mix: carbonyl index (I_{CO}) and sulfoxide index (I_{SO}). To quantify the change in indices due to aging, the initial unaged I_{CO} need to be known for different binders. In this study, a total of eight unaged binders were studied to estimate the base value of I_{CO} and I_{SO} . Indices for unaged binders are provided in Figure 53 and 54. It can be mentioned that average value of the indices for each binder is calculated from 10 separate spectra and the plot in Figure 53 for unaged binder contains eight binder samples. So, the box plot is made of a total of eighty data points.

From Figure 53, it can be observed that the spread of I_{CO} for unaged binder is higher than the aged binder. Unaged binders possess very low peak height in the absorbance spectra corresponding to carbonyl group because the concentration of carbonyl group is very low in unaged binder. This value can be affected by the variation of the absorption value of the valley on either side of the peak. But aged binders have significantly higher peak height value, which is less likely to be affected by the variation of the absorption value of

the valley. In case of I_{SO} , the variation is much higher for aged binder than the unaged binder. The cause of the variation can be attributed to the variation of the intensity of the sulfoxide group itself. As the carbonyl index possesses less variability for aged binder, this index can be considered as a stronger marker to quantify the aging phenomenon more confidently than the sulfoxide index.

Increase in Carbonyl Index (I_{CO}) Due to Laboratory Aging

The effect of laboratory aging on the increase of carbonyl index was observed through binder and mix aging. Five different binders were aged up to 80 hours in PAV and the carbonyl indices were recorded at 20-hour intervals. It was observed that for some cases there exists significant difference in carbonyl index due to variation of the binder grade or source. But the maximum deviation of carbonyl content of a binder from the mean value of all the binders at a certain aging level is around 12% for all four aging conditions. So, irrespective to binder grade or sources, the carbonyl indices were grouped together based on the aging level. Figure 19 is the change in I_{CO} because of laboratory aging of binder as well as for the mix. All four subplots of Figure 19 exhibit a general trend that the carbonyl index increases with the duration of the aging process. Contrary to the findings from several researchers, the I_{CO} does not linearly increase with duration of the aging process [58]. At the beginning of the aging process, the rate of increase is higher, but with time the rate diminishes. RTFO can create similar aging index (0.0376) in 24 hours which can be attained by PAV in 80 hours (0.0372). Although at the end, the indices are equal, the beginning RTFO ages the binder at faster rate than the PAV which can be qualitatively understood from the Figure 55(a) and 55(b).

Long term mix aging is performed in two different ways. Loose mix was aged in force draft oven at 135°C for maximum 24 hours at 85°C for maximum 5 days. Mix was collected at a regular interval and extracted to monitor the aging condition. Aging at 85°C temperature creates slightly less (0.0254) index than that obtained in 12 hours of aging at 135°C (0.0296). Careful observation of Figure 55(a) and 55(c) reveals that 4, 12 and 24 hours of mix aging at 135°C have equivalent effects of binder aging of 1-PAV, 2-PAV, and 4-PAV respectively.

Figure 53. Carbonyl index of unaged binder and comparison of those indices to 1-PAV aged binder

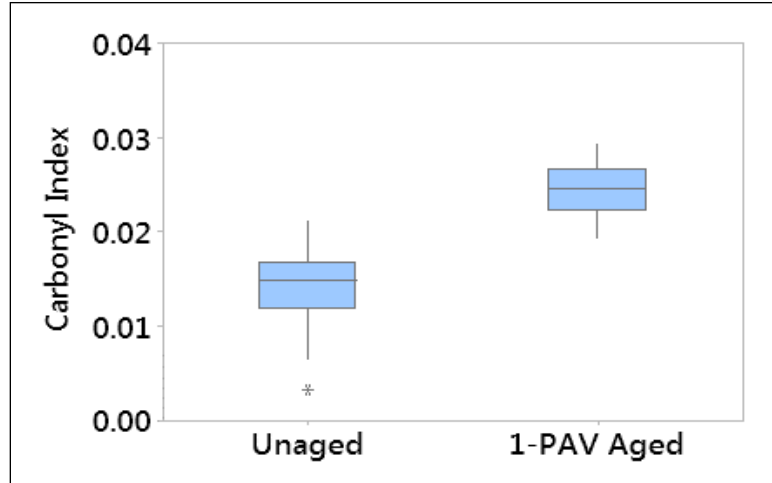


Figure 54. Sulfoxide index of unaged binder and comparison of those indices to 1-PAV aged binder

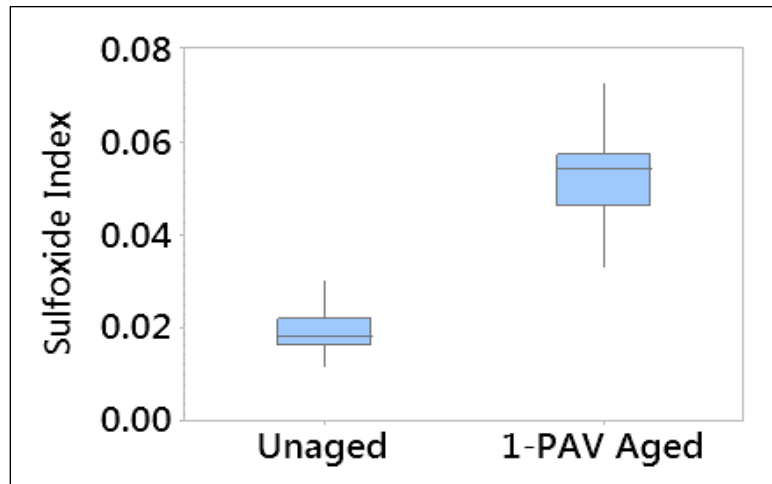
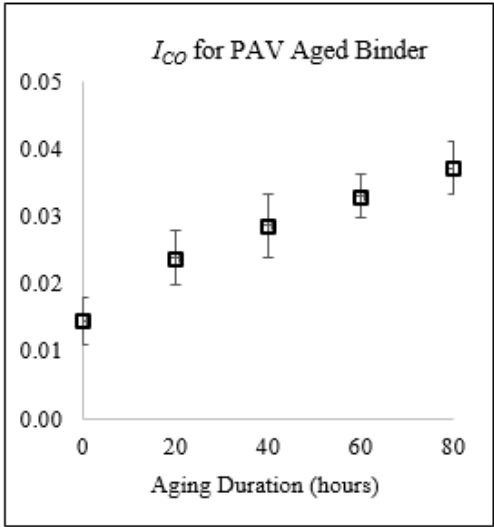
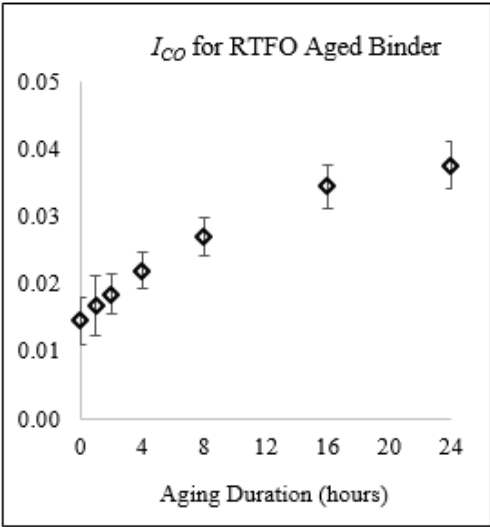


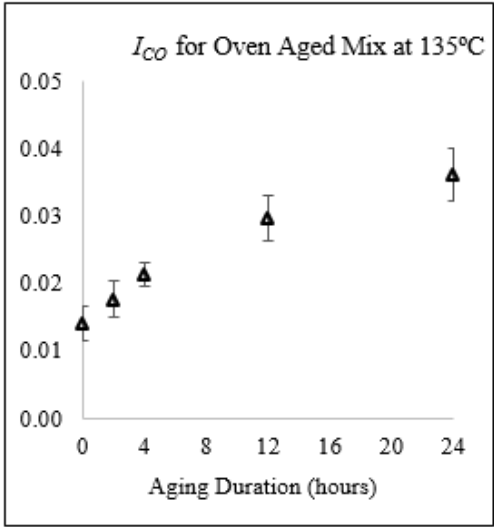
Figure 55. Increase in carbonyl index with the duration of different laboratory aging methods: (a) PAV aging, (b) RTFO aging, (c) oven aging at 135°C and (d) oven aging at 85°C



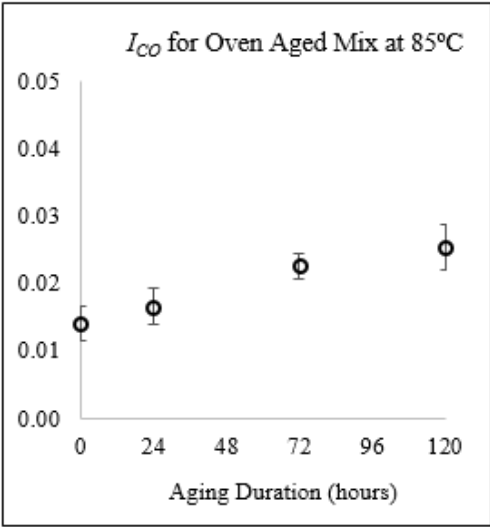
(a)



(b)



(c)



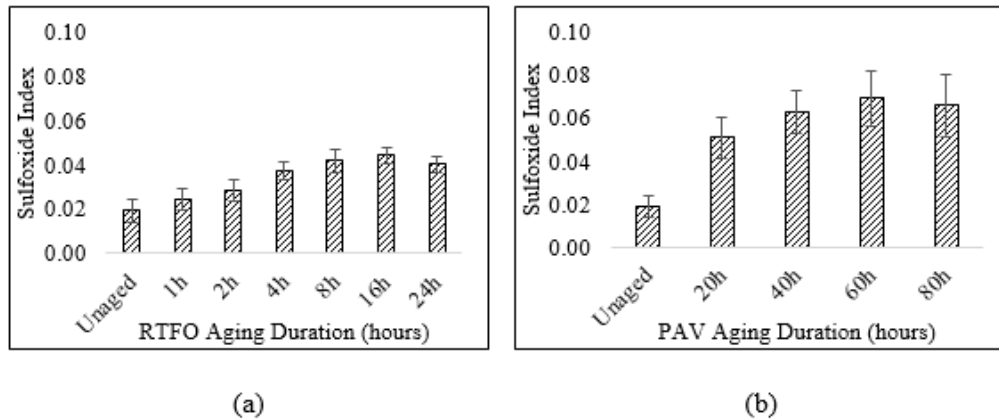
(d)

Variation of Sulfoxide Index (I_{SO}) Due to Laboratory Aging

Sulfoxide index (I_{SO}) for all four types of aged sample was determined and index for aged binder are shown in the Figure 56. It is observed that I_{SO} keeps increasing up to a certain aging level and beyond that point it starts decreasing, which corroborates with some previous studies [77]. There is a probability that some sulfoxide might decompose to sulfones which reduced the intensity of sulfoxide after extended duration of accelerated aging process [48]. This trend is similar for both the RTFO and PAV aged binder. So, by observing only the I_{SO} of a certain binder it is not possible to conclusively determine the aging state because of its indecisive trend.

More importantly, in case of mix aging, the I_{SO} does not follow any noticeable trend. It was also observed that S=O functional group in extracted binder exhibited a wide absorbance spectrum which is not proportional to the aging product. This larger absorbance around 1030 cm^{-1} was resulted from the overlap with Si=O functional group present in the aggregate [18, 78]. As I_{SO} is not providing any conclusive results, this parameter is not used for determining the aging state of RAP or mixes.

Figure 56. Sulfoxide index for laboratory aged binder



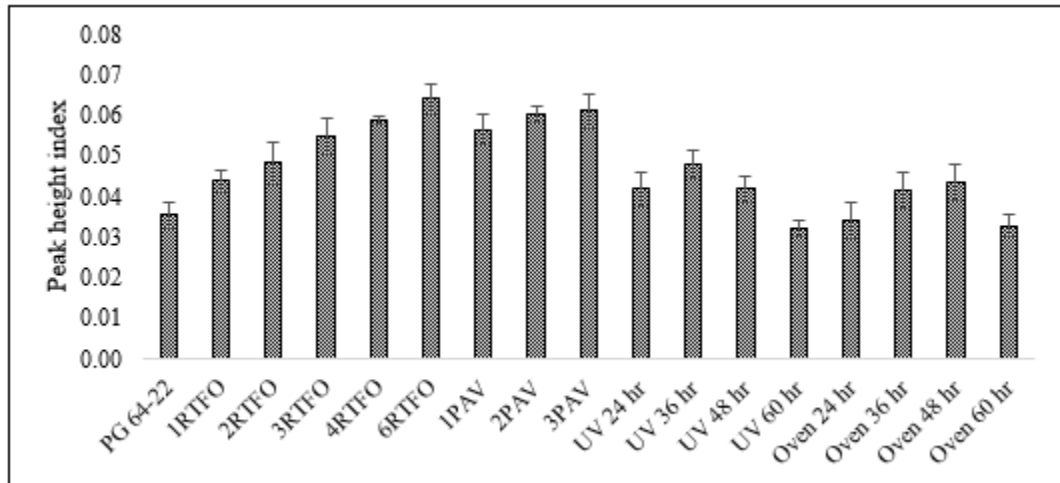
Analysis of Aging at Similar Stiffness

Figure 57 shows the carbonyl (I_{CO}) peak height index of original, RTFO, PAV, UV, and oven aged PG 64-22 binder. Due to oxidation, oxygen containing functional group, I_{CO} increases in asphalt binder. The carbonyl index was calculated based on the Eq. 5.

$$I_{CO} = \frac{\text{Peak height at } 1695 \text{ cm}^{-1}}{\text{Peak height at } 2920 \text{ cm}^{-1} \text{ or peak height at } 1375 \text{ cm}^{-1}} \quad (5)$$

After 1-RTFO, 2-RTFO, 3-RTFO, 4-RTFO, and 6-RTFO aging, I_{CO} index of PG 64- 22 binder was increased by 23%, 36%, 54%, 65%, and 81% respectively. In the case of 1-PAV, 2-PAV, and 3-PAV aging, index was increased by 59%, 70%, and 72% respectively. It was observed that, after 40 hours of PAV aging, change in I_{CO} index was not significant. UV and oven aged binder showed increment of I_{CO} index up to 36hr of aging. After 36hr of aging, I_{CO} index was reduced in both the case of UV and oven aging. Increment of I_{CO} functional group can make the asphalt binder more viscous which will lead to brittle and harder asphalt binder.

Figure 57. I_{CO} peak height index ($1695 \text{ cm}^{-1}/1456 \text{ cm}^{-1}$) for PG 64-22 original and aged binder



From the DSR temperature sweep test, stiffness ($G^*/\sin\delta$) and phase angle (δ) values of different RTFO and PAV aged PG 64-22 binders were obtained. It was observed that 3RTFO and 1PAV, 4RTFO and 2PAV, and 6RTFO and 3PAV aged binders have similar stiffness and similar phase angle at 64°C as shown in Figure 58. Base binder's stiffness increased by 12 times after 3RTFO and 1PAV, 7 times after 4RTFO and 2PAV, and 10 times after 6RTFO and 3PAV aging (Figure 58a). Again, base binder's phase angle decreased by 11% after 3RTFO and 1PAV, 18% after 4RTFO and 2PAV, and 25% after 6RTFO and 3PAV aging (Figure 58b). Rutting depends on the binder's stiffness and phase angle. It can be concluded that extreme aging increased stiffness and reduced phase angle of the base binder which indicated poor rutting resistance.

It can be observed from Figure 59 that at similar stiffness, the C=O index of RTFO and PAV aged binder was the same for two different types of indices calculation. It can be concluded that, at similar stiffness of unmodified aged binder, the C=O index was similar which indicated the C=O index has a direct correlation with the stiffness of the binder.

Figure 58. RTFO and PAV aged (W/O RTFO) PG 64-22 binder at 64°C (a) stiffness (b) phase angle

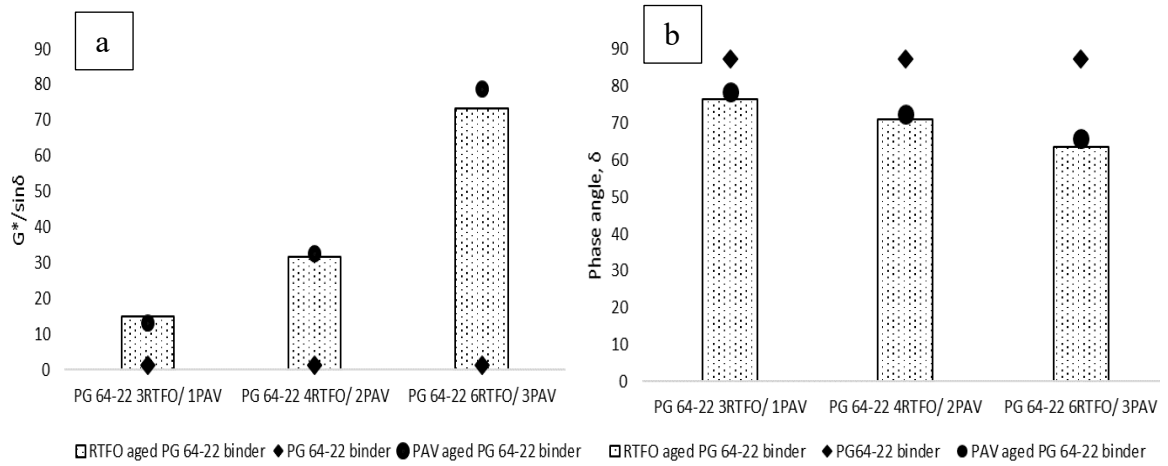
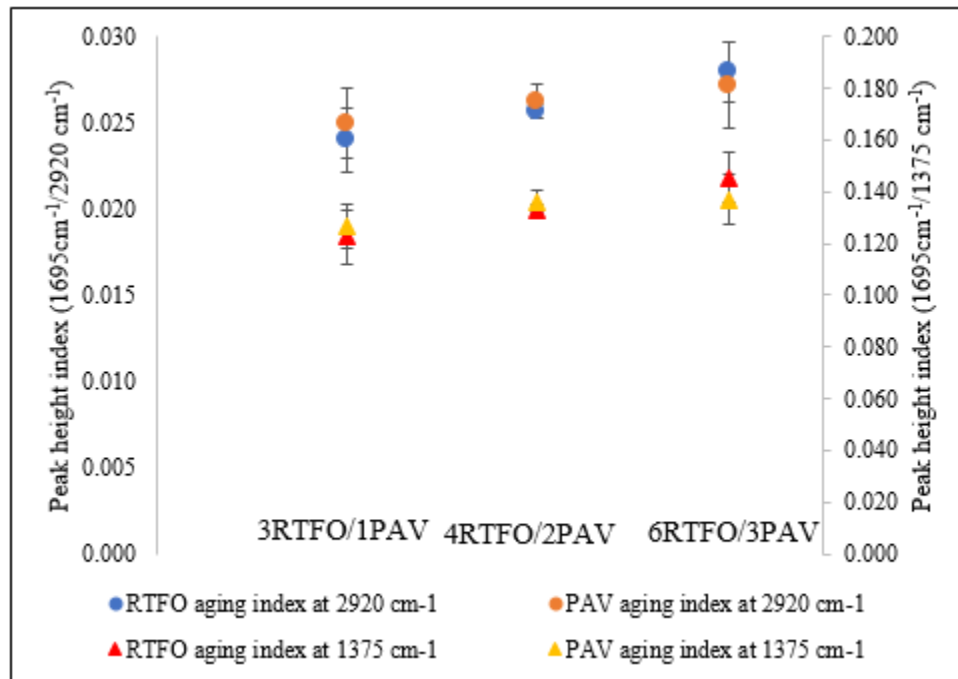


Figure 59. Comparison of C=O index of RTFO and PAV aged PG 64-22 binder at similar stiffness



RAP Content Determination

Understanding the Aging State of RAP

As mentioned earlier, one of the objectives of this study is to characterize the RAP based on their extent aging. In most cases, RAP are the blends from different sources and the life history of RAP is mostly unknown. An estimate of the base value of different indices need to be made irrespective to binder grade or sources to determine the state of aging of the RAP.

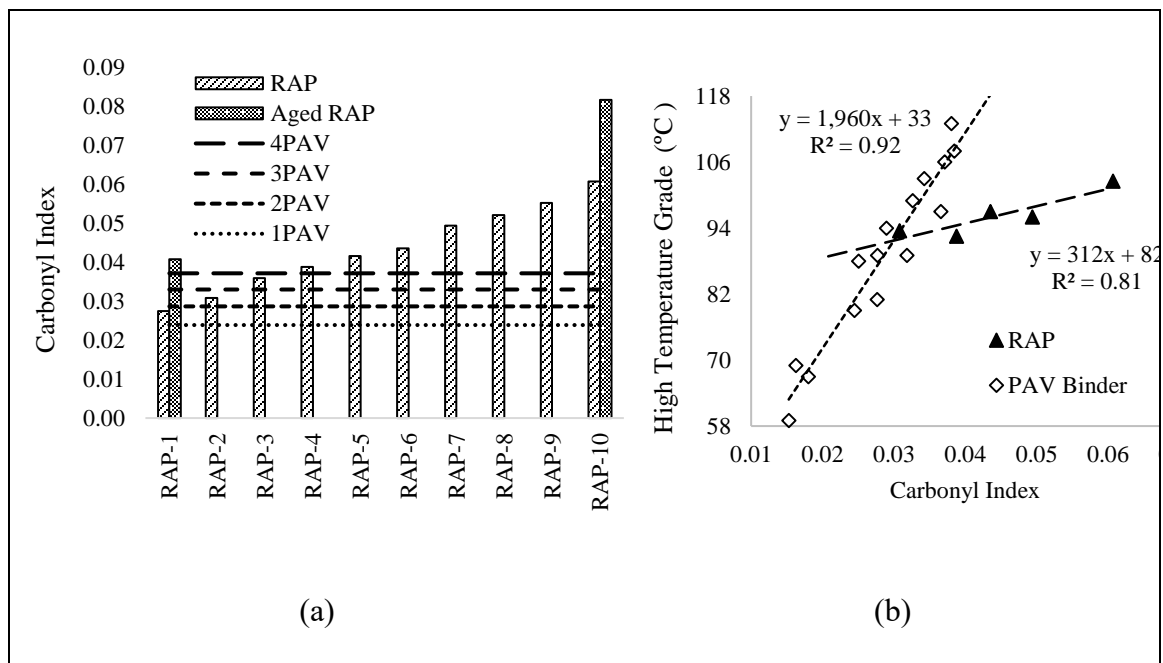
Because of variability of sources and inadequate information regarding the history of the reclaimed asphalt pavement, it is a challenging task to characterize the RAP based on the severity of aging. Traditional binder extraction from the RAP is not a convenient option to determine the aging state as it requires time and use of huge amount of solvent. The extracted binder provides the information regarding the stiffness of RAP binder but does not provide any insight regarding the chemical change because of oxidative aging. The aging process of course increases the stiffness of the binder but measuring the stiffness alone might not be a true estimate of aging. Figure 60(a) shows the carbonyl index of 10 different RAPs collected from different plants and sites. They are named based on the carbonyl content arranged in ascending order. The average carbonyl index for each RAP binder is computed from 10 individual spectra obtained from two different extractions of each RAP. Carbonyl index of the RAP, studied here, varies from 0.0274 to 0.0607 with maximum coefficient of variation of 12%. So, it is observed that the I_{CO} of naturally occurring RAP varies at a wide range. FT-IR can be used to characterize the RAP based on their extent of aging. Instead of fixing the maximum amount of RAP in HMA irrespective to their severity of aging the quantity can be adjusted. Higher amount of RAP with lower I_{CO} can be recommended whereas the use of RAP with high I_{CO} can be restricted. Of course, further study on mix properties should be conducted to adjust the amount of RAP use based on the carbonyl index.

Four horizontal dotted lines in the plot indicate the carbonyl index corresponding to different PAV aging levels. Age of the RAP used for this study varies from 3 years to over 20 years. So, it can be expected that a large age distribution of RAP is covered in the study. All the RAP binders are aged above the 1-PAV aging level. Seven out of 10 RAPs are aged above 4-PAV level. PAV aging is showing the limitation to predict the actual aging that a binder undergoes in real life. The results indicate that, in service life, aging of

binder produces much higher carbonyl content than that of the laboratory mix aging method practiced by different agencies.

To investigate the potential of further aging of RAPs: RAP-1 and RAP-10 are aged in a forced draft oven at 135°C for 24 hours. The reason behind the selection of those two RAPs is that they possess the least and most carbonyl index respectively. Increase in carbonyl index for RAP-1 and RAP-10 are 48% and 34% respectively because of oven aging. It can be inferred that even though RAP contains highly aged binder it possesses the potential to get more aged with time. A hypothesis can be made that the oxidative aging is a never-ending process. Further study must be conducted to prove this hypothesis.

Figure 60. Comparison of PAV aged binder and naturally aged RAP: (a) carbonyl index, (b) high temperature grade



Stiffness of the binder is a parameter that might not truly quantify the chemical changes due to oxidative aging. Figure 60(b) is the plot of high temperature grade (temperature in degree Celsius at which $G^*/\sin\delta = 1$ kPa) for both PAV aged and traditionally extracted RAP binder against the carbonyl index. High temperature grade follows linear relationship with carbonyl index for both the cases with satisfactory R^2 values of over 0.80. An intriguing observation from the plot is that, PAV aged binder with similar carbonyl index to RAP binder possess higher stiffness than that of the RAP binder. The

rate of increase of stiffness of PAV aged binder is much higher than that of RAP binder. In the field, the aging process increases the carbonyl content without increasing the stiffness at the same rate that happens in PAV aging. Stiffness of a binder is contributed by the concentration of oxidative aging products as well as the dispersion of those molecules. Agglomerated molecules can produce more stiffness although the concentration of the aging product is the same. The accelerated aging method may facilitate the molecular agglomeration at faster rate than what happens in the field by the natural aging process in a longer course of time. This might be the reason for higher stiffness of the laboratory aged binder.

Quality Control of Plant Mix Using FT-IR Spectrometer

Quality control of RAP contained HMA during the production is a challenge. Quality control involves making sure that the mix contains the specified amount of RAP and the RAP is homogeneously blended. To investigate the potential of handheld FT-IRS in quality control of plant mix the research team visited two different plants in Louisiana. Design RAP content for the mixes was 15% as Louisiana specification does not allow more than that in surface course. At each plant, the ATR-FTIR spectra of the asphalt binder as well as the quickly extracted RAP binder were recorded before the plant started the operation. The process of quick extraction of RAP and recording 10 FTIR spectra of both virgin and extracted binder required less than 30 minutes. Three mix samples were collected at different time intervals and FT-IR spectra were recorded.

For quantifying the RAP content in the mix, it is assumed that the carbonyl index in a binder blend increases linearly with an increased amount of aged binder in a blend. Two extreme ends of the carbonyl index of the binder blend is limited by the carbonyl index of the unaged binder and the highly aged RAP binder respectively. If the carbonyl index of a binder blend can be determined provided that both the upper and lower limits are known, the percentage of aged binder in the blend can be calculated. To establish this assumption of linear change in carbonyl index, four binder blends were prepared with 10%, 20%, 40% and 80% of aged binder. It is understandable that 0% and 100% represents the unaged and highly aged binder. For this study, a 4-PAV aged binder was used instead of the RAP binder for convenience. Figure 61 shows the increase of carbonyl index from 0.0163 (for unaged binder) to 0.0381 (for aged binder) with an increase of percentage of aged binder. It is observed from Figure 61 that all the points lie around the straight line obtained by connecting the lowest and highest values with R^2 value of 0.98.

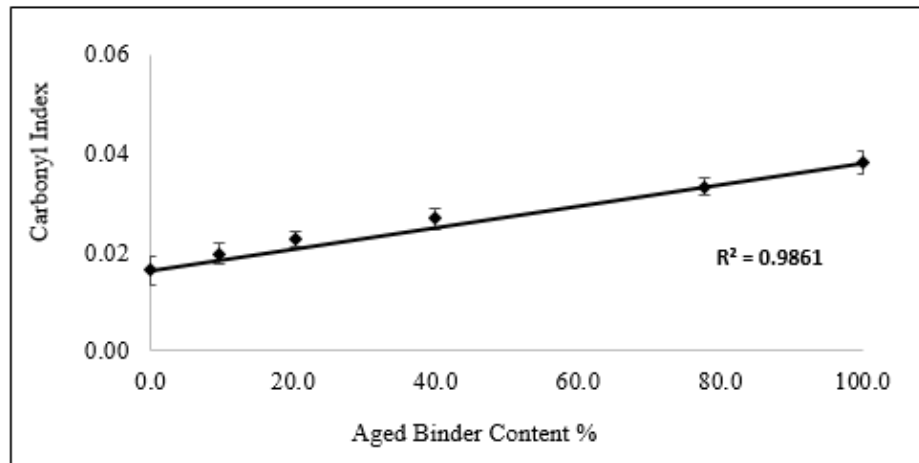
Figure 62 is the test results for plant mix containing RAP-8. The mix was made of 15% RAP aggregate with design asphalt content of 5.0%. Contribution of binder from RAP was 0.8% which yielded the RAP binder ratio of 0.16 or 16%. The carbonyl index of unaged binder and RAP binder were found to be 0.0158 and 0.0521 respectively. The predicted carbonyl index of the mix made of 16% of the RAP binder was calculated to be 0.0216 by the following equation:

$$I_{CO} (\text{calculated}) = 0.0158 * (1 - 0.16) + 0.0521 * 0.16 \quad (9)$$

Figure 62(a) shows the carbonyl index for three different samples collected from the same plant. There is a slight difference in the carbonyl index which can be utilized to calculate the corresponding RAP binder percent in the mix. If I_{CO} of the unaged binder corresponds to 0% and I_{CO} of RAP binder corresponds to 100% RAP binder, for a given value of I_{CO} the percentage of RAP binder in the mix can be determined by the following equation:

$$RAP\% = \frac{I_{CO} (\text{Mix}) - I_{CO} (\text{Unaged binder})}{I_{CO} (\text{RAP}) - I_{CO} (\text{Unaged binder})} * 100 \quad (10)$$

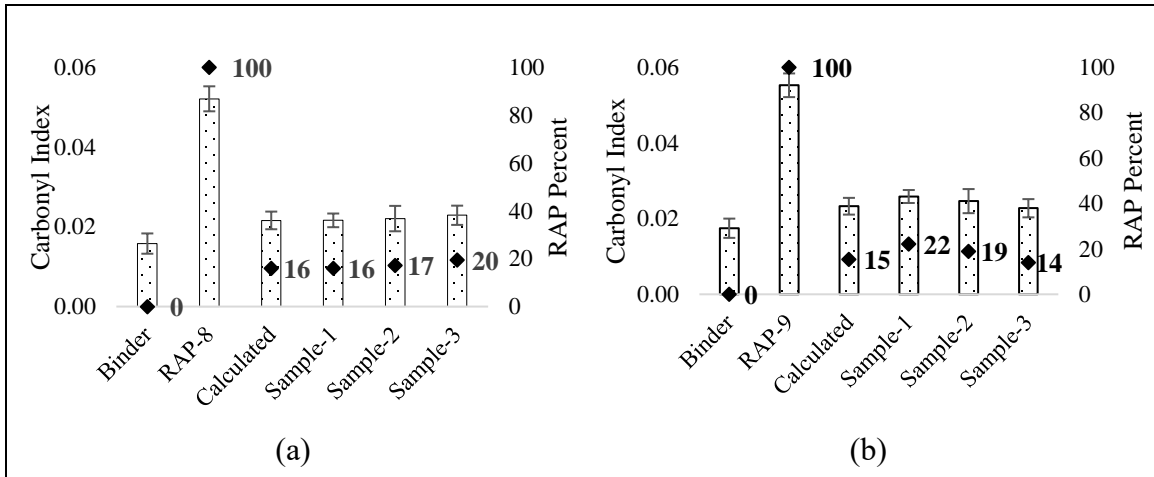
Figure 61. Linear increase in carbonyl index with increase of aged binder



The percentage of RAP binder in the mix made of RAP-8 with 16% design RAP binder, varies from 16% to 20%. For the other mix made of 15.4% design RAP binder the amount was found to be between 14% and 22%. There might be a probability of using higher amount of RAP in the mix or the RAP was not properly blended from where the sample was collected. Whatever the reasons are, the FT-IRS can detect the variation in

carbonyl index and dictates the investigation of mix production anomaly. The procedure of determining carbonyl index is very straight forward. It does not require any laboratory support. One person can control the quality of the asphalt mix in the plant or in the construction site using a handheld FT-IR spectrometer with minimal accessories in just 30 minutes.

Figure 62. Prediction and validation of RAP content in plant produced mix of (a) RAP-8 with 16% design RAP binder, (b) RAP-9 with 15.4% design RAP binder



Change in Carbonyl Index with Increased RAP Content

It was presumed that the carbonyl index of a mix varies linearly with increased amount of RAP in the mix. Six mixes were prepared in the laboratory with 0%, 10%, 20%, 40%, 80%, and 100% of RAP. Total 100 grams of mix were taken in a small jar and all the mix was used to extract the binder. Two ends of the carbonyl index of the mix are limited by the I_{CO} of the unaged mix and the RAP respectively. Figure 63 shows the increase of I_{CO} from 0.0166 (for unaged binder) to 0.0634 (for RAP) with increase of the percentage of RAP. It is observed from Figure 63 that all the points lie around the straight line obtained by connecting the lowest and highest values of the carbonyl index. The R^2 value of the trend line (not shown in the Figure 63) was found to be 0.9935 which is an indication of very good linear correlation.

Effect of Short-Term Aging in the Plant

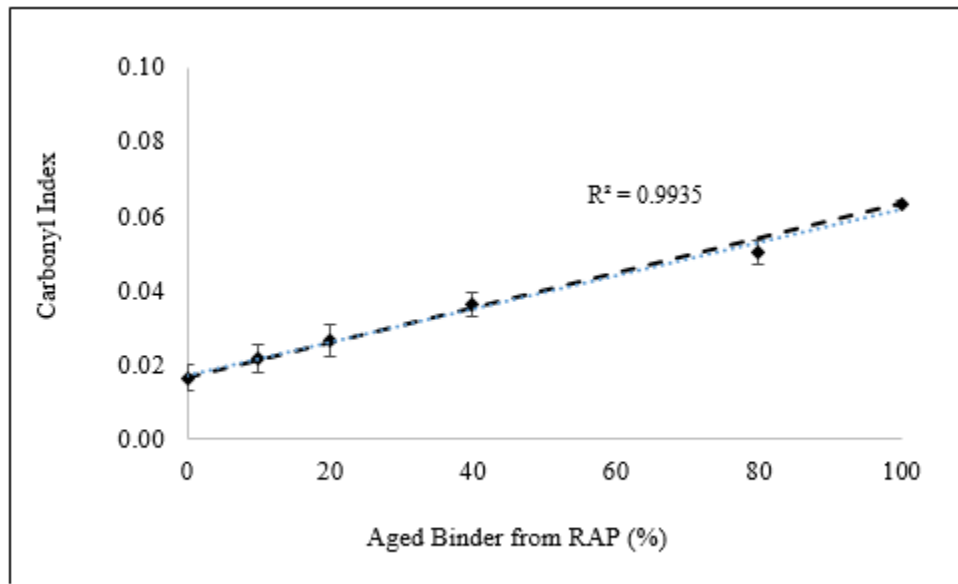
All the mixes were collected from two different locations in the plant: from the ‘drum’ and from the ‘truck.’ Carbonyl index were measured for all the mixes and based on this

measurement the percentage of RAP could be determined. In Figure 64, carbonyl index of four mixes are shown where ‘mix D’ is collected from the drum and remaining three were collected from the truck. The bar charts are representing the carbonyl index of the unaged binder, used RAP, and predicted value of carbonyl index if designed RAP were used. For example, the carbonyl index of unaged binder and RAP in ‘mix D’ has the carbonyl index of 0.0196 and 0.0697 respectively. The predicted carbonyl index of the mix made of 16% of the RAP binder was calculated to be 0.0276 by the following equation:

$$I_{CO} (calculated) = 0.0196 * (1 - 0.16) + 0.0697 * 0.16 \quad (8)$$

Except ‘mix D’, all other mixes showed a significant increase in the carbonyl index than the predicted value. It can be mentioned that ‘mix D’ was collected from the drum whereas, other three mixes were collected from the truck. There is a chance that ‘mix B’, ‘mix E’, and ‘mix H’ were short-term aged when they were being stored in silo. If the carbonyl indices were used to calculate the RAP percent in the mix it would give a much higher percentage although RAP content might be in the design limit. So, it is important to choose the location from where the sample should be collected. In the case of ‘mix D’, the carbonyl index was obtained around the predicted value. So, ‘mix D’ and other mixes collected from the drum were used to determine the RAP content in the mix. Further study will be conducted to investigate the effect of short-term aging of mix in the silo.

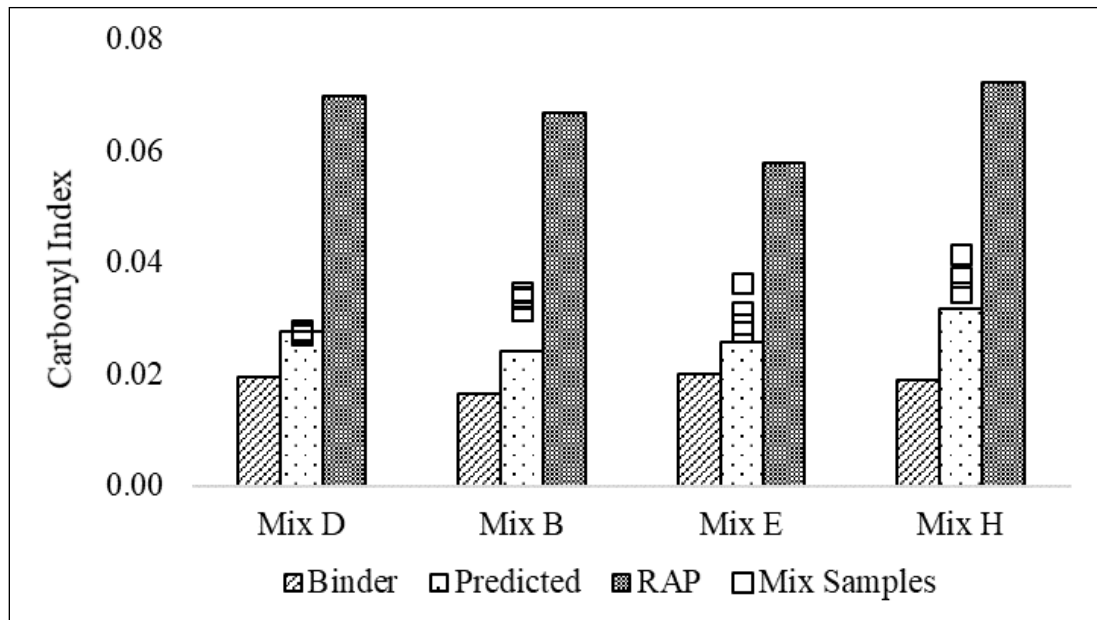
Figure 63. Linear increase in carbonyl index with increase in RAP content in the laboratory mix



Determination of RAP Content in Fresh Mix

Figure 65 is the test results of six different mixes which were collected from the drum. Design RAP content for each mix is shown on the plot. Carbonyl index for different samples of same mix are slightly different which can be utilized to calculate the corresponding RAP binder percent in the mix. For example, unaged binder and RAP in 'mix A' has the carbonyl index of 0.0219 and 0.0758 respectively. Carbonyl index of one sample from 'mix A' was found to be 0.0285. If I_{CO} of the unaged binder corresponds to 0% and I_{CO} of RAP binder corresponds to 100% RAP binder, for a given value of I_{CO} of 0.2875, the percentage of RAP binder in the mix was found to be 12% by the following equation 7.

Figure 64. Carbonyl index of short-termed aged mixes in the plant



Percentage of RAP in the 'mix A', varies from 12% to 21% where the design RAP was 16%. For all the mix tested here the RAP content were found within $\pm 5\%$ range, the only exception of one sample from 'mix F.' There might be a probability of using a higher amount of RAP in the mix or the RAP was not properly blended from where the sample was collected. Whatever the reasons are, the FT-IRS can detect the variation in carbonyl index and dictates the investigation of mix production anomaly. The detailed information regarding the RAP content in plant mix is represented in Table 18.

Figure 65. RAP content determined by handheld FT-IRS in the plant

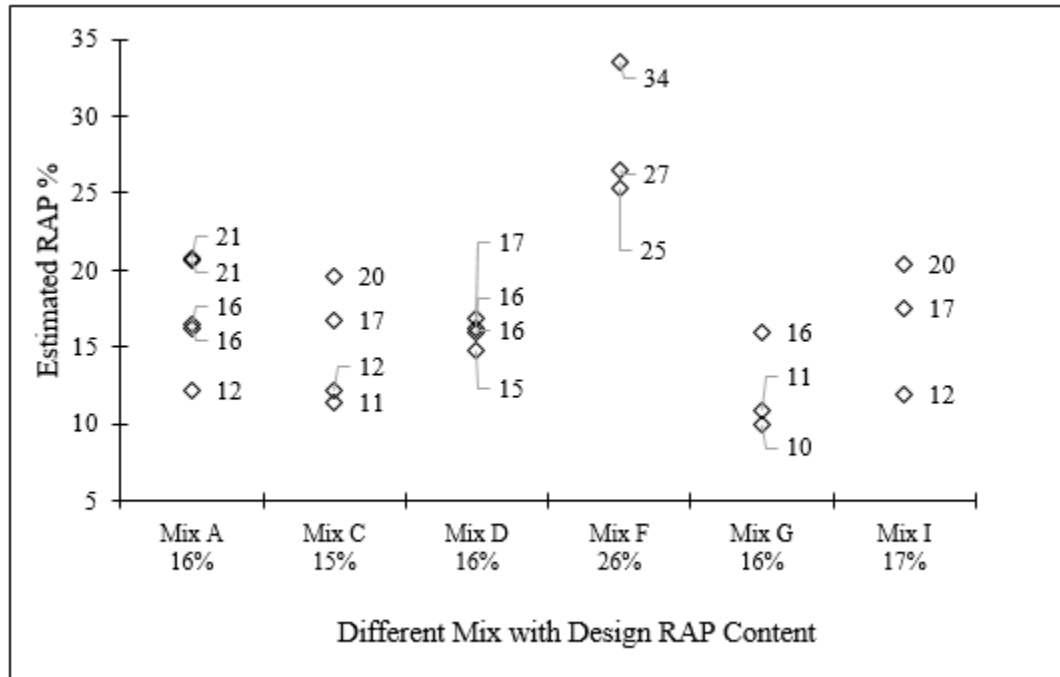


Table 18. Details information regarding the plant mix

	Mix Designation								
	A	B	C	D	E	F	G	H	I
NMS (inch)	0.5	0.5	0.5	0.5	0.5	0.75	0.5	1.0	0.75
RAP %	15.0	14.3	14.3	14.2	15.0	23.8	14.2	19.0	14.9
Design Asphalt %	4.8	4.7	4.7	5.0	4.6	4.6	5.0	4.2	4.6
Binder from RAP %	0.8	0.7	0.7	0.8	0.7	1.2	0.8	1.0	0.8
RAP to Binder Ratio	0.167	0.149	0.148	0.160	0.152	0.260	0.160	0.238	0.174
Binder PG	67-22	64-22	70-22	64-22	67-22	76-22	64-22	70-22	70-22
Virgin Binder Ico	0.0219	0.0167	0.0283	0.0196	0.0200	0.0193	0.0209	0.0190	0.0190
RAP Binder Ico	0.0758	0.0667	0.0689	0.0697	0.0577	0.0924	0.0725	0.0722	0.0722
Mix Collected From	Drum	Truck	Drum	Drum	Truck	Drum	Drum	Truck	Truck

Identification and Quantification of Rejuvenators

Qualitative Analysis

For qualitative analysis neat spectra of the asphalt binder, aromatic rejuvenator, and bio rejuvenator were studied to identify their representative functional groups. Figure 66 and 67 showed the representative functional groups present in aromatic and bio rejuvenator. The characteristic functional groups in the fingerprint region of the aromatic rejuvenator are: bending vibration of C=C at 1600 cm^{-1} ; asymmetric bending of CH₂ and CH₃ at 1455 cm^{-1} ; symmetric bending of CH₃ at 1375 cm^{-1} ; stretching vibration of S=O at 1034 cm^{-1} ; out of plane deformation CH at $870, 817, 745\text{ cm}^{-1}$; and aromatic ring vibration of CH at 721 cm^{-1} . On the other hand, representative functional groups of the bio rejuvenator in the fingerprint region are stretching vibration: of C=O at 1744 cm^{-1} ; bending vibration of C=C at 1653 cm^{-1} ; stretching vibration of CH₂ and CH₃ at 1453 cm^{-1} ; bending vibration of CH at 1377 cm^{-1} ; stretching vibration of C-O at $1243, 1162, 1118, 1097\text{ cm}^{-1}$; and ring vibration of CH₂ at 721 cm^{-1} .

The functional groups in fingerprint region of aromatic rejuvenator are the same as the asphalt binder [18]. When bio rejuvenator added with unmodified asphalt binder, spectra showed two distinct functional groups in the fingerprint region—stretching vibration of C=O at 1744 cm^{-1} and stretching vibration of C-O at 1162 cm^{-1} . These two functional groups were also apparent when bio rejuvenator added in polymer modified binder and RAP induced unmodified and polymer modified binder. From qualitative analysis, it was determined that these two functional groups can be a good representation for identification of bio rejuvenator in asphalt binder. Since, fingerprint region of asphalt binder and aromatic rejuvenator are composed of same functional groups, no distinctive peaks were observed when aromatic rejuvenator mixed with asphalt binder. Figure 68, 69, 70, and 71 showed the effect of bio rejuvenator and aromatic rejuvenator addition in unmodified binder, polymer modified binder, and RAP induced unmodified and polymer modified binder.

Quantitative Analysis

From the qualitative analysis, it was apparent that bio rejuvenator added two functional groups in asphalt binder which can be used for quantification of bio rejuvenator in asphalt binder. The fact that absorbance in ATR-FTIR spectra is linearly proportional to the concentration which directed to conduct a linear regression analysis based on the

absorbance intensity, absorbance height and absorbance area at wavenumber 1744 cm^{-1} and 1163 cm^{-1} , responsible for bio rejuvenation. The base lines for height and area measurement were drawn from wavenumber $1764\text{--}1720\text{ cm}^{-1}$ for C=O stretching vibration at 1744 cm^{-1} and $1200\text{--}1129\text{ cm}^{-1}$ for C-O stretching vibration at 1162 cm^{-1} . Table 19 and 20 showed the results of the regression analysis in these wavenumbers.

Figure 66. Absorbance spectra of aromatic rejuvenator in ATR-FTIR a) spectral region from $650\text{--}4000\text{ cm}^{-1}$ b) fingerprint spectral region from $650\text{--}1800\text{ cm}^{-1}$

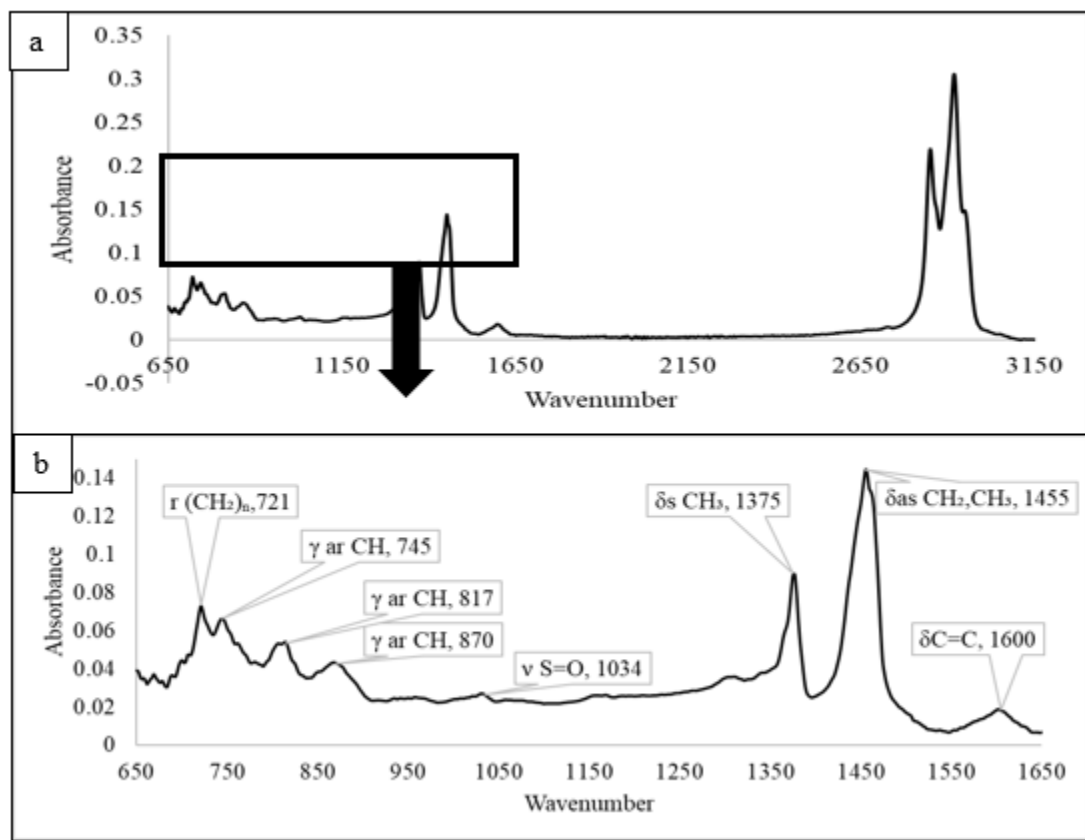
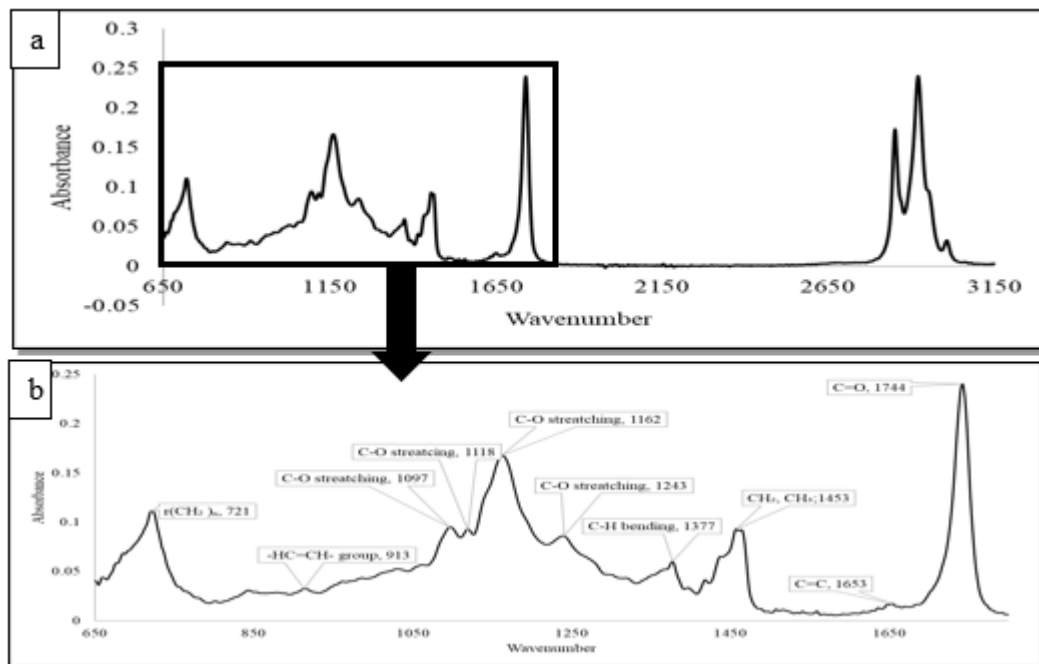


Figure 67. Absorbance spectra of bio rejuvenator in ATR-FTIR a) spectral region from 650-4000 cm^{-1} 1 b) fingerprint spectral region from 650- 1800 cm^{-1}



Results presented that absorbance height method exhibited a good linear relationship with R^2 ranges from 0.97 to 0.99 than the other two methods. It was also found that linear regression based on the stretching vibration of C=O (1744 cm^{-1}) was more fitted than the stretching vibration of C-O (1163 cm^{-1}). From these two-inference, additional conclusion was carried out based on the regression equation established from absorbance height measurement at wavenumber 1744 cm^{-1} . It is noted here that, slope and intercept of the regression line did not vary significantly when bio rejuvenator was added to the unmodified and polymer modified binder, which indicated that quantification of bio rejuvenator did not affect the presence of SBS polymer. Again, the addition of RAP binder caused a significant decrease in C=O functional group as well as slope and intercept of the regression equations. It suggested that quantification of bio rejuvenator can also be supportive to comment on if any RAP binder is added with the unmodified binder or polymer modified binder. A reduction in absorbance intensity of C=O stretching vibration occurs due to the addition of the RAP binder. This was caused by the electron distribution between the stretching vibrations of C=O at 1744 cm^{-1} and the adjacent 1694 cm^{-1} , which was responsible for oxidation in the RAP binder. Figure 72 and 73 showed the regression line at wavenumber 1744 cm^{-1} and 1162 cm^{-1} , respectively.

Figure 68. Effect of BR (bio rejuvenator) on unmodified and SBS-modified binder spectra in 650-1800 cm^{-1} spectral region

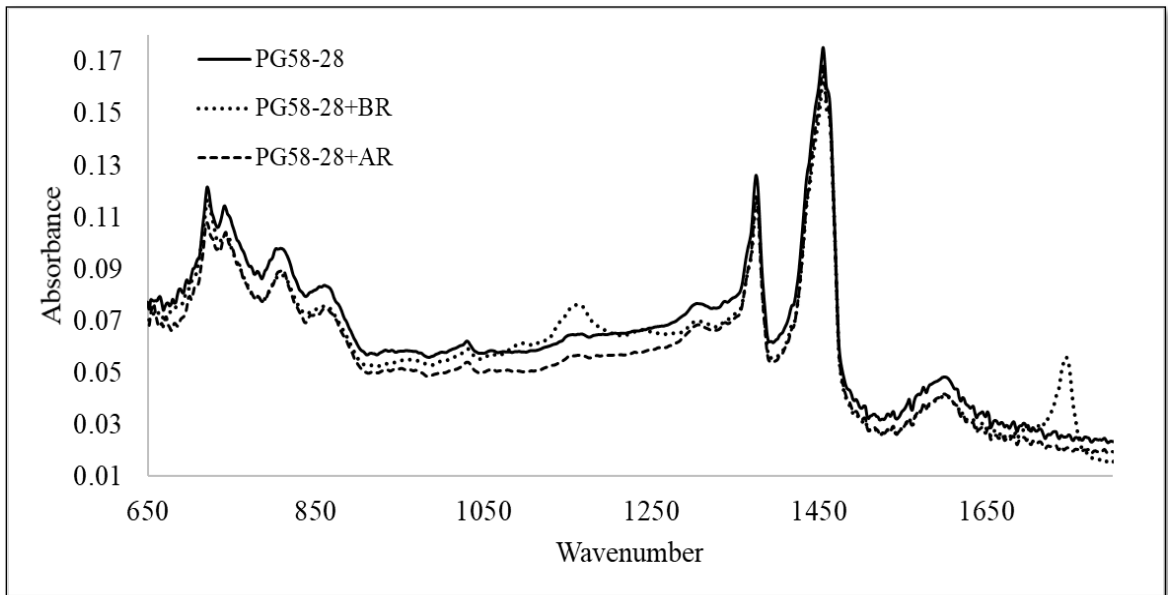


Figure 69. Effect of AR (aromatic rejuvenator) on unmodified and SBS-modified binder spectra in 650-1800 cm^{-1} spectral region

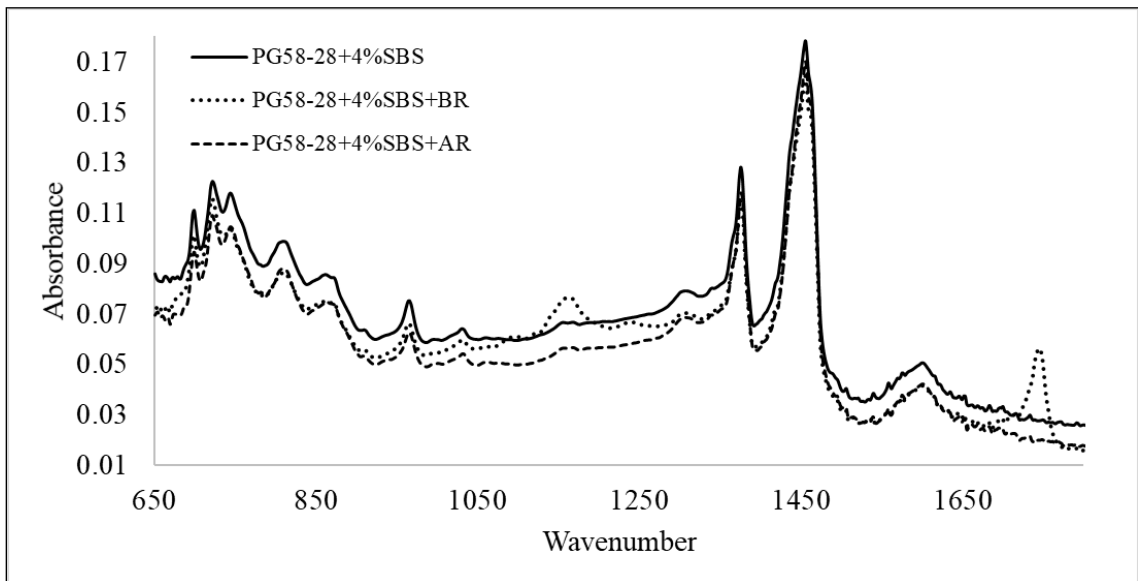


Table 19. Properties of linear regression curves due to bio rejuvenation process at 1744 cm⁻¹

Functional Group	Analysis Method	Samples	Regression Equation		
			Slope	Intercept	R ²
Stretching vibration of C=O at 1744cm ⁻¹	Absorbance value	UMB+BR	0.0161	0.0082	0.997
		PMB+BR	0.0147	0.0106	0.969
		20%RAP+UMB+BR	0.0056	0.0220	0.979
		20%RAP+PMB+BR	0.0064	0.0216	0.989
	Absorbance Height	UMB+BR	0.02	-0.01	0.994
		PMB+BR	0.02	-0.02	0.983
		20%RAP+UMB+BR	0.0055	-0.0055	0.970
		20%RAP+PMB+BR	0.0066	-0.0065	0.990
	Absorbance Area	UMB+BR	0.30	-0.24	0.992
		PMB+BR	0.31	-0.30	0.984
		20%RAP+UMB+BR	0.1072	-0.0796	0.968
		20%RAP+PMB+BR	0.1310	-0.1033	0.991

UMB= Unmodified binder; PMB= Polymer modified binder, BR= Bio Rejuvenator, AR= Aromatic Rejuvenator

Figure 70. Effect of BR (bio rejuvenator) on unmodified and SBS-modified binder spectra modified with 20% RAP binder in 650-1800 cm⁻¹ spectral region

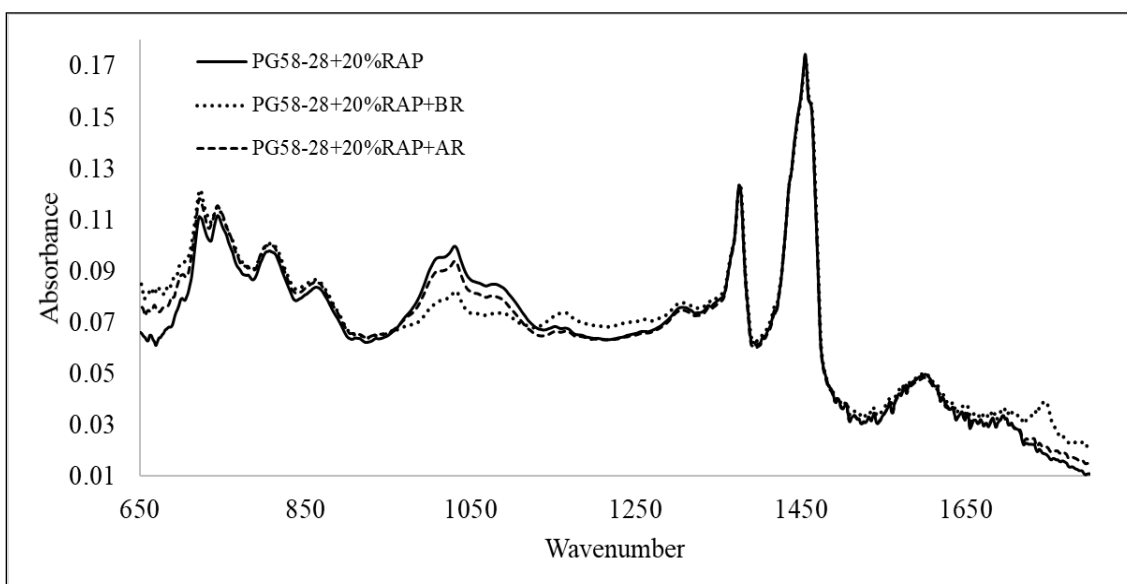


Figure 71. Effect of AR (aromatic rejuvenator) on unmodified and SBS-modified binder spectra modified with 20% RAP binder in 650-1800 cm⁻¹ spectral region

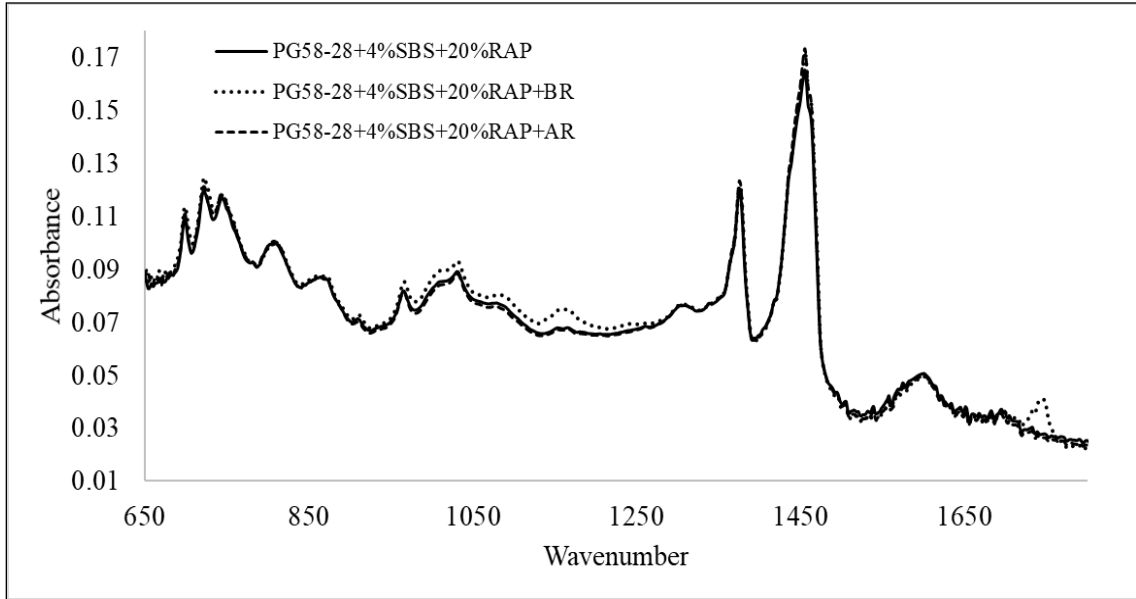


Table 20. Properties of linear regression curves due to bio rejuvenation process at 1162 cm⁻¹

Functional Group	Analysis Method	Samples	Regression Equation		
			Slope	Intercept	R ²
Stretching vibration of C-O at 1162 cm ⁻¹	Absorbance value	UMB+BR	0.0054	0.0598	1.000
		PMB+BR	0.0046	0.0612	0.811
		20% RAP+UMB+BR	0.0020	0.0674	0.906
		20% RAP+PMB+BR	0.0027	0.0668	0.990
	Absorbance Height	UMB+BR	0.0049	-0.0024	0.9976
		PMB+BR	0.0052	-0.0032	0.9808
		20% RAP+UMB+BR	0.0017	-0.0001	0.968
		20% RAP+PMB+BR	0.0021	-0.0006	0.978
	Absorbance Area	UMB+BR	0.11	0.08	0.945
		PMB+BR	0.18	-0.11	0.983
		20% RAP+UMB+BR	0.0627	-0.0083	0.962
		20% RAP+PMB+BR	0.0753	-0.0203	0.978

UMB= Unmodified binder; PMB= Polymer modified binder, BR= Bio Rejuvenator, AR= Aromatic Rejuvenator

Figure 72. Linear regression analysis for bio rejuvenated FT-IR spectra at wavenumber 1744 cm⁻¹

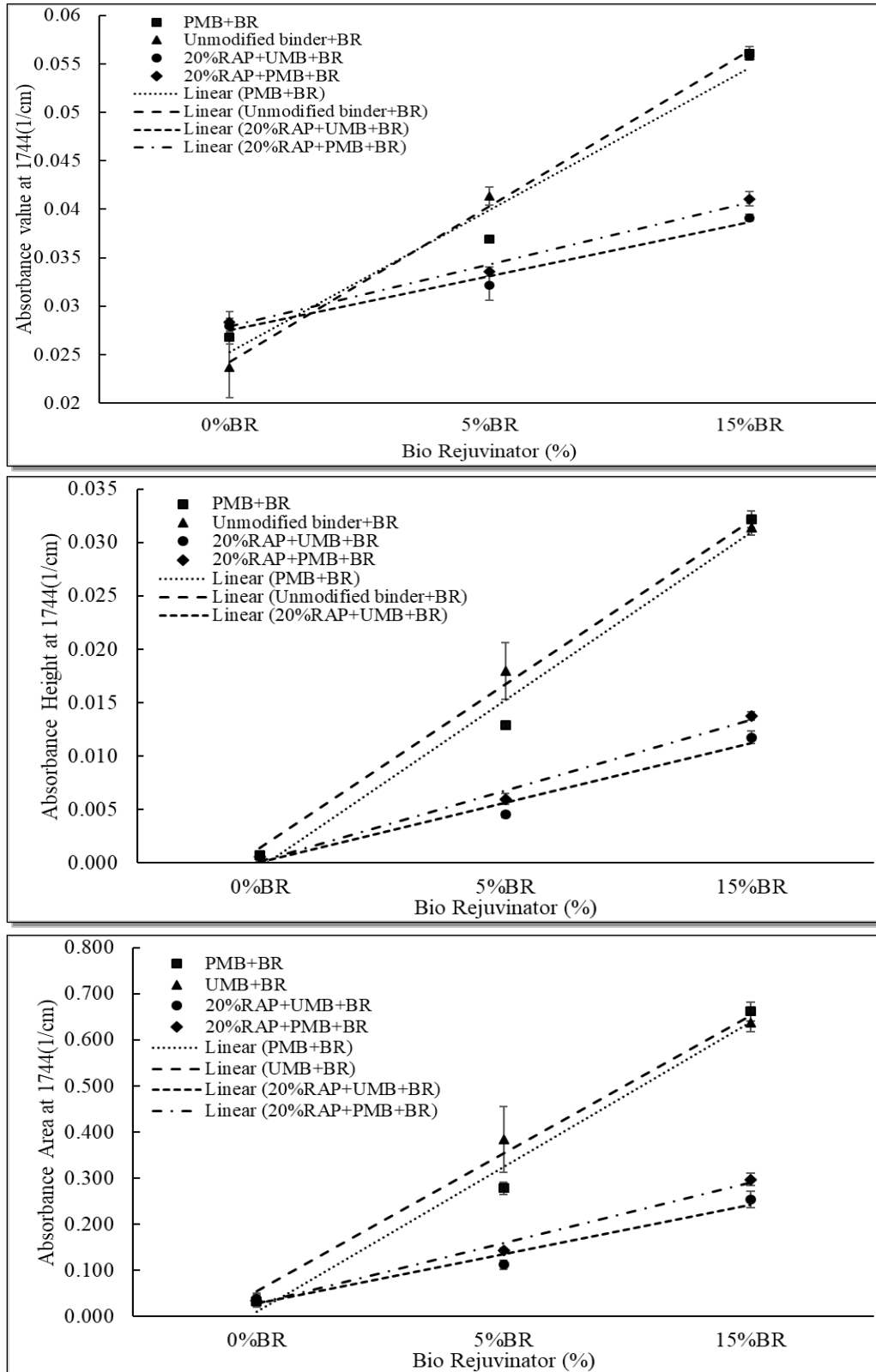
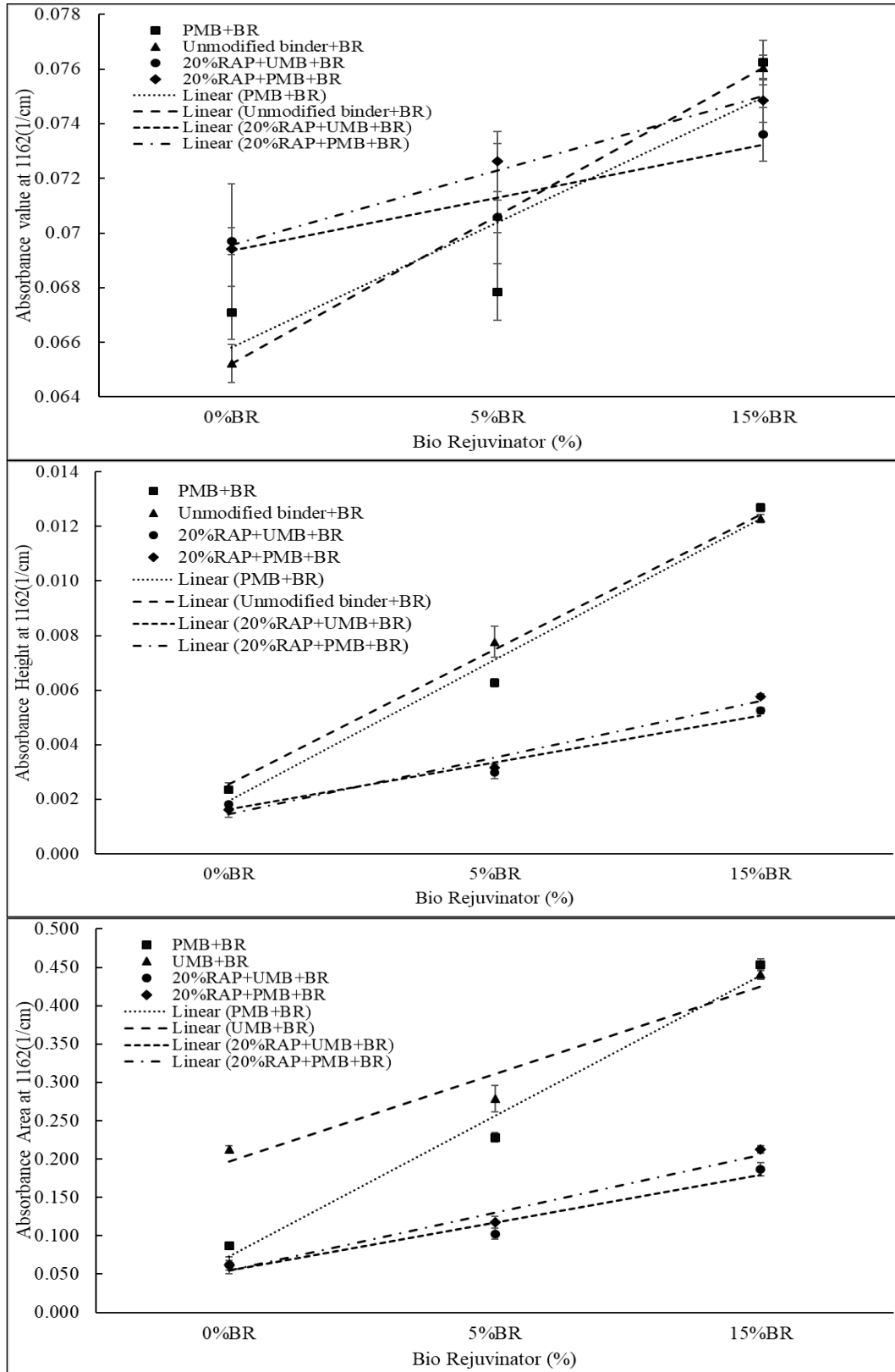


Figure 73. Linear regression analysis for bio rejuvenated FT-IR spectra at wavenumber 1162 cm⁻¹



Conclusions

Findings on Quantification of SBS Content

One of the principal goals of this study was to implement a handheld FT-IR spectrometer in the field to predict the SBS percentage in the modified asphalt binder for quality control. For predicting the SBS percentage, a universal curve was developed by linear regression analysis. The findings from this study are stated below-

1. From the qualitative analysis, it was found that SBS addition in asphalt binder incorporated two additional functional groups at 965 cm^{-1} accountable for polybutadiene block and at 699 cm^{-1} named as polystyrene block. However, the difference in SBS polymer structure (linear, radial, and diblock) and the addition of cross-linking agents (sulfur) did not add any new functional group in the asphalt binder. Also, peak shape and position were unaffected by these factors.
2. SBS quantification at 965 cm^{-1} was unaffected by the variation in base binder performance grades and sources, SBS polymer structures, and presence of cross-linking agent. Peak height measurement was found to be highly correlated with SBS concentration with a correlation value of 0.97.
3. Regression model developed in this study based on the peak height measurement and SBS concentration (%) exhibited prediction performance with $R^2=0.94$, $RMSE=0.0014$ and $MAE=0.0010$. In addition, percent error for predicting SBS concentration (%) in laboratory prepared samples was ranged from 0%-5%.
4. Prediction result of SBS (%) in Field measurement justified the specified SBS (%) range stated by the manufacturer. Also, the percentage error of the predicted SBS concentration (%) was 5% when the actual amount of SBS (%) was known. The total process for sample collection and data processing for SBS (%) prediction in each field demonstration required 15 minutes by the handheld FT-IR.

Findings on Degradation of SBS Due to Aging

The model developed earlier in this study to quantify the SBS content in the modified binder was used to predict the SBS content (%) in SBS-modified asphalt binder after RTFO and PAV aging. The following conclusions can be drawn from this study:

1. After RTFO and PAV aging, SBS content (%) decreased which indicated SBS polymer degraded after aging. After RTFO aging, 7.5-14.5% SBS content (%) was decreased and after PAV aging 16-30% SBS content (%) was decreased.
2. The result obtained from the predictive model for evaluating the degradation of SBS polymer due to aging was also verified by the novel DSR-based extensional deformation test method.

Findings on Selection of Asphalt Binder Aging Parameter

1. Both the carbonyl and sulfoxide functional groups in asphalt binder are affected by the aging process. The change in concentration of sulfoxide with the extent of asphalt binder or mixture aging was not consistent. Moreover, in case of mixture aging, the index values were influenced by the fines present in the mixture. Therefore, sulfoxide index should not be considered as a reliable indicator to quantify the aging rate of an asphalt binder or mixture.
2. Carbonyl index calculated by peak height ratio at wavenumber 1696 cm^{-1} to 2920 cm^{-1} provide accurate result to quantify laboratory binder and mix aging.
3. For quantification of RAP content in the mix, the area ratio at 1696 cm^{-1} to 1456 cm^{-1} yields more consistent results than the other indices.

Findings on Effect of Laboratory Binder and Mix Aging

A comparative study between four different types of aging (RTFO, PAV, UV and forced draft oven) was performed to understand the rheological and chemical behaviors of original and aged unmodified binder. For better understanding of asphalt binder aging in mixture, a detailed study was also performed. The following conclusions can be drawn:

1. Carbonyl index can successfully quantify binder and mix aging. For all types of laboratory aging methods, carbonyl index gradually increases with duration

- of aging. Rate of increase of I_{CO} is not linear; it rather slows down while the aging progresses.
2. A quick extraction process developed in this study can produce enough binder from the mix for testing in FT-IR.
 3. DCM solvent does not affect the absorbance value of the ATR spectra. So, this solvent is suitable for extraction of aged mix.
 4. In the case of UV and oven aging, I_{CO} increased up to a certain time then decreased. I_{CO} index of RTFO and PAV aged binders was the same at similar stiffness.
 5. FT-IR can precisely detect the presence of aged binder in the mix within a very short time and using a small amount of mix. So, the handheld FT-IR has the potential to be used as a quality control tool in the field.

Findings on RAP Content Determination

The other goal of this study is to implement the handheld FT-IR as a quality control tool in the field by monitoring the quantity of added RAP. FT-IR spectral analysis was performed on plant produced mix as well as RAP to estimate the RAP content in fresh mix. Laboratory aged binder and mix were analyzed at the beginning to comprehend and compare the aging processes in terms of carbonyl index. From this study, the following conclusions can be drawn:

1. Generally available RAPs possess much higher carbonyl index than that of the laboratory aged binder or mix. But laboratory aged asphalt shows higher stiffness than the RAPs at similar carbonyl content. FT-IR can be used for screening of RAP based on their extent of aging.
2. The carbonyl index of a mix increases linearly with increase in the RAP content. This linear relationship can be utilized to determine the RAP content in the mix.
3. FT-IRS can successfully determine the RAP content in the mix within $\pm 5\%$ range of the design RAP content.
4. Mix sample should be collected from the outlet of the drum before it reaches to the silo to minimize the effect of short-term aging.
5. This study indicates that handheld FT-IRS has the potential to be used as an effective quality control tool.

Findings on Identification and Quantification of Rejuvenator

The performance of the handheld FT-IR as an individual technique in identification and quantification of the bio and aromatic rejuvenator in asphalt binder was focused on in this study. Since chemical characterization of the rejuvenator is a demanding phenomenon, FT-IR showed its applicability to differentiate between aromatic and bio rejuvenator by analyzing their functional group incorporated in the asphalt binder. The key findings of this study are listed below:

1. From the qualitative analysis of the FT-IR spectra, it was apparent that bio rejuvenator added two functional groups (at 1744 cm^{-1} and at 1162 cm^{-1}) which can be used to identify bio rejuvenator in asphalt samples.
2. Absorbance height method showed good linear relationship with a R^2 value of 0.96 in quantifying bio rejuvenator in asphalt binder.
3. The quantification process of the bio rejuvenator having no effect due the presence of polymer (SBS). On the other hand, presence of RAP having significant effect on the bio rejuvenator quantity.
4. Unlike bio rejuvenator, aromatic rejuvenator did not add any significant functional group in the asphalt binder.

Recommendations

Ten plant RAP mixes that were utilized in this study that justifies the viability of using a handheld FT-IR spectrometer for quality control of SBS-modified asphalt binder and RAP mixes. A handheld FT-IR spectrometer can determine the percent of SBS/SB in asphalt binder and percent of RAP content in RAP mixes in the field precisely, accurately, and quickly. The outcome of this study is immediately implementable. The authors would like to recommend the use of FT-IR spectrometer following the procedure used in this study.

The authors used the ATR-FT-IR method that needs binder or extracted binder. The authors proposed a 15-min field extraction method. The ATR-FT-IR method was performed because of higher accuracy in the ATR method compared to the DR method. In the future, further study should be performed on DR-FT-IR (diffuse reflectance) method so that the 15-min field extraction process can be eliminated.

The FT-IR method has the potential to be used for pavement maintenance purposes. Thresholds can be developed using aging indices that will trigger maintenance actions. Also, investigations need to be performed on the potential use of the FT-IR spectrometer for identifying cracking susceptible, extremely aged surfaces. Forensic analyses can be performed using the FT-IR method to find the possible causes of premature failure. In forensic analyses, the FT-IR method can detect segregation of polymer, degradation of polymer, excessive usage of RAP, extremely oxidized RAP usage, presence of rejuvenators, etc.

Based on the findings of this study, the authors recommend immediate implementation of the FT-IR spectrometer as well as studies for viability of extensive usage of a handheld FT-IR spectrometer in various potential other applications as mentioned before.

Acronyms, Abbreviations, and Symbols

Term	Description
AASHTO	American Association of State Highway and Transportation Officials
ATR	Attenuated Total Reflectance
CV	Coefficient of Variation
DCM	Dichloromethane
DOTD	Louisiana Department of Transportation and Development
DR	Diffuse Reflectance
DSR	Dynamic Shear Rheometer
FHWA	Federal Highway Administration
FT-IR	Fourier Transform Infrared Spectroscopy
HMA	Hot Mix Asphalt
LTRC	Louisiana Transportation Research Center
LTOA	Long-term Oven Aging
NMN	Nonmodified Nano Clay
NS	Nano Silica
PAV	Pressure Aging Vessel
PG	Performance Grade
PMN	Polymer Modified Nano Clay
PPA	Polyphosphoric Acid
RAP	Reclaimed Asphalt Pavement
RTFO	Rolling Thin Film Oven Aging
SBS	Styrene-Butadiene-Styrene
SBSMA	SBS-modified Asphalt
UV	Ultra-violet
WMA	Warm Mix Asphalt

References

- [1] Ren, R., Han, K., Zhao, P., Shi, J., Zhao, L., Gao, D., and Yang, Z. (2019). Identification of Asphalt Fingerprints Based on Atr-Ftir Spectroscopy and Principal Component-Linear Discriminant Analysis. *Construction and Building Materials*, 198, 662-668.
- [2] Hou, X., Lv, S., Chen, Z., and Xiao, F. (2018). Applications of Fourier Transform Infrared Spectroscopy Technologies on Asphalt Materials. *Measurement*, 121, 304-316.
- [3] Cortizo, M. S., Larsen, D. O., Bianchetto, H., and Alessandrini, J. L. (2004). "Effect of the Thermal Degradation of SBS Copolymers During the Ageing of Modified Asphalts." *Polymer Degradation and Stability*, 86: 275-282.
- [4] Zhao, Y., Gu, F., Xu, J., and Jin, J. (2010). Analysis of Aging Mechanism of SBS Polymer Modified Asphalt Based on Fourier Transform Infrared Spectrum. *Journal of Wuhan University of Technology-Mater. Sci. Ed.*, 25(6), 1047-1052.
- [5] Singh, B., and Kumar, P. (2019). Effect of Polymer Modification on the Ageing Properties of Asphalt Binders: Chemical and Morphological Investigation. *Construction and Building Materials*, 205, 633-641.
- [6] Huang, W., Yan, C., and Jiang, X. (2019). Chemical and Rheology Evaluation on The Field Short-Term Aging of High Content Polymer Modified Asphalt. Presented at 98th Annual Meeting of the Transportation Research Board, Washington, D. C., 2019.
- [7] Li, Y., Moraes, R., Lyngdal, E., and Bahia, H. (2016). Effect of Polymer and Oil Modification on the Aging Susceptibility of Asphalt Binders. *Transportation Research Record*, 2574(1), 28-37.
- [8] Tang, N., Huang, W., and Xiao, F. (2016). Chemical and Rheological Investigation of High-Cured Crumb Rubber-Modified Asphalt. *Construction and Building Materials*, 123, 847-854.

- [9] Wang, C., and Wang, Y. (2019). Physico-Chemo-Rheological Characterization of Neat and Polymer-Modified Asphalt Binders. *Construction and Building Materials*, 199, 471-482.
- [10] Mansourkhaki, A., Ameri, M., and Daryaei, D. (2019). Application of Different Modifiers for Improvement of Chemical Characterization and Physical-Rheological Parameters of Reclaimed Asphalt Binder. *Construction and Building Materials*, 203, 83-94.
- [11] Yusoff, N. I. M., Alhamali, D. I., Ibrahim, A. N. H., Rosyidi, S. A. P., and Hassan, N. A. (2019). Engineering Characteristics of Nanosilica/Polymer-Modified Bitumen and Predicting their Rheological Properties using Multilayer Perceptron Neural Network Model. *Construction and Building Materials*, 204, 781-799.
- [12] AASHTO T302, (2015). Standard Method of Test for Polymer Content of Polymer-Modified Emulsified Asphalt Residue and Asphalt Binders, American Association of State Highway and Transportation Officials (AASHTO).
- [13] Lu, X., and Isacsson, U. (2000). "Artificial Aging of Polymer Modified Bitumens." *Journal of Applied Polymer Science*, 76(12):1811–24.
- [14] Zhang, F., Yu, J., and Han, J. (2011). "Effects of Thermal Oxidative Ageing on Dynamic Viscosity, TG/DTG, DTA And FTIR of SBS- and SBS/Sulfur-Modified Asphalts." *Construction and Building Materials*, 25(1): 129-137.
- [15] Kaseer, F., A. E. Martin, and E. Arámbula-Mercado (2019). "Use of Recycling Agents in Asphalt Mixtures with High Recycled Materials Contents in The United States: A Literature Review." *Constr. Build. Mater.*, 211, <https://doi.org/10.1016/j.conbuildmat.2019.03.286>.
- [16] Chen, J. S., Liao, M. C., and Shiah, M. S. (2002). "Asphalt Modified by Styrene–Butadiene–Styrene Triblock Copolymer: Morphology and Model." *Journal of Materials In Civil Engineering*, 14(3): 224–9.
- [17] Abdelaziz, A., Ho, C. H., and Snyder, M. (2018). "Evaluating the Influence of Polymer Modified Asphalt Binders on Low Temperature Properties." *MATEC Web Of Conferences*, 2018. 163: 05012.

- [18] Liang, Y., Wu, R., Harvey, J. T., Jones, D., and Alavi, M. Z. (2019). Investigation into the Oxidative Aging of Asphalt Binders. *Transportation Research Record*, 0361198119843096.
- [19] Davis, R., and Mauer, L. J. (2010). Fourier Transform Infrared (FT-IR) Spectroscopy: A Rapid Tool for Detection and Analysis of Foodborne Pathogenic Bacteria. Current Research, *Technology And Education Topics In Applied Microbiology And Microbial Biotechnology*, 2, 1582-1594.
- [20] Derrick, M. R., Stulik, D., and Landry, J. M. (2000). Infrared Spectroscopy in Conservation Science. Getty Publications.
- [21] Birkel, E., and Rodriguez-Saona, L. (2011). Application of a Portable Handheld Infrared Spectrometer for Quantitation of Trans Fat in Edible Oils. *Journal Of The American Oil Chemists' Society*, 88(10), 1477-1483.
- [22] Hu, K., Han, S., Liu, Z., and Niu, D. (2018). Determination of Morphology Characteristics of Polymer-Modified Asphalt by a Quantification Parameters Approach. *Road Materials And Pavement Design*, 1-16.
- [23] Singh, S. K., Kumar, Y., and Ravindranath, S. S. (2018). Thermal Degradation of SBS in Bitumen During Storage: Influence of Temperature, SBS Concentration, Polymer Type and Base Bitumen. *Polymer Degradation And Stability*, 147, 64-75.
- [24] Wang, Y., Chong, D., and Wen, Y. (2017). Quality Verification of Polymer-Modified Asphalt Binder used in Hot-Mix Asphalt Pavement Construction. *Construction And Building Materials*, 150, 157-166.
- [25] Wang, K., Yuan, Y., Han, S., and Yang, Y. (2017). Application of FTIR Spectroscopy with Solvent-Cast Film and PLS Regression for the Quantification of SBS Content in Modified Asphalt. *International Journal of Pavement Engineering*, 1-6.
- [26] Ye, Z. C., Chen, D., Ling, C., and Guan, F. Y. (2015). Quantifying Sbs Content in Modified Asphalt using Fourier Transform Infrared Spectroscopy. *In Advanced Materials Research* (Vol. 1065, Pp. 691-695). Trans Tech Publications.

- [27] Lu, Q., Gunaratne, M., and Guo, L. (2015). Field Test Method to Determine Presence and Quantity of Modifiers in Liquid Asphalt (No. BDV25-977-06). Florida. Dept. of Transportation.
- [28] Masson, J. F., Pelletier, L., and Collins, P. (2001). Rapid FTIR Method for Quantification of Styrene-Butadiene Type Copolymers in Bitumen. *Journal of Applied Polymer Science*, 79(6), 1034-1041.
- [29] Zhao, Y., Gu, F., Xu, J., and Jin, J. (2010). "Analysis of Aging Mechanism of SBS Polymer Modified Asphalt Based on Fourier Transform Infrared Spectrum." *Journal of Wuhan University of Technology-Mater. Sci. Ed.*, 25(6), 1047-1052.
- [30] Lu, X., and Isacsson, U. (1998). "Chemical and Rheological Evaluation of Ageing Properties of SBS Polymer Modified Bitumens." *Fuel*, 77(9–10): 961-972.
- [31] Zhang, D., Zhang, H. and Shi, C. (2017). "Investigation of Aging Performance of SBS-Modified Asphalt with Various Aging Methods." *Construction and Building Materials*, 145: 445-451.
- [32] Wu, S., Pang, L., Mo, L., Chen, Y., and Zhu, G. (2009). "Influence of Aging on The Evolution of Structure, Morphology and Rheology of Base and SBS-Modified Bitumen." *Construction and Building Materials*, 23(2) 1005-1010.
- [33] Nivitha, M., Prasad, E. and Krishnan, J. (2016). "Ageing in Modified Bitumen Using FTIR Spectroscopy." *Int. J. Pavement Eng.* 17(7): 565-577.
- [34] Marsac, P., Piérard, N., Porot, L., Grenfell, J., Mouillet, V., Pouget, S., Besamusca, J., Farcas, F., Gabet, T. and Hugener, M. (2014). "Potential and Limits of FTIR Methods for Reclaimed Asphalt Characterisation." *Mater. Struct.* 47(8): 1273-1286.
- [35] Yao, H., Dai, Q. and You, Z. (2015). "Fourier Transform Infrared Spectroscopy Characterization of Aging-Related Properties of Original and Nano-Modified Asphalt Binders." *Constr. Build. Mater.* 101: 1078-1087.

- [36] Zofka, A. (2013). Evaluating Applications of Field Spectroscopy Devices to Fingerprint Commonly used Construction Materials. Transportation Research Board.
- [37] Yut, I. and Zofka, A. (2011). "Attenuated Total Reflection (ATR) Fourier Transform Infrared (FT-IR) Spectroscopy of Oxidized Polymer-Modified Bitumens." *Appl. Spectrosc.* 65(7): 765-770.
- [38] Salomon, D., and I. Yut. (2016). Monitoring Oxidation Signals of Asphalt Pavement Surfaces by Portable Infrared Spectroscopy: In-Situ Testing of % RAP in HMA. Presented at Construction and Materials Subcommittee Meeting, Western Association Of State Highway And Transportation Officials (WASHTO), Salt Lake City, Utah.
- [39] Dehdezi, P. K., and J. Tuck. (2014). Optical Spectroscopy of Binder Condition at Traffic Speed. Publication ARPS 223(4/45/12), Prepared For The Highways England.
- [40] Bowers, B. F., Huang, B., Shu, X. and Miller, B. C. (2014). "Investigation of Reclaimed Asphalt Pavement Blending Efficiency Through GPC and FTIR." *Constr. Build. Mater.* 50: 517-523.
- [41] Sun, L., Wang, Y. and Zhang, Y. (2014). "Aging Mechanism and Effective Recycling Ratio of SBS-Modified Asphalt." *Constr. Build. Mater.* 70: 26-35.
- [43] Martin, K. L., Davison, R. R., Glover, C. J., and Bullin, J. A. (1990). Asphalt Aging in Texas Roads and Test Sections. *Transportation Research Record*, 1269, 9–19.
- [44] Liu, F., Zhou, Z, Wang, Y. (2019). Predict the Rheological Properties of Aged Asphalt Binders using a Universal Kinetic Model. *Construction And Building Materials*, 195, 283-291.
- [45] Zhang, H., Chen, Z., Xu, G., and Shi, C. (2018). Evaluation of Aging Behaviors of Asphalt Binders through Different Rheological Indices. *Fuel*, 221, 78-88.
- [46] Glover, C. J., A. E. Martin, A. Chowdhury, R. Han, N. Prapaitrakul, X. Jin, and J. Lawrence. (2009). Evaluation of Binder Aging and Its Influence in Aging of Hot

Mix Asphalt Concrete: Literature Review and Experimental Design (No. FHWA/TX-08/0-6009-1). Texas Transportation Institute.

- [47] Fernandez-Berridi, M.J., N. Gonzalez, A. Mugica, and C. Bernicot. (2006). Pyrolysis-FTIR and TGA Techniques As Tools In The Characterization Of Blends Of Natural Rubber And SBR. *Thermochimica Acta*, Vol. 444, No. 1, Pp. 65-70.
- [48] Hossain, R., and Wasiuddin, N. M. (2019). "Evaluation of Degradation of SBS-Modified Asphalt Binder because of RTFO, PAV, and UV Aging Using a Novel Extensional Deformation Test." *Transportation Research Record*, 2673(6), 447–457. <https://doi.org/10.1177/0361198119847471>
- [49] Huang, S. C., and W. Grimes. (2010). "Influence of Aging Temperature on Rheological and Chemical Properties of Asphalt Binders." *Transp. Res. Rec.*, 2179(1), <https://doi.org/10.3141/2179-05>.
- [50] Qin, Q., J. F. Schabron, R. B. Boysen, and M. J. Farrar. 2014. "Field Aging Effect on Chemistry and Rheology of Asphalt Binders and Rheological Predictions for Field Aging." *Fuel*, 121, <https://doi.org/10.1016/j.fuel.2013.12.040>
- [51] Ge, D., S. Chen, Z. You, X. Yang, H. Yao, M. Ye, and Y. K. Yap, 2019. "Correlation of DSR Results and FTIR's Carbonyl and Sulfoxide Indexes: Effect of Aging Temperature on Asphalt Rheology." *J. Mater. Civ. Eng.*, 31(7), [https://doi.org/10.1061/\(ASCE\)MT.1943-5533.0002781](https://doi.org/10.1061/(ASCE)MT.1943-5533.0002781)
- [52] Jing, R., A. Varveri, X. Liu, T. Scarpas, and S. Erkens. (2018). "Chemo-Mechanics of Ageing on Bituminous Materials." In 97th Annual Meeting Of The Transp. Res. Board, Washington, DC.
- [53] Hofko, B., L. Porot, A. F. Cannone, L. Poulidakos, L. Huber, X. Lu, and H. Grothe. (2018). "FTIR Spectral Analysis of Bituminous Binders: Reproducibility and Impact of Ageing Temperature." *Mater. Struct.*, 51(2), <https://doi.org/10.1617/S11527-018-1170-7>
- [54] Hung, A.M. and Fini, E.H. (2019). Absorption Spectroscopy to Determine the Extent and Mechanisms of Aging in Bitumen and Asphaltenes. *Fuel*, 242, Pp.408-415.

- [55] Kaveh, F., and S. A. Hesp. (2011). “Spectroscopic Analysis of Pressure Aging Vessel Protocols for The Accelerated Laboratory Aging of Asphalt Cements.” In *Proc., 1st Conf. Of Transp. Res. Group Of India*, Bangalore, India
- [56] Nguyen, D., Haghshenas Fatmehsari, H., Kommidi, S., and Kim, Y. R. (2016). Optimizing Chemical & Rheological Properties of Rejuvenated Bitumen.
- [57] Zhu, H., Xu, G., Gong, M., and Yang, J. (2017). Recycling Long-Term-Aged Asphalts using Bio-Binder/Plasticizer-Based Rejuvenator. *Construction and Building Materials*, 147, 117-129.
- [58] Cavalli, M. C., Zaumanis, M., Mazza, E., Partl, M. N., and Poulikakos, L. D. (2018). Effect of Ageing on the Mechanical and Chemical Properties of Binder from RAP Treated with Bio-Based Rejuvenators. *Composites Part B: Engineering*, 141, 174-181.
- [59] Zhang, R., You, Z., Wang, H., Ye, M., Yap, Y. K., and Si, C. (2019). The Impact of Bio-Oil as Rejuvenator for Aged Asphalt Binder. *Construction and Building Materials*, 196, 134-143.
- [60] Cai, X., Zhang, J., Xu, G., Gong, M., Chen, X., and Yang, J. (2019). Internal Aging Indexes to Characterize the Aging Behavior of Two Bio-Rejuvenated Asphalts. *Journal Of Cleaner Production*, 220, 1231-1238.
- [61] Whelan, A., and Whelan, T. (1994). *Polymer Technology Dictionary*. Springer Science & Business Media.
- [62] Behnood, A., and Gharehveran, M. M. (2018). Morphology, Rheology and Physical Properties of Polymer-Modified Asphalt Binders. *European Polymer Journal*.
- [63] Marcelo, M. C. A., Mariotti, K. C., Ferrão, M. F., and Ortiz, R. S. (2015). Profiling Cocaine by ATR–FTIR. *Forensic Science International*, 246, 65-71.
- [64] Diefenderfer, S. (2006). Detection of Polymer Modifiers in Asphalt Binder. Publication FHWA/VTRC 06-R18, A Cooperative Organization Sponsored Jointly By The Virginia Department Of Transportation And The University Of Virginia, Charlottesville, Virginia.

- [65] Ghebremeskel, G.N. and S. R. Shield. (2003). Characterization of Binary/Tertiary Blends of SBR, NBR and PVC by IR Spectroscopy. *Rubber World*, Vol. 227, No. 4, Pp. 26-46.
- [66] Curtis, C.W., D. I. Hanson, S. T. Chen, G. J. Shieh, and M. Ling. (1995). Quantitative Determination of Polymers in Asphalt Cements and Hot-Mix Asphalt Mixes. In *Transportation Research Record*, Pp. 52-61.
- [67] Nasrazadani, S., D. Mielke, T. Springfield, and N. Ramasamy. (2010). Practical Applications of FTIR to Characterize Paving Materials. Publication FHWA/TX-11/0-5608-1. University Of North Texas, Denton, Texas, Texas Department Of Transportation.
- [68] Tazreiter, M., Christian, P., Schennach, R., Grießer, T., and Coclite, A. M. (2017). Simple Method for The Quantitative Analysis of Thin Copolymer Films On Substrates by Infrared Spectroscopy Using Direct Calibration. *Analytical Methods*, 9(36), 5266-5273.
- [69] Xue, Y., Hu, Z., Wang, C., and Xiao, Y. (2019). "Evaluation of Dissolved Organic Carbon Released from Aged Asphalt Binder in Aqueous Solution." *Construction and Building Materials*, 218 465-476.
<https://doi.org/10.1016/j.conbuildmat.2019.05.060>.
- [70] Yut, I., Bernier, A. and Zofka, A. (2015). "Field Applications of Portable Infrared Spectroscopy to Asphalt Products." *Introduction To Unmanned Aircraft Systems*: 127.
- [71] Chen, C., F. Yin, P. Turner, R. C. West, and N. Tran. (2018). "Selecting A Laboratory Loose Mix Aging Protocol for The NCAT Top-Down Cracking Experiment." *Transp. Res. Rec.*, 2672(28),
<https://doi.org/10.1177/0361198118790639>.
- [72] Munteanu, S. B., and Vasile, C. (2005). Spectral and Thermal Characterization of Styrene-Butadiene Copolymers with Different Architectures. *Journal Of Optoelectronics And Advanced Materials*, 7(6), 3135.

- [73] Lee, L. C., Liong, C. Y., and Jemain, A. A. (2017). A Contemporary Review On Data Preprocessing (DP) Practice Strategy in ATR-FTIR Spectrum. *Chemometrics And Intelligent Laboratory Systems*, 163, 64-75.
- [74] Hofko, B., Alavi, M. Z., Grothe, H., Jones, D., and Harvey, J. (2017). Repeatability and Sensitivity of FTIR ATR Spectral Analysis Methods for Bituminous Binders. *Materials And Structures*, 50(3), 187.
- [75] Cook, R. D. (1979). Influential Observations in Linear Regression. *Journal Of The American Statistical Association*, 74(365), 169-174.
- [76] Bruce, P., and Bruce, A. (2017). Practical Statistics for Data Scientists: 50 Essential Concepts. " O'Reilly Media, Inc."
- [77] James, G., Witten, D., Hastie, T., and Tibshirani, R. (2013). An Introduction to Statistical Learning (Vol. 112, P. 18). New York: Springer.
- [78] Petersen, J. C. and R. Glaser. 2011. "Asphalt Oxidation Mechanisms and the Role of Oxidation Products on Age Hardening Revisited

Appendix

APPENDIX A: Quick Extraction Process in the Field

- [1] Loose asphalt mix is collected in the plant. Loose mix can be collected either from the truck or from the outlet of the mixing drum. The mix needs to be air cooled for enough time to reach an ambient temperature. During the air-cooling process, the mix should be stirred frequently to prevent sticking to the pan.

Figure A 1. Collection of loose mix



- [2] When the mix reaches to ambient temperature, around 100 grams of loose mix is poured into a mason jar. The size of the jar used in this study was 16 oz. The size of the jar should be chosen in a way that the height of the loose mix in the jar should be around 1 in.

Figure A 2. Pour the mix into the mason jar



[3] Dichloromethane (DCM) is used as a solvent to extract the binder from the mix. Around 100 milliliters of DCM is poured into the jar containing the loose mix. Immediately after pouring the DCM, the jar should be shaken well for around 30 seconds. After that the jar should be left for five minutes to get the binder dissolved into the solvent.

Figure A 3. Pour the mix into the mason jar



[4] After five minutes, the solvent with dissolved asphalt was filtered through an 80-micron nylon mesh. Proper care should be taken so that the filter is not clogged by the fine particles drained from the jar. The liquid is collected on a wide metal pan. In this case, a 5-in. metal pan was used to collect the filtered liquid.

Figure A 4. DCM with dissolved asphalt binder is being filtered



[5] The pan was kept on a table at an open space in the plant. Because the place was open, it was nicely ventilated. Most of the DCM evaporated within five minutes. After five more minutes, 10 minutes after filtration, all the DCM was evaporated and the binder residue was left on the metal pan. The amount of the binder was enough to record the FT-IR spectra for 10 replicates.

Figure A 5. Most of the DCM is evaporated (left), all the DCM is evaporated in 10 minutes (right)



[6] Binder residue is collected using a spatula and placed on the diamond crystal of the FT-IR for recording the spectra.

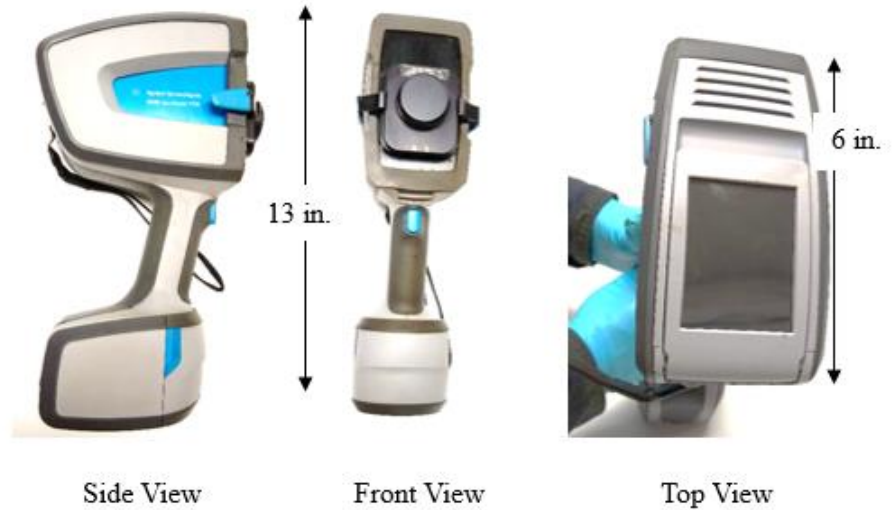
Figure A 6. Sample is placed on the diamond crystal



APPENDIX B: Instruction of Operation of Handheld FT-IR

STEP 1

The figure shows the Agilent 4300 Handheld FTIR viewed from different angles.



STEP 2

Insert two batteries into the slot to operate the equipment at any place without AC power supply. Then turn the power 'ON.'



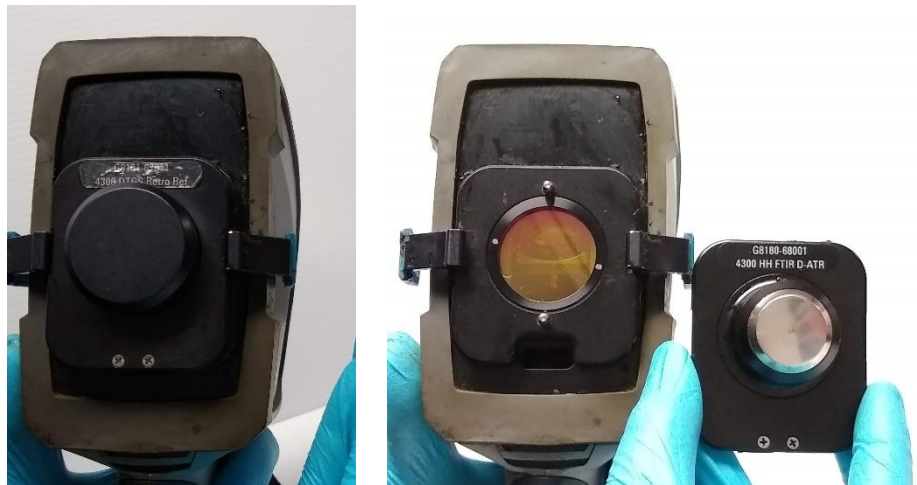
STEP 3

The screen of the handheld FT-IR will appear like this. Insert the password and press 'login.'



STEP 4

Replace the cover by a Diamond ATR fixture.



STEP 5

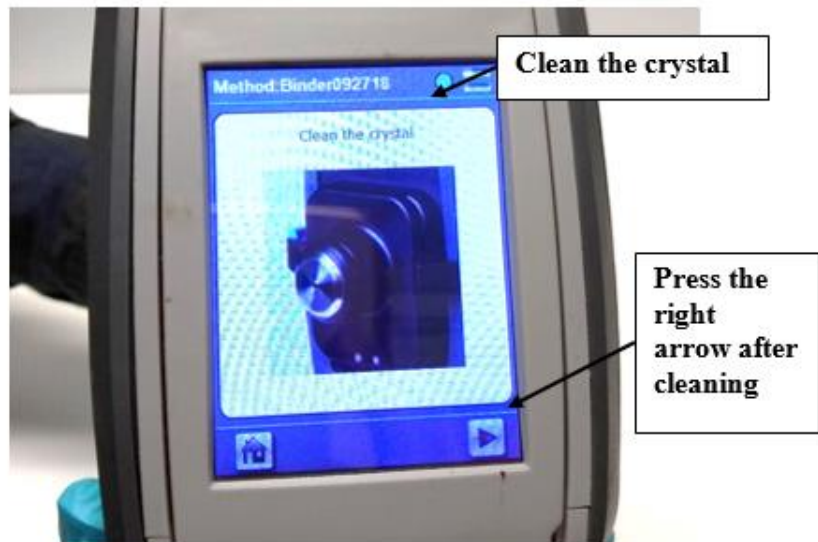
Press on 'Start'
to begin the
data collection.



STEP 6

The system
will ask to
clean the
crystal.

Time required
for the step: 3
min.



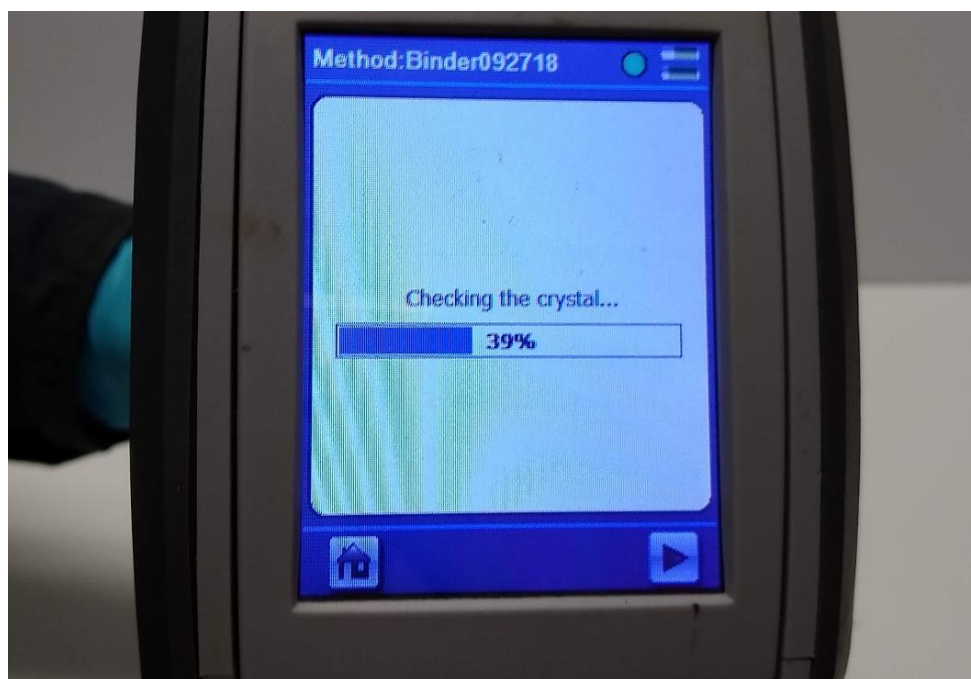
STEP 7

Clean the crystal gently using a paper towel soaked with isopropyl alcohol.



STEP 8

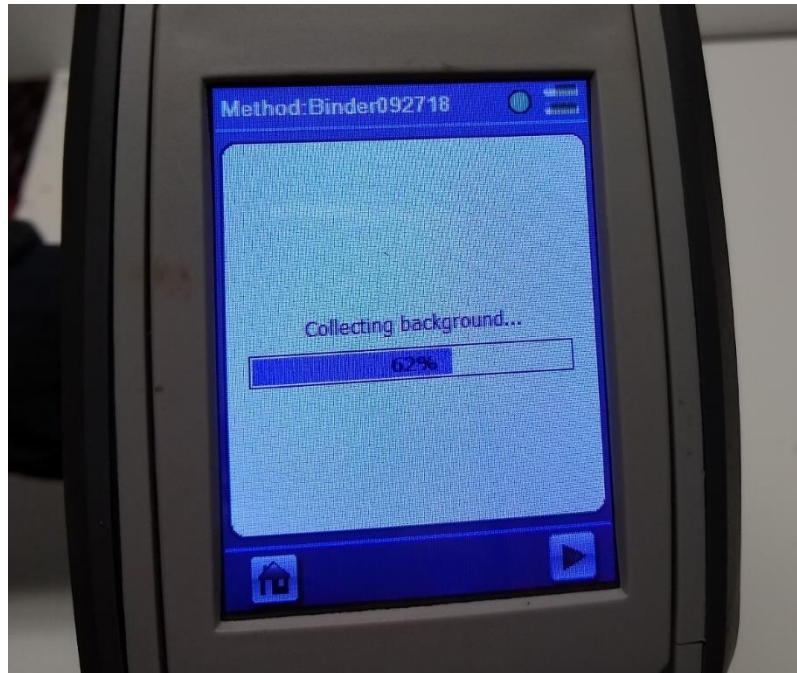
The system will check the crystal.



STEP 9

The system will then collect the background spectra automatically.

Time required for the step: 1 min.



STEP 10

After the collection of background, the software will ask for the sample.

Ensure contact with sample



STEP 11

The binder is kept on a hot plate during the data collection time. A small amount (around 1 gram) of liquid binder is collected using a spatula.



STEP 12

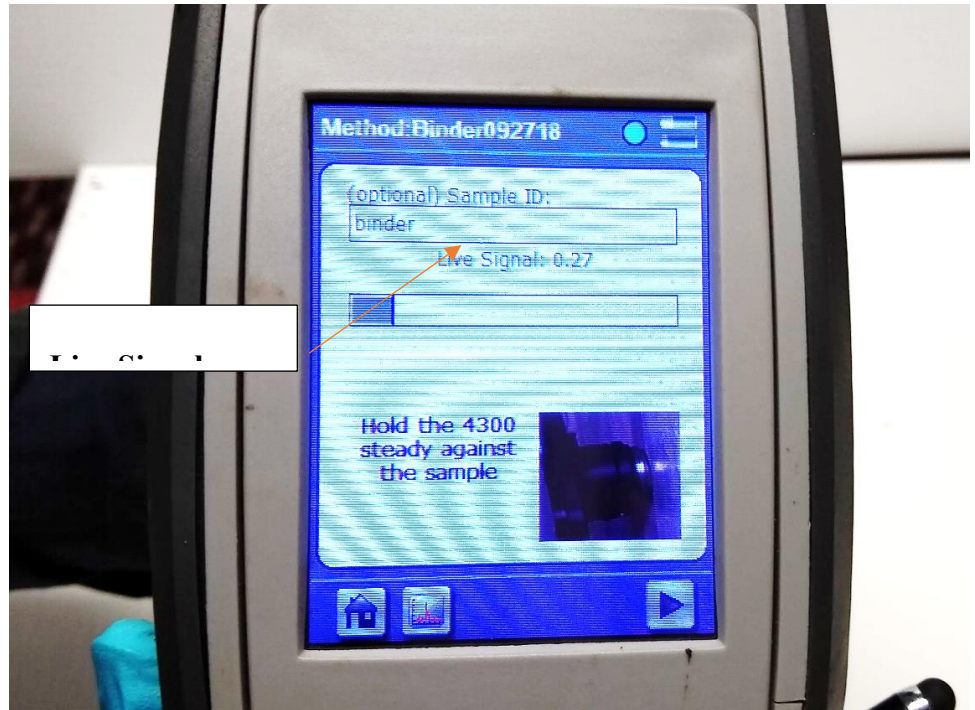
The binder is placed on the diamond crystal of the ATR sensor instantly.

Time required for the step: 1 min.



STEP 13

If the contact is perfect, the live signal value will show above 0.10. The equipment is now ready to collect the spectra. At this point, a sample name should be inserted for future reference.



STEP 14

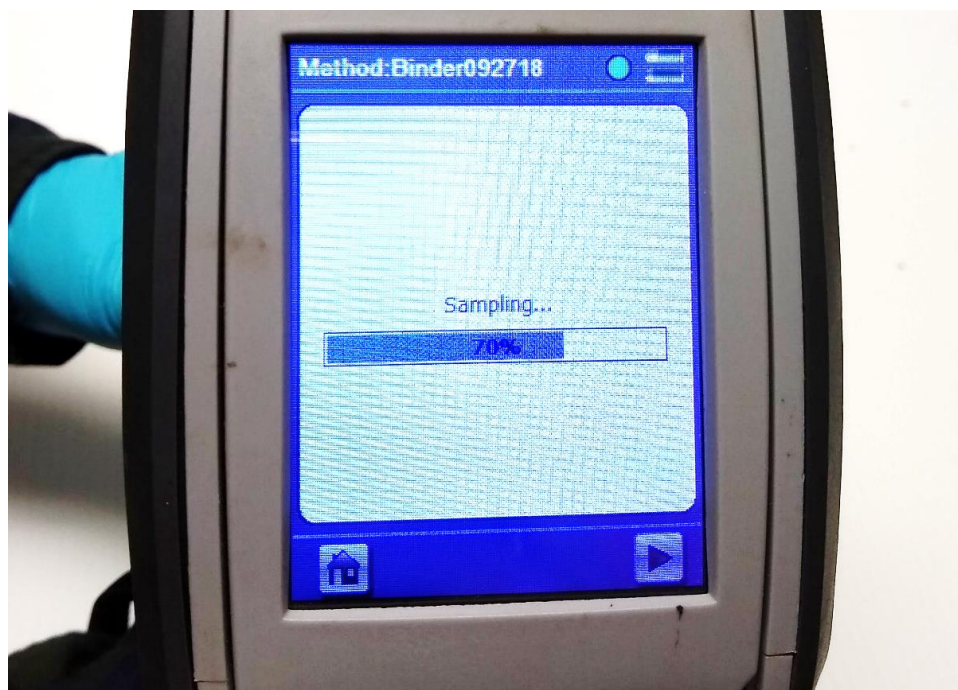
Press the trigger once, to start the data collection.



STEP 15

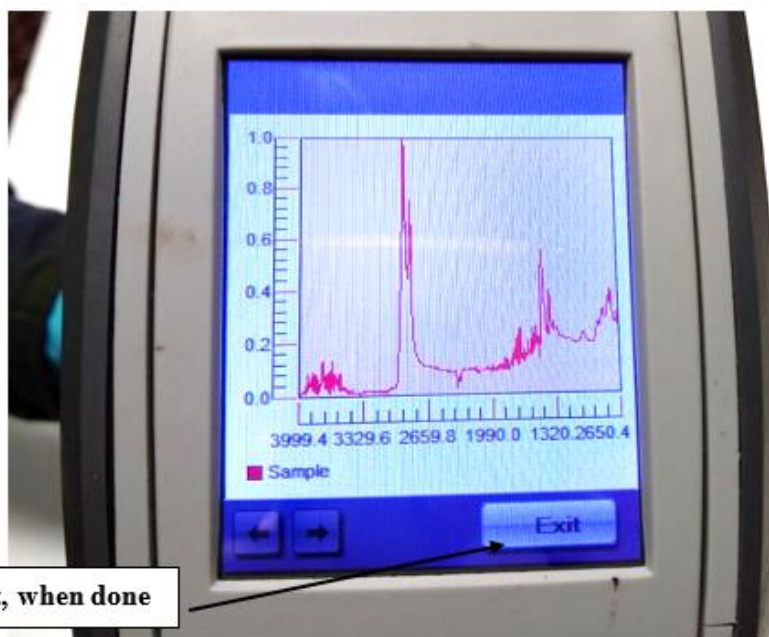
Sampling is in progress.

Time required for the step: 2 min.



STEP 16

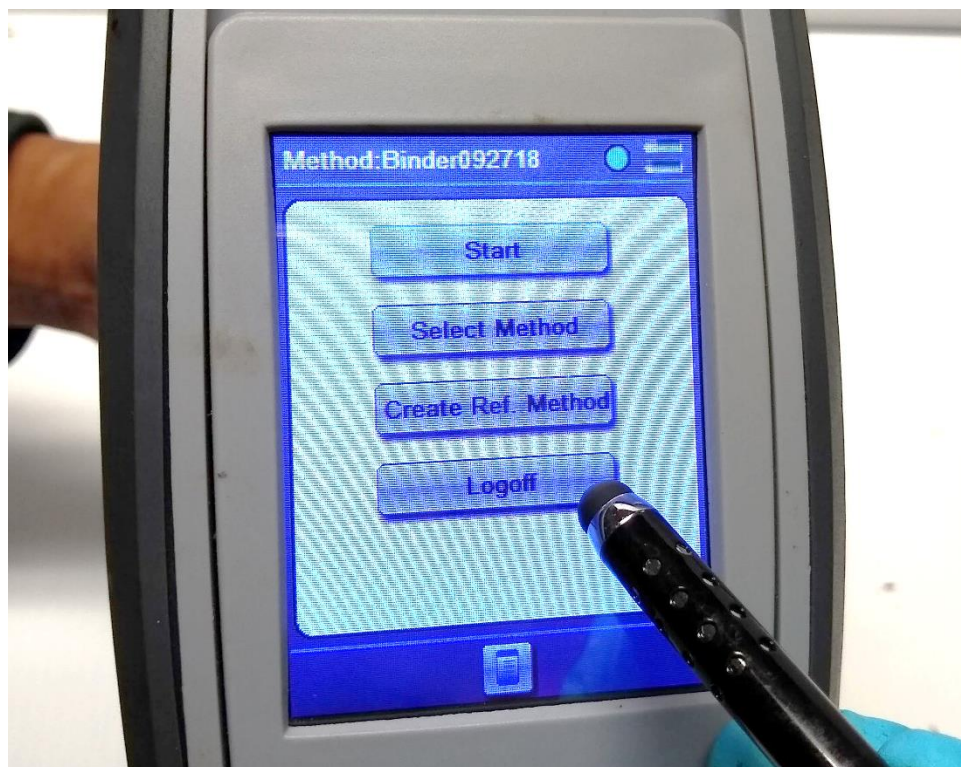
The spectra will appear on the screen.



Press Exit, when done

STEP 17

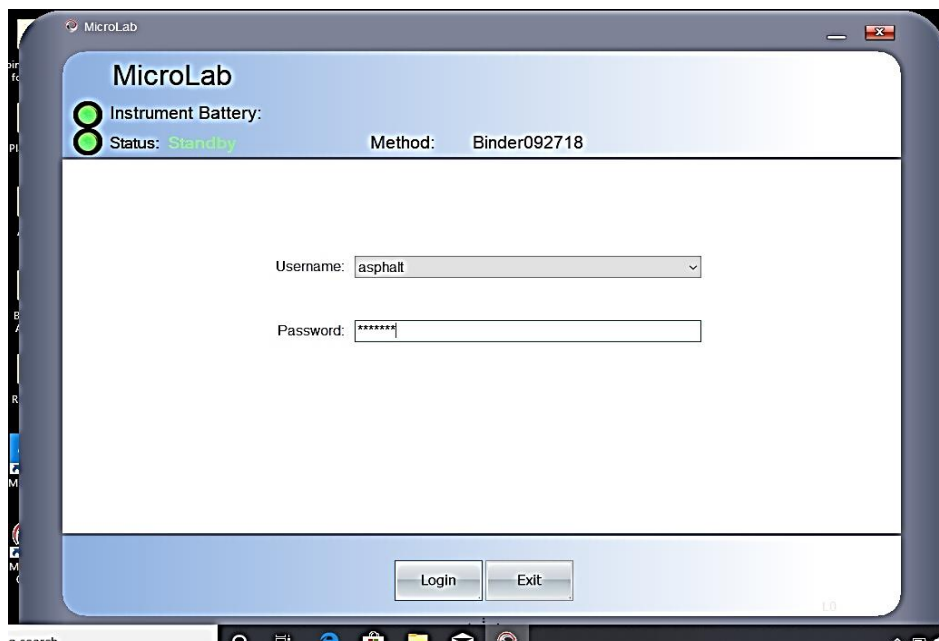
Press 'Start' to begin new sampling.
Press 'Logoff' if done.



APPENDIX C: Import Data File from FT-IR to the PC

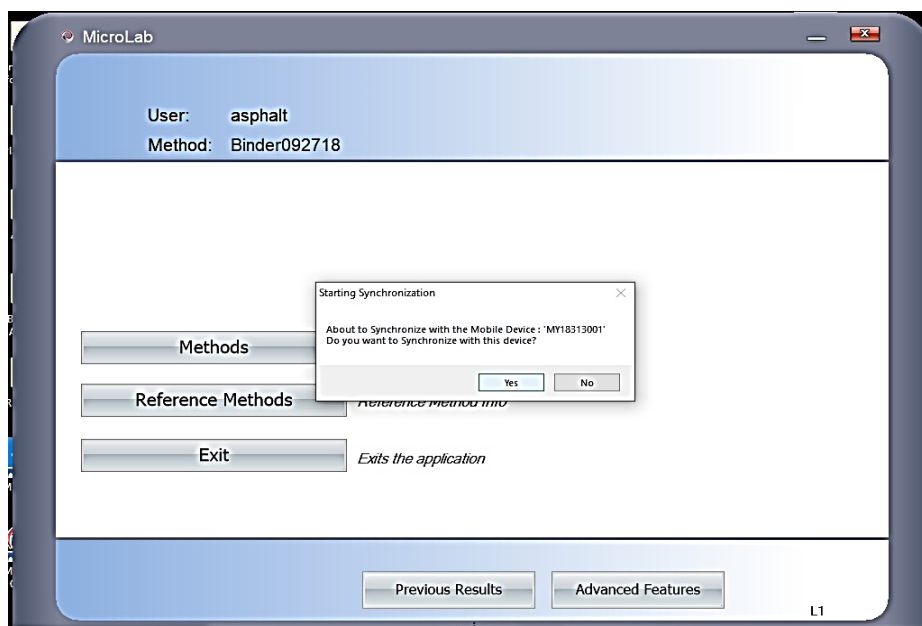
STEP 1

Open the
'MicroLab Lite'
on the PC.
Insert the
password and
press 'login.'



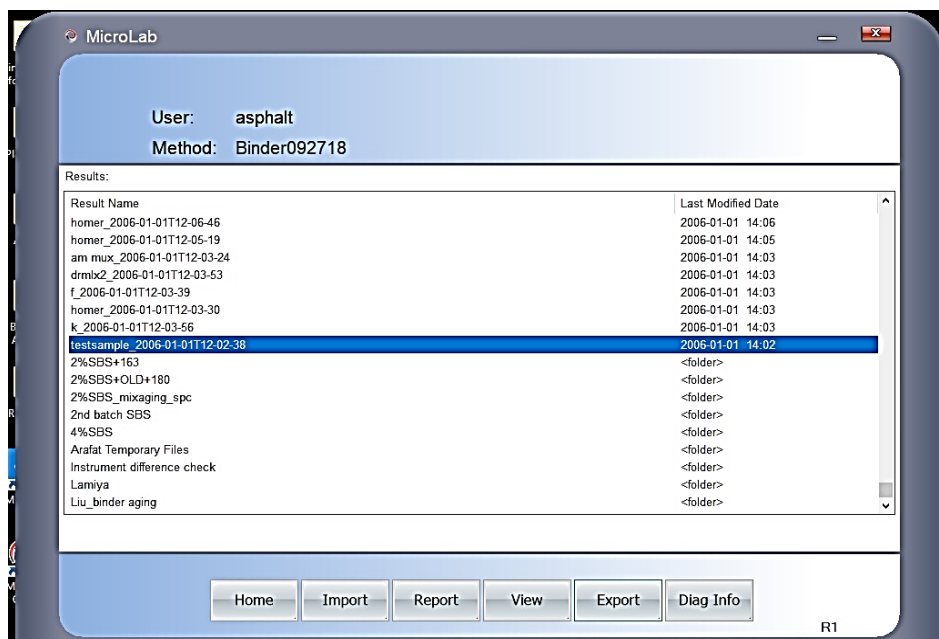
STEP 2

It will automatically ask to synchronize the data. The spectra saved in the FTIR memory will be transferred to the hard drive of the PC. Press 'yes' to wait till synchronization is done. Press 'Precious Result' to see the spectra data files.



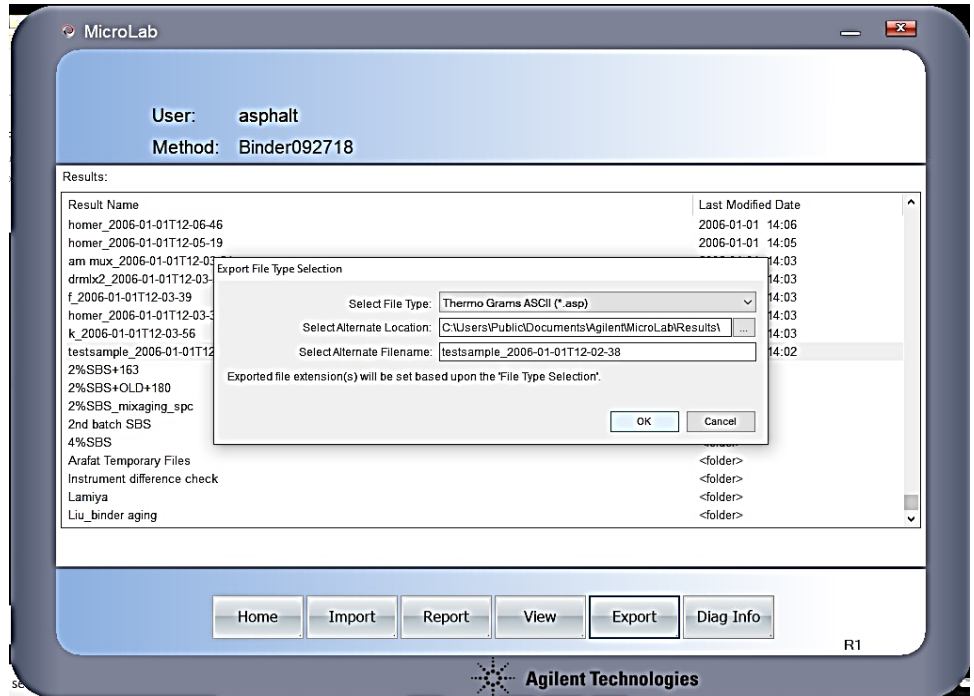
STEP 3

Select one file that needs to be used for analysis.



STEP 4

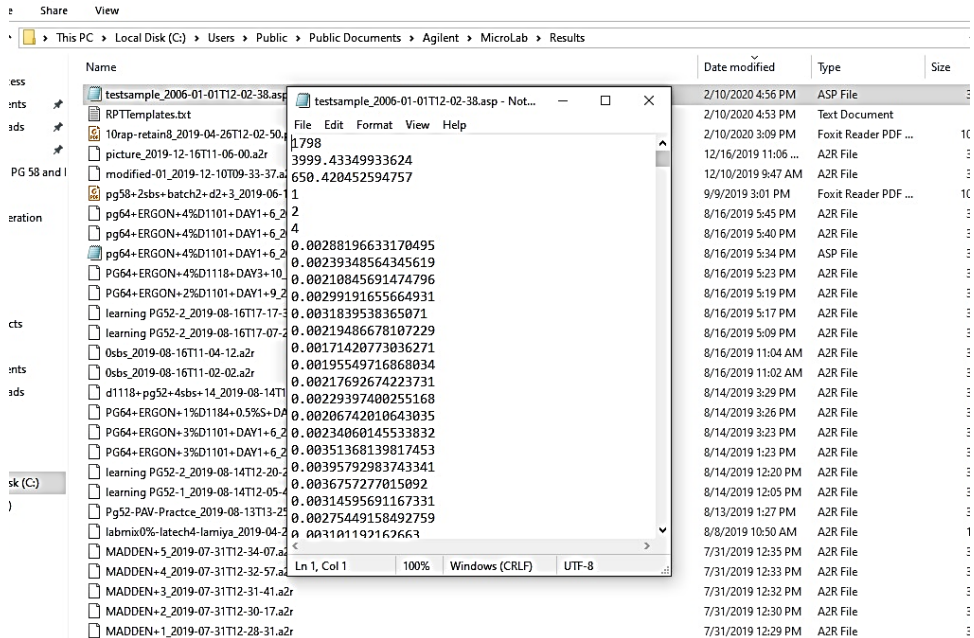
Press 'Export' to convert it to text file.



STEP 5

The text file will be saved in the same directory. Copy the data into the excel file for further data processing and analysis.

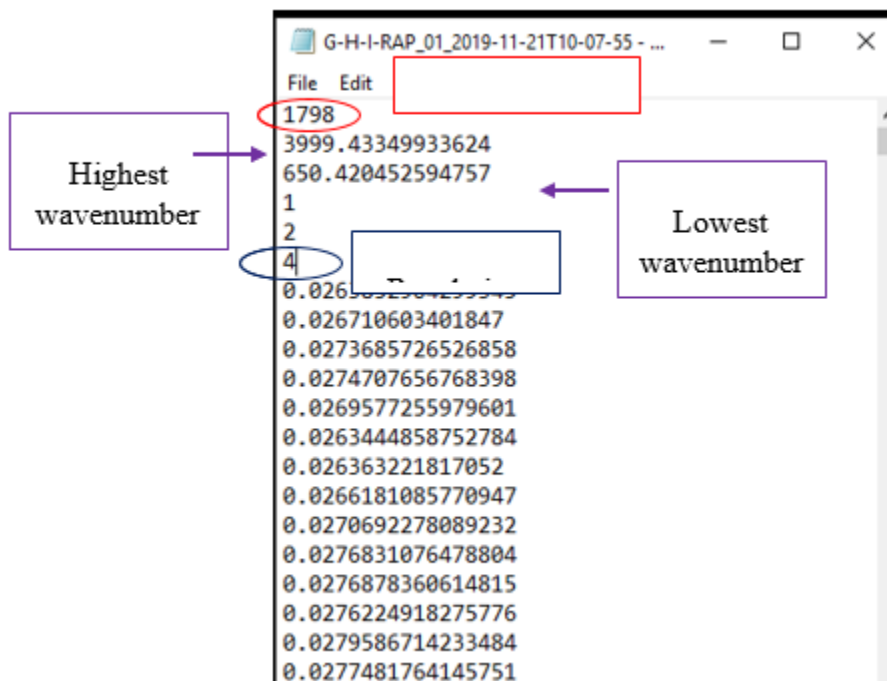
Time required to convert the data: 2 min.



APPENDIX D: FT-IR Spectra Analysis Method

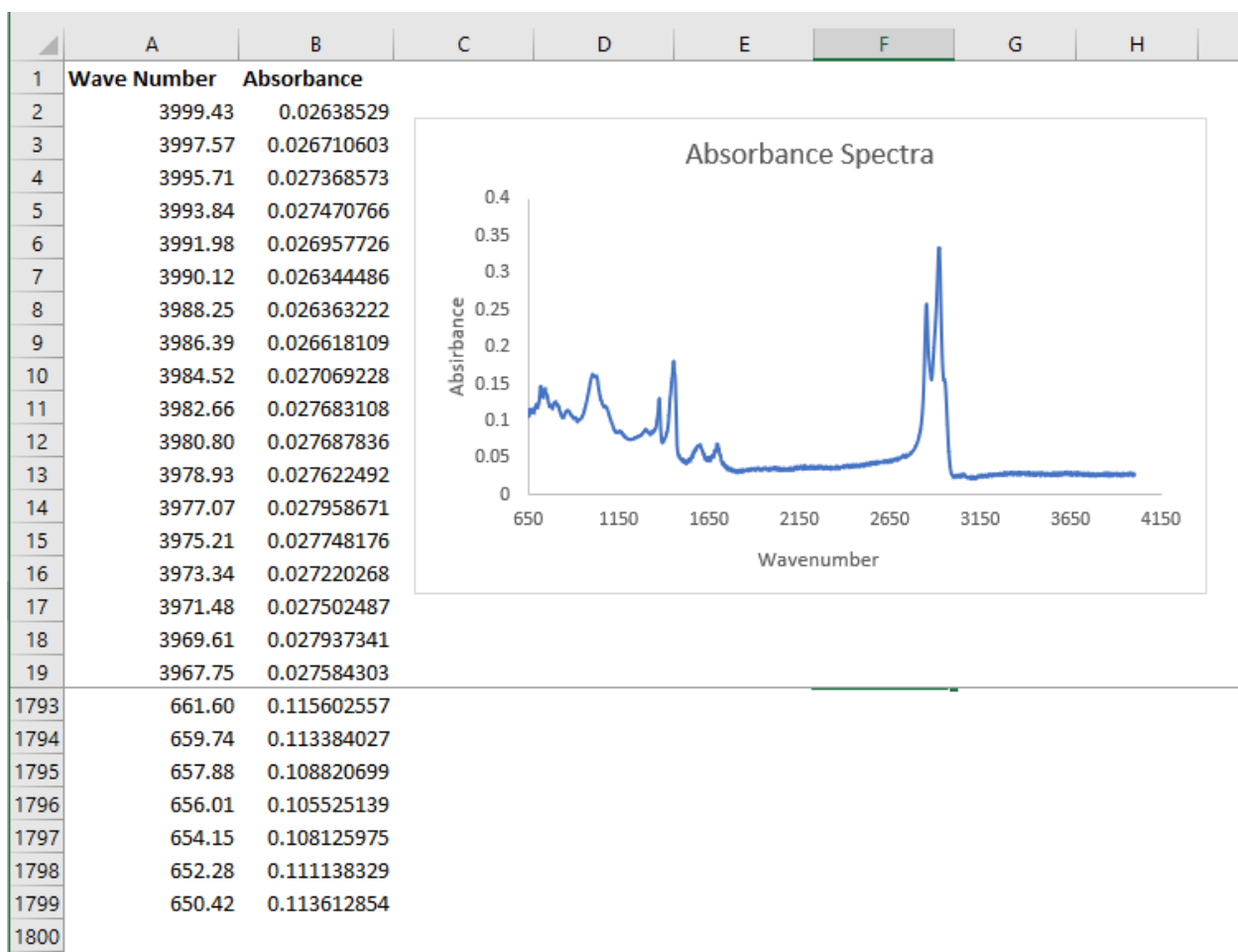
- [1] Open the text file where the absorbance values are stored at different wavenumbers.

Figure D 1. Typical text file with absorbance spectra value



- [2] Create a column in Excel with the heading 'Wavenumber'
Value of first row of the data set = 3999.433
Value of last row of the data set = 650.420
Number of rows = 1798
Increment = $(3999.433 - 650.420)/(1798 - 1) = 1.8636$
The number of rows will vary if the scanning range or rate is changed. During the study the resolution was kept fixed to 4 cm^{-1} .
- [3] Create another column with heading 'Absorbance'
Copy the absorbance value directly from the text file to excel.
- [4] Plot the scatter diagram to check if there is any anomaly in the shape of the spectra.

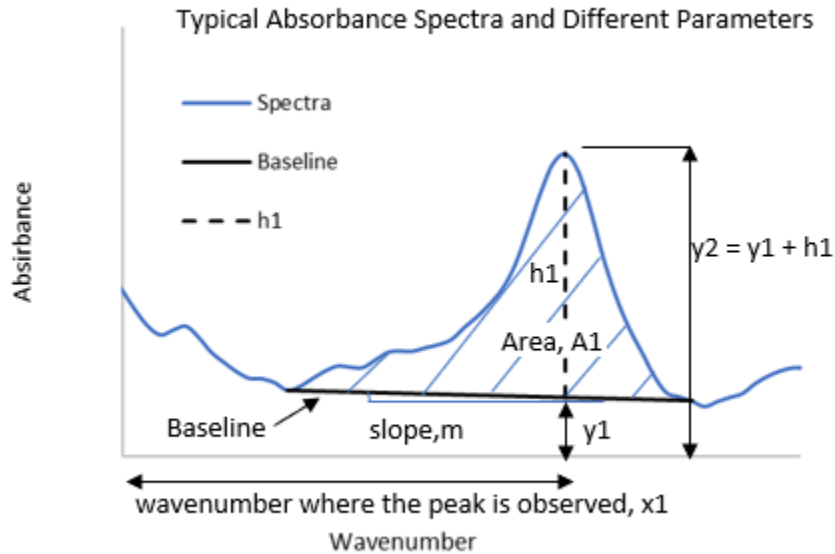
Figure D 2. Typical absorbance spectra plotted in excel



[5] At specific wavenumber, the peak height as well as the area under the peak high enclosed by the spectra and the base line need to be calculated to determine different indices. A baseline is needed to be drawn first to calculate those values.

- Baseline is the straight line connecting the lowest point on either sides of a peak.
- 'm' is the slope of the baseline.
- 'x1' is the wavenumber corresponding to certain functional group of interest.
- 'y1' is the y-value on the baseline at x1.
- 'y2' is the absorbance value on the spectra at x1.
- 'h1' is the peak height at x1, which is the distance between the peak and the baseline at x1.
- 'A1' is the area under the curve and above the baseline.

Figure D 3. Segment of a spectra for Peak height and area calculation



[6] Detailed calculation of peak height and the area determination at wavenumber $x_1 = 1456 \text{ cm}^{-1}$ is demonstrated here.

- It is determined that the valley or the lowest point on the left side of the peak corresponding to wavenumber 1456 cm^{-1} is 1394 cm^{-1} and the valley on the right side is 1487 cm^{-1} . Wavenumbers at the valley remained unchanged irrespective to the different types of samples.
- For this example, the absorbance value at 1394 cm^{-1} is 0.0714 and at 1487 cm^{-1} is 0.0517 . Peak value of absorbance at 1456 cm^{-1} is $y_2 = 0.1805$.
- A baseline is constructed connection the points $(1394, 0.0714)$ and $(1487, 0.0517)$. The equation of baseline is assumed to be, $y = m \cdot x + C$.
- Here, $m = (0.0517 - 0.0714) / (1487 - 1394) = -0.0002113$.
- And, $C = 0.0517 - 1487 \cdot (-0.0002113) = 0.3660$.
- $y_1 = (-0.0002113) \cdot 1456 + 0.3660 = 0.0584$.
- $h_1 = 0.1805 - 0.0584 = 0.1221$.
- A_1 is calculated using the trapezoidal rule.

**Figure D 4. Calculation of peak height and area at wavenumber 1456 cm⁻¹:
screenshot of the excel file**

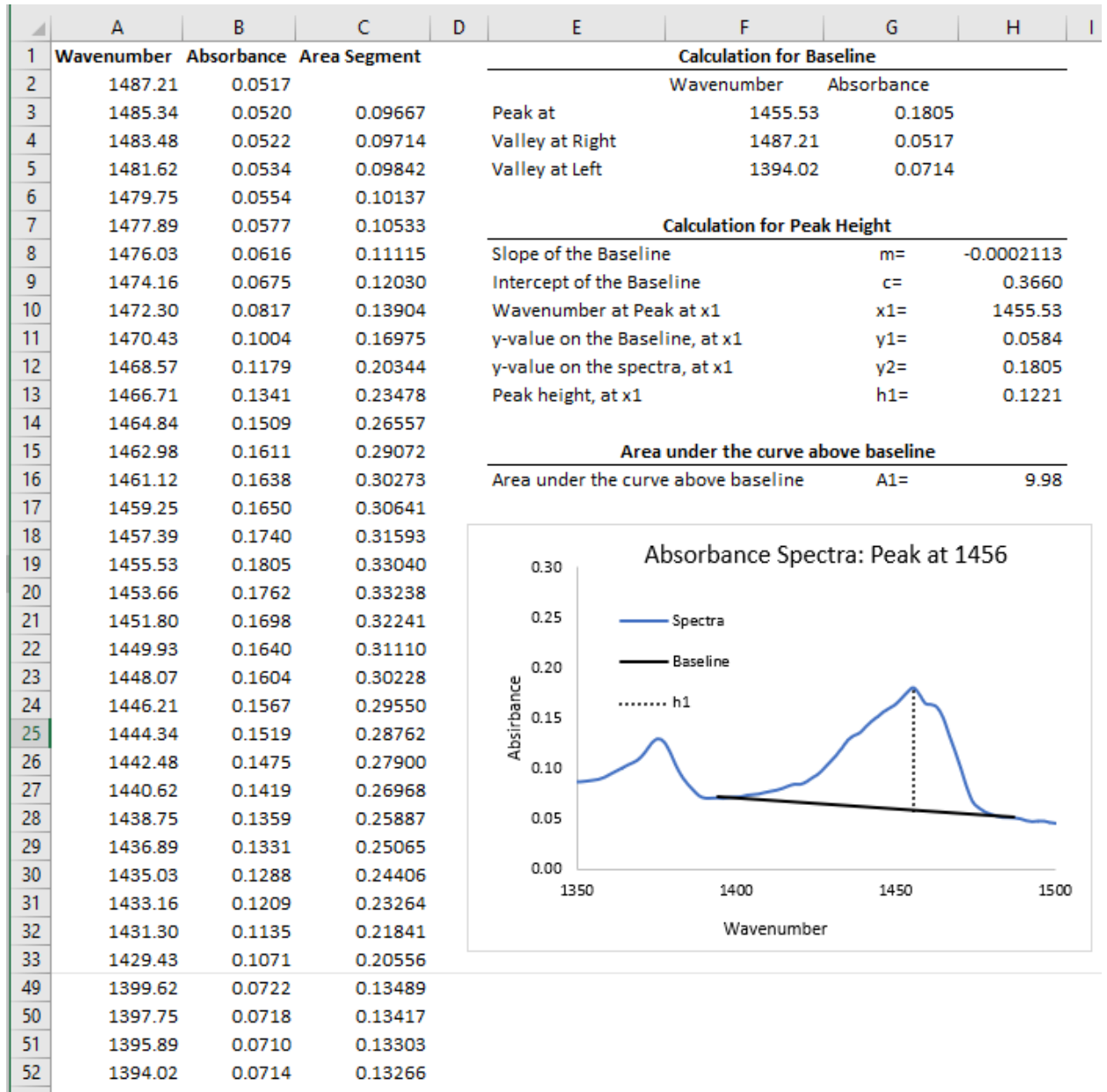


**Figure D 5. Calculation of peak height and area at wavenumber 1032 cm⁻¹:
screenshot of the excel file**

Calculation for Baseline			
	Wavenumber	Absorbance	
Peak at	1032.47	0.0796	
Valley at Right	1080.93	0.0612	
Valley at Left	980.29	0.0674	

Calculation for Peak Height			
Slope of the Baseline	m=	-0.0000613	
Intercept of the Baseline	c=	0.1275	
Wavenumber at Peak at x1	x1=	1032.47	
y-value on the Baseline, at x1	y1=	0.0642	
y-value on the spectra, at x1	y2=	0.0796	
Peak height, at x1	h1=	0.0155	

Area under the curve above baseline			
Area under the curve above baseline	A1=	7.1709	

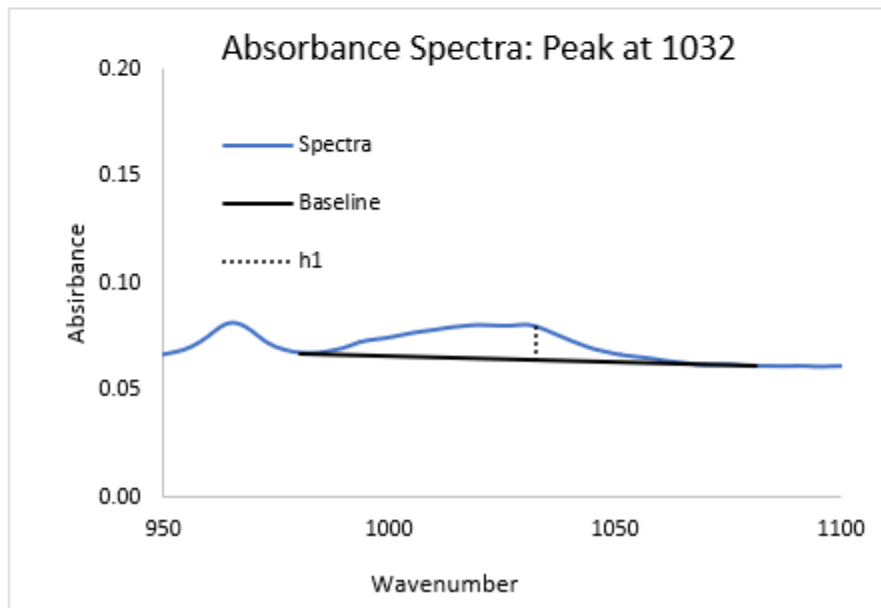
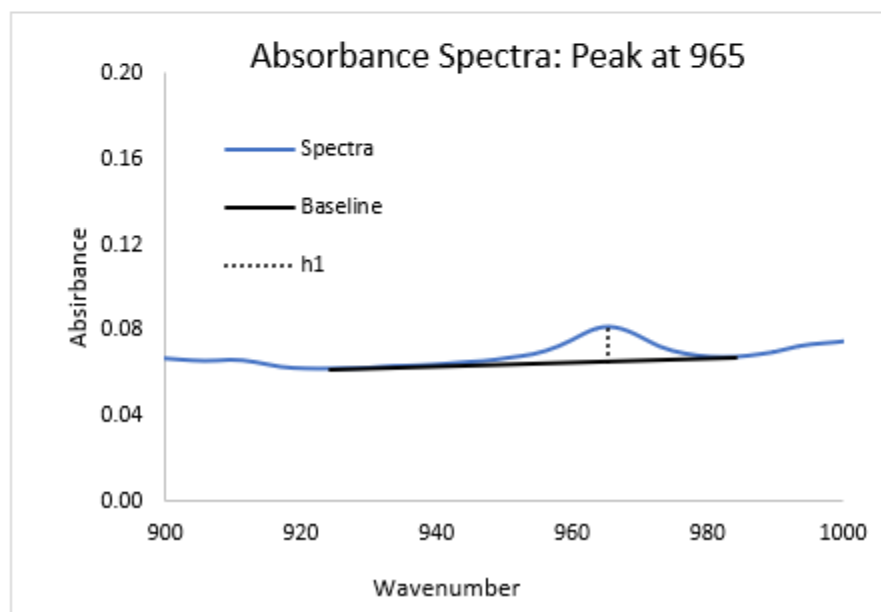


Figure D 6. Calculation of peak height and area at wavenumber 965 cm⁻¹: screenshot of the excel file

Calculation for Baseline		
	Wavenumber	Absorbance
Peak at	965.38	0.0814
Valley at Right	984.02	0.0673
Valley at Left	924.38	0.0619

Calculation for Peak Height		
Slope of the Baseline	m=	0.0000917
Intercept of the Baseline	c=	-0.0229
Wavenumber at Peak at x1	x1=	965.38
y-value on the Baseline, at x1	y1=	0.0656
y-value on the spectra, at x1	y2=	0.0814
Peak height, at x1	h1=	0.0158

Area under the curve above baseline		
Area under the curve above baseline	A1=	4.0993



**Figure D 7. Calculation of peak height and area at wavenumber 1375 cm⁻¹:
screenshot of the excel file**

Calculation for Baseline		
	Wavenumber	Absorbance
Peak at	1375.39	0.1245
Valley at Right	1394.02	0.0644
Valley at Left	1341.84	0.0793

Calculation for Peak Height		
Slope of the Baseline	m=	-0.0002847
Intercept of the Baseline	c=	0.4613
Wavenumber at Peak at x1	x1=	1375.39
y-value on the Baseline, at x1	y1=	0.0697
y-value on the spectra, at x1	y2=	0.1245
Peak height, at x1	h1=	0.0547

Area under the curve above baseline		
Area under the curve above baseline	A1=	4.7247

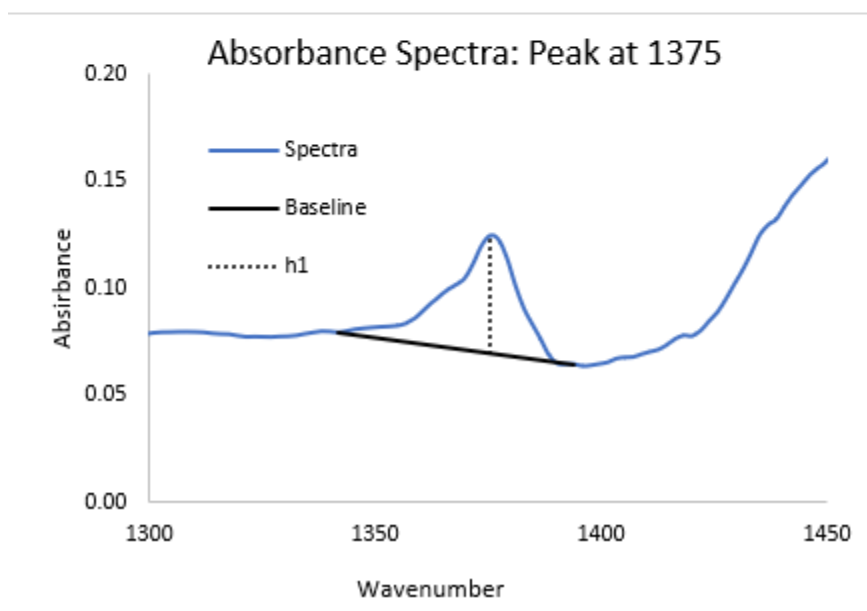


**Figure D 8. Calculation of peak height and area at wavenumber 1696 cm^{-1} :
screenshot of the excel file**

Calculation for Baseline		
	Wavenumber	Absorbance
Peak at	1695.94	0.0379
Valley at Right	1720.17	0.0283
Valley at Left	1686.62	0.0329

Calculation for Peak Height		
Slope of the Baseline	m=	-0.0001370
Intercept of the Baseline	c=	0.2640
Wavenumber at Peak at x1	x1=	1695.94
y-value on the Baseline, at x1	y1=	0.0316
y-value on the spectra, at x1	y2=	0.0379
Peak height, at x1	h1=	0.0062

Area under the curve above baseline		
Area under the curve above baseline	A1=	1.1542

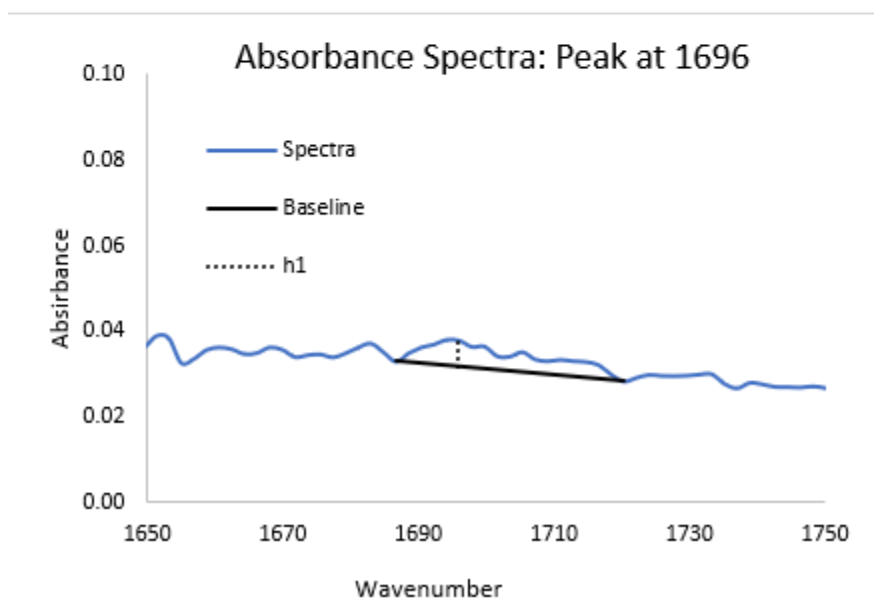


**Figure D 9. Calculation of peak height and area at wavenumber 2920 cm^{-1} :
screenshot of the excel file**

Calculation for Baseline		
	Wavenumber	Absorbance
Peak at	2920.37	0.3114
Valley at Right	2996.78	0.0230
Valley at Left	2754.50	0.0435

Calculation for Peak Height		
Slope of the Baseline	m=	-0.0000844
Intercept of the Baseline	c=	0.2760
Wavenumber at Peak at x1	x1=	2920.37
y-value on the Baseline, at x1	y1=	0.0295
y-value on the spectra, at x1	y2=	0.3114
Peak height, at x1	h1=	0.2819

Area under the curve above baseline		
Area under the curve above baseline	A1=	32.41

